ANALYTICAL STUDIES OF THE DEGRADATION OF CELLULOSE NITRATE ARTEFACTS

by

Robert A. Stewart

A thesis submitted to the Department of Pure and Applied Chemistry, University of Strathclyde, in partial fulfilment of the requirements for the degree of Doctor of Philosophy.

April 1997

ABSTRACT

The deterioration of cellulose nitrate artefacts in museum and art collections is a complex problem facing conservators and conservation scientists. This study has looked at several aspects of the degradation by analysing artefacts and model samples. Initial work concentrated on a survey of a collection of artefacts, many of which showed active degradation, by visual inspection and FTIR spectroscopy. A more thorough analysis of the artefacts was carried out, using ion chromatography, x-ray fluorescence spectroscopy and atomic absorption spectroscopy, to identify compositional differences between samples, which may relate to degradation. The results of these studies suggested that residual sulphate in the plastics is a cause of increased degradation. The presence of oxalate in degraded artefacts also indicated that chain scission is occurring during deterioration. Later work using gel permeation chromatography confirmed this. Work has also involved the use of accelerated ageing tests to study the effect of sulphate in the degradation and also the influence of inorganic fillers, iron and humidity. It has been concluded that the degradation of cellulose nitrate artefacts is dependent on the presence of sulphate and humidity. The process is diffusion controlled which indicates that loss of plasticiser is a vital factor. This work also suggests simple procedures that can be used to assess an artefact's stability.

ACKNOWLEDGEMENTS

I would like to express my thanks to my supervisors Prof. David Littlejohn, Prof. Richard Pethrick at the University of Strathclyde and Dr Anita Quye at the Royal Museum of Scotland, in Edinburgh. Their technical knowledge and guidance have been an asset to this research. Thanks also to Dr Norman Tennent for being on hand to provide his advice.

Thanks also to all the staff and colleagues of the Analytical Department and the Physical Chemistry Department for their support. Particular thanks is given to John Carruthers for helping me with the GPC work. Thanks also to all the staff at the Royal Museum in Edinburgh, in Conservation and Analytical Research and the Geology Department for allowing me to use their facilities and providing technical advice.

I would also like to thank Colin Williamson, Yvonne Shashoua, John Morgan and the Museum of London for donation of degraded samples of cellulose nitrate. Also, the Royal Ordnance factory, Bishopton for allowing me to tour their site and for providing me with samples of cellulose.

Finally, I wish to acknowledge the financial support of the Engineering and Physical Sciences Research Council and the Scottish Conservation Bureau (Historic Scotland).

CONTENTS OF THESIS

CHAPTER ONE

INTRODUCTION

Chapter One - Contents

1.1 Introduction

The importance of plastics in society today is immense. Since the development of the first synthetic plastics almost 150 years ago, their introduction into almost every aspect of our lives has been phenomenal. World-wide production today is approximately 100 million tonnes per year [1]. However, plastics have acquired a rather tarnished image and are generally perceived as dull, cheap and mass produced. But, their social and economic importance has meant that they are now represented in many museum collections across the world

The semi-synthetic plastic cellulose nitrate is of particular historical value, being the first plastic produced commercially, and is widely found in collections. Unfortunately, museums are discovering that the other popular misconception about plastics - that they last forever - is not necessarily true, especially with early cellulose nitrate. Examination of these plastic artefacts in recent years has shown that many of the objects exhibit signs of degradation and this problem is therefore becoming an increasingly important issue [2, 3]. Museum conservators are faced with a problem of trying to halt the degradation of these artefacts, but their task is hindered by the lack of suitable research on which to base appropriate storage conditions or treatment strategies.

1.2 History and uses of cellulose nitrate

Cellulose nitrate, sometimes incorrectly referred to as nitrocellulose, was the first plastic produced commercially. It was responsible for many changes in science, industry and the arts as well as being a forerunner to the current plastics industry [4].

The early half of the nineteenth century marked a time when chemical thought was rapidly changing. The impact of technology on industry was great enough to affect the lives of most people. Like many naturally occurring substances, uses for cellulose were being studied. Although a Frenchman, Henri Braconnet, had investigated the effect of concentrated nitric acid on potato starch in 1833, [5] and a similar experiment on paper was conducted by Theophile Jules Pelouze a few years later, the discovery of cellulose nitrate is generally accredited to Christian Schobein. In 1845, he perfected the nitration process using a mixture of nitric and sulphuric acids [6, 7]. Schobein, however, failed to realise the potential of his discovery and

did not continue this work. The major breakthrough for cellulose nitrate as a plastic came in 1862 when Alexander Parkes displayed a variety of moulded cellulose nitrate objects at the International Exhibition in London [8]. Parkes continued to experiment with plasticisers for cellulose nitrate, but his product was not a commercial success and his company went bankrupt shortly afterwards. Although Parkes had experimented with camphor as a plasticiser, he had not recognised its importance. The preparative mixture was perfected by John Wesley Hyatt, an American, in 1869, who produced the first commercially successful plastic, Celluloid [5]. Around the same time in England, Daniel Spill was producing a similar material called Xylonite.

Applications for Celluloid and Xylonite were widespread and an enormous range of everyday objects was produced. The plastic could be moulded into almost any conceivable shape or size , from combs to billiard balls. By using additives in the cellulose nitrate - camphor mix, coloured objects, imitation ivory, amber and tortoiseshell could be manufactured [9-11].

In the following years, cellulose nitrate also found applications in several other fields. It was used as a protective layer for many objects and as an adhesive [12-14]. It was also developed by Henry Reichenbach to produce a base for photography and later, in cinematography [8]. A more nitrated form of cellulose nitrate than that used in plastics and lacquers was developed in 1889 by Frederick Abel [15]. This was used in the explosives industry and was seen as the major break from the traditional use of gunpowder [16].

The production of cellulose nitrate declined towards the turn of the century due to the development of plastics such as cellulose acetate and formaldehyde-condensed plastics which were stronger, cheaper and had wider applications. Cellulose nitrate also became notorious for being unstable and extremely flammable, which hastened the decline of its use.

1.3 Chemistry of cellulose nitrate artefacts

Cellulose nitrate is the oldest known derivative of cellulose [15] and its solid structure retains the form of the cellulose from which it is derived. Therefore, the

chemistry of the derivative cannot be understood without a basic knowledge of the parent material.

1.3.1 Cellulose

Cellulose is the polysaccharide which forms the bulk of the structural material for all plants. Cotton is the usual starting material for the synthesis of cellulose nitrate. The seed hairs or linters of the cotton plant are almost pure cellulose, but also contain pectin, fats and waxes [17, 18]. Other sources of cellulose used for the production of cellulose nitrate are wood (average cellulose content of 50%) and less commonly, bast fibres (65 - 80% cellulose) [19].

The structure of cellulose is very complex and varied, but basically consists of long chain polysaccharides which combine to form a fibrous material. The molecular structure of cellulose (see Figure 1.1) indicates that it is comprised of linear, unbranched chains of 1- 4 linked β - D - glucopyranose residues [20]. Due to various intermolecular interactions the chain adopts a helical nature. The degree of polymerisation depends on the cellulose source and the level of degradation. In cotton linters, for example, the degree of polymerisation may be in the region of 1000 - 3000 glucopyranose units.

Cellulose is naturally fibrous, formed from individual cellulose chains which wrap around each other to form a thicker portion known as the elementary fibril. These then group together to form microfibrils which in turn entwine to produce fibrils and then finally the fibre. The whole process is likened to the configuration of rope [21] (see Figure 1.2). Cellulose is known to have a highly ordered crystalline structure (over 70%) [19]. This is maintained by a high degree of intermolecular and intramolecular chain hydrogen bonding between hydroxyl groups. These are sufficiently strong enough to make cellulose relatively insoluble, such that it is impossible to plasticise it directly.

In its natural state, cellulose does not behave as a plastic. It has a glass transition temperature of 220 °C and degrades at higher temperatures [17]. However, cellulose can be processed to form semi-synthetic plastics, i.e. man made plastics using a natural starting material.

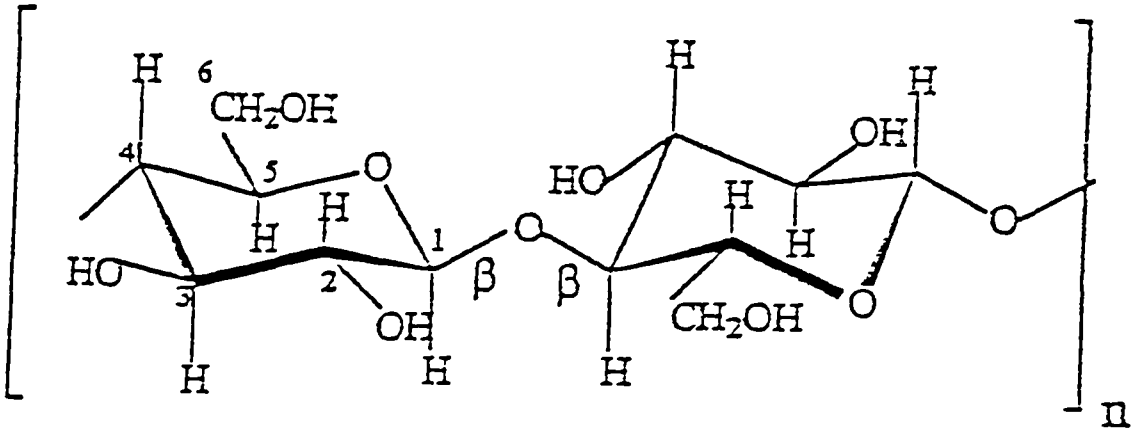

Figure 1.1 **Chemical structure of cellulose.**
The three hydroxyl groups may be replaced or partially replaced by nitrate groups in the formation of cellulose nitrate.

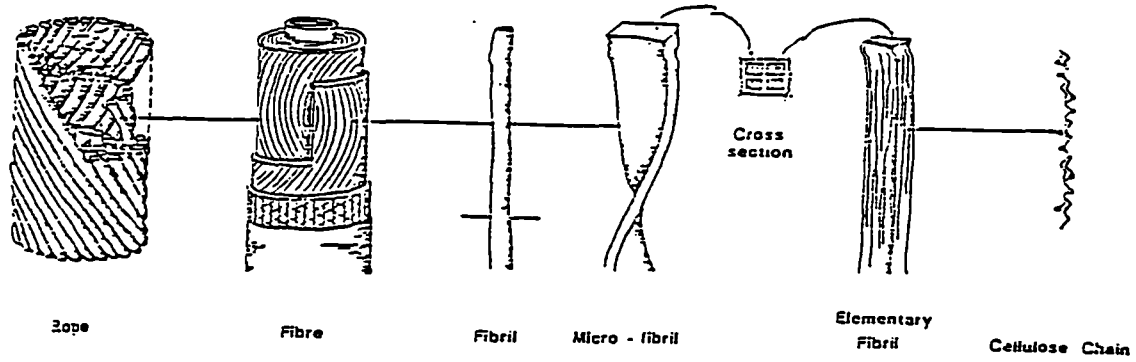

Figure 1.2 **Schematic diagram of the different structural levels of a cellulose fibre, compared with that of a rope [21].**

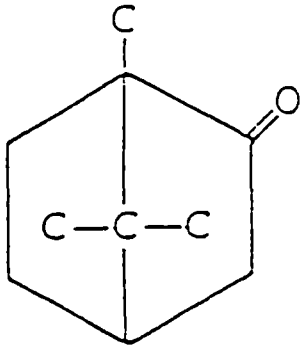

Figure 1.3 **Chemical structure of camphor**

1.3.2 Nitration

The conversion from cellulose to cellulose nitrate is more correctly an esterification rather than a nitration process, although it is still referred to as nitration in cellulose nitrate manufacturing literature. Nitration is carried out by the addition of nitric acid, sulphuric acid and water to the cellulose under controlled conditions. Each glucose residue in the cellulose chain contains three hydroxyl groups, two secondary and one primary (see Figure 1.1). Theoretically, each of the three hydroxyls could be substituted by a nitrate group, to obtain a product with a maximum of 14.1 % nitrogen (of total weight) [22-24]. In practice, a nitrogen content of 14.1 % is not possible, due to the instability of the trinitrate, and a maximum of 13.5 % is the most that can be achieved.

By varying the reaction conditions, i.e. temperature, relative concentrations of acids, etc., it is possible to control the number of hydroxyl groups that are replaced and hence the nitrogen content. It is therefore possible to produce cellulose nitrate with varying levels of nitrogen, from 10 % to 13.5 %. These products have contrasting properties and different applications.

1.3.3 Plasticisation

As cellulose nitrate still retains the fibrous nature of the original cellulose, it is necessary to process it with a plasticiser to form a homogeneous gel before moulding or casting. Plasticisers are compounds which are added to a material in order to improve its flexibility and processibility. A plasticiser can decrease the glass transition temperature and modulus of elasticity without changing the chemical nature of the plasticised material [25]. Plasticisers also aid the processing of plastics by reducing adhesion to metal surfaces and lowering processing temperatures.

In order for a plasticiser to be used with a compound it must be able to satisfy two requirements [26].

a) It should be compatible with the polymer, i.e. the polymer and plasticiser should be mutually soluble.
b) It should not exude out of the system, through volatilisation or bleeding, during the life of the plastic.

The number of substituted hydroxyl groups in cellulose increases during the nitration process thereby reducing the degree of hydrogen bonding in the polymer. This decrease in polarity lends to cellulose nitrate's solubility in volatile solvents and its compatibility with a wide range of plasticisers. The most commonly used plasticiser in the manufacture of early plastics was camphor, a white crystalline material extracted from the camphor laurel [20]. The structure of camphor is shown in Figure 1.3. Other plasticisers have been used throughout history, such as dibutylphthalate, triphenylphosphate and glycerol, but certainly not to the same extent as camphor [12, 27].

There has been much speculation as to the exact nature of the camphor - cellulose nitrate system [15, 28]. As the solubility parameters of cellulose nitrate and camphor differ considerably, it is likely that there is some form of specific interaction between the two, such as some degree of hydrogen bonding between cellulose nitrate and the camphor carbonyl group.

1.4 Manufacture of cellulose nitrate artefacts

The production of cellulose nitrate plastics has remained relatively unchanged over the last one hundred years. It is a straightforward, two stage process; the production of cellulose nitrate from cellulose and then the production of plasticised cellulose nitrate from which the articles are made An outline of both stages is shown in Figures 1.4 and 1.5.

There is a vast amount of literature concerning the manufacturing process; the better reviews are by Miles [28], Barsha [15], Yarsley [22] and DeBussy [24].

1.4.1 Cellulose: sources and preparation

Raw material for the production of cellulose nitrate is usually cotton fibres, although woodpulp may be used. Cotton cellulose contains a small amount of impurities (about 2 %), mainly the protective film of wax, oil from the seed, pectin and colouring matter. The cotton linters (seed hairs) must therefore be purified prior to use, but this requires

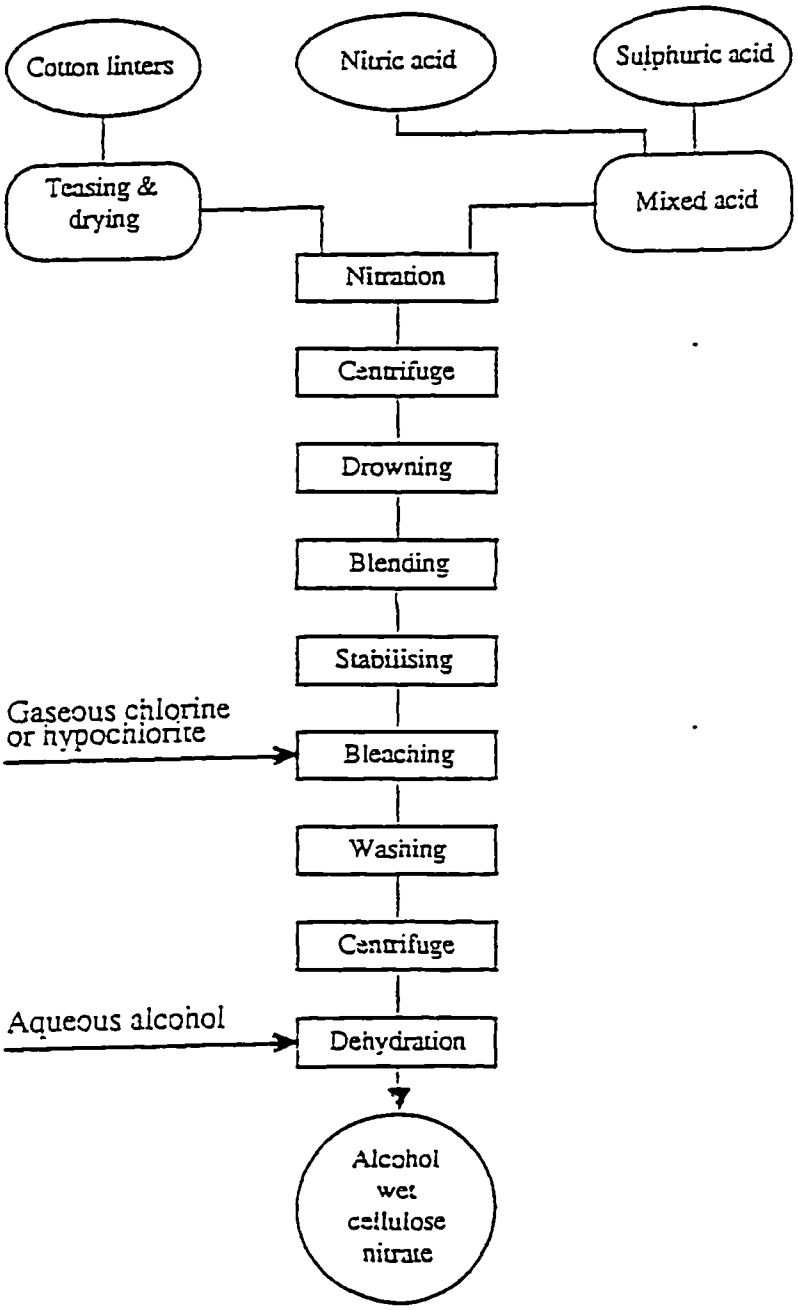

Figure 1.4 Manufacturing steps in the production of cellulose nitrate [22].

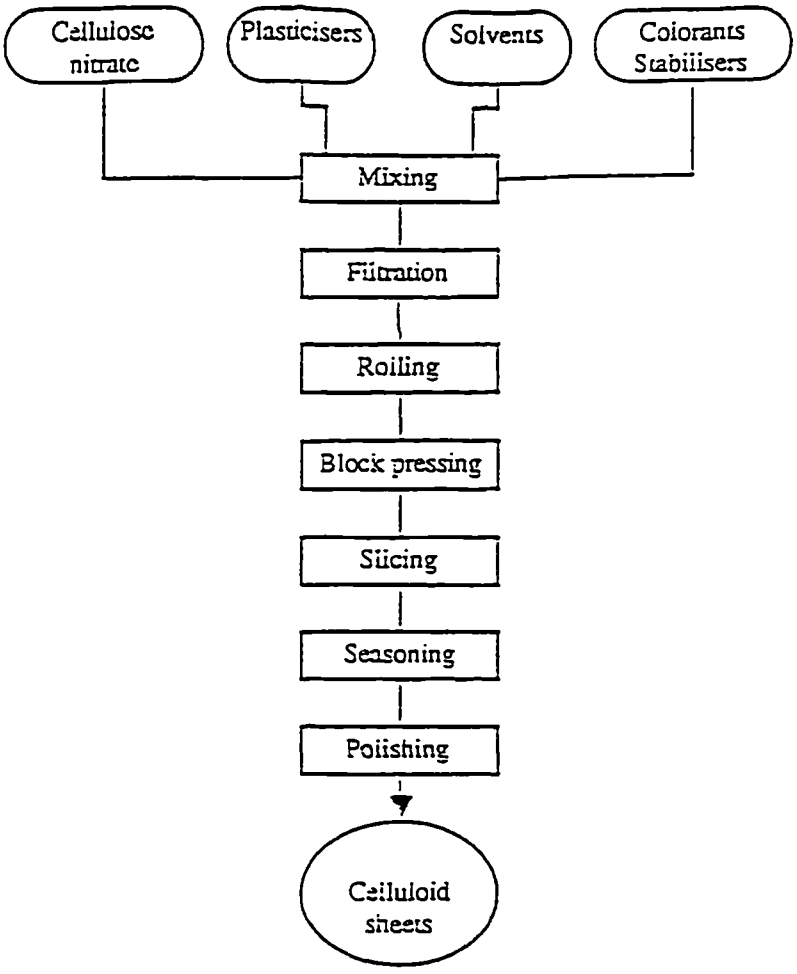

Figure 1.5 Manufacturing steps in the production of celluloid

careful control to avoid degradation of the cellulose molecule[29]. The linters are boiled with dilute sodium hydroxide solution. This reaction may produce soluble acidic degradation products, mainly oxalic acid but also formic, acetic, glycolic and lactic acids [28]. These must be removed, along with any residual alkali, by washing. The cellulose can then be bleached using dilute sodium hypochlorite. The purified cotton is then dried to give a final product of 3 % moisture, before nitrating.

1.4.2 Nitration with mixed acid

Cellulose nitration can be achieved using a number of reagent mixtures, for example, nitric acid-phosphoric acid and nitric acid-acetic anhydride [30]. However, cellulose nitrate plastics are most commonly manufactured from a nitric acid-sulphuric acid mixture.

The purified cotton linters are placed in a nitration bath and a mixture of nitric acid, sulphuric acid and water added. The reaction scheme is summarised as follows:

$$C_6H_7O_2(OH)_{3n} + 3nHNO_3 \xrightarrow{H_2SO_4/H_2O} C_6H_7O_2(NO_3)_{3n} + 3nH_2O$$

Hydroxyl groups are initially esterified with sulphate ions, then substituted with nitrate ions [31]. Since the reverse reaction also takes place, an equilibrium forms between cellulose, acid, water and cellulose nitrate. To force the reaction to completion, it is necessary to displace the equilibrium by adding sulphuric acid to combine with water formed. Excess water also causes the cellulose fibres to swell into a gel-like substance which hinders the diffusion of the acid into the cellulose. The use of sulphuric acid as a condensing agent prevents this swelling and the product retains its fibrous nature.

The reaction time, temperature and concentration of acids all influence the degree of nitration of the cellulose. Typical reaction conditions of around 30 minutes at 25 °C using 25 % HNO_3, 55 % H_2SO_4 and 20 % H_2O gives a product with around 11 % nitrogen content, suitable for producing plastics. After nitration, the cellulose nitrate is spun in a centrifuge to remove the bulk of the acid, followed by steeping in water to considerably dilute any acid still present.

1.4.3 Stabilisation

Although steeping lowers the acidity, the nitrated cellulose still contains significant levels of nitric and sulphuric acids. Their presence will cause instability within the cellulose nitrate. Sulphate esters may also be formed as a secondary product during the nitration process. These sulphate esters may form free sulphuric acid if not removed and hence initiate the decomposition of the cellulose nitrate. An after treatment or stabilisation stage is therefore essential. The stabilisation stage proceeds in large vats where the cellulose nitrate has accumulated. The material is usually boiled in water until an overall acidity of <0.2 % is achieved, which may take several days [32].

The sulphate esters may be divided into two types: an acid sulphate half-ester (Cell - OSO_3H) which is easily removed; and a more resilient form, generally considered a neutral sulphate ester, (Cell - O - SO_2 - Cell) [15], although other investigators have concluded that it is physically absorbed sulphuric acid [28]. Slightly acidic water enhances the removal of this impervious sulphate, whilst boiling has been shown to be necessary to swell the cellulose nitrate sufficiently to release the sulphate ester groups [33]. Long stabilisation stages are necessary to obtain a product with very high stability. However, the nitrogen content and the molecular weight of the cellulose nitrate may be reduced if lengthy stabilisation stages are used [22].

1.4.4 Further processing

1.4.4.1 Bleaching

Cellulose nitrate produced as described above, generally has a faint brown colour and it may require to be bleached for the manufacture of clear objects. Bleaching agents were usually gaseous chlorine (later removed by sodium sulphite) or were sodium hypochlorite and oxalic acid [15, 34]. The cellulose nitrate may be washed after this and soaked in alcohol to remove the water, making it more stable for storage and transport.

1.4.4.2 Plasticisation

The alcohol wet cellulose nitrate still resembles the original fibrous cellulose at this stage. To convert it into the finished plastic article it must go through several further stages, shown in Figure 1.5. First it is kneaded with camphor. The alcohol and camphor cause the cellulose nitrate fibres to swell as gelatinisation proceeds, eventually forming a dough. The amount of camphor used in the mixing may vary from 5 % to 50 % of the total weight.

Until around 1920, camphor had typically around 2 % impurities, which were mainly oils [35]. After this time, better quality camphor was used and also a synthetic camphor produced from turpentine became available. Other plasticisers were used over time such as phthalates, castor oil and glycerol, but not to any great extent.

1.4.4.3 Additives

Aside from plasticisers, other components are often added to the cellulose nitrate mix at this stage. These are used to change the mechanical properties or the appearance of the plastic. The three main groups of additives are as follows.

Stabilisers

The degradation of cellulose nitrate may occur through processing or during the life of the plastic, and is often brought on by exposure to heat, light, chemicals, etc. As cellulose nitrate is particularly prone to degradation, many attempts were made as far back as 1897 to stabilise the plastics. Stabilisers are components which are compatible with cellulose nitrate and are relatively inert. They function either by preventing the initiation reactions of the degradation processes or by scavenging degradation products hence preventing further deterioration [36]. There are two types of stabilisers generally used with cellulose nitrate. Antioxidants (e.g. phenols and secondary amines), which inhibit oxidative degradation and ultraviolet stabilisers (e.g. salicylates), which absorb UV light more readily than cellulose nitrate, without decomposing.

Fillers

Certain compounds are often added to the mix to add bulk and to give an opaque appearance to the plastic. Fillers are generally inexpensive inorganic minerals such

as zinc oxide, titanium oxide and even calcium carbonate [37]. As much as 10 % of the weight of a plastic may be filler. Cellulose nitrate artefacts containing fillers are often in very good condition and it is likely that the filler is acting as some kind of stabiliser by neutralising compounds which cause degradation.

Colourants

There are three types of colourant used in the manufacture of cellulose nitrate articles. Pigments (inorganic and organic) are insoluble in the plastic material and are widely used. Dyes are soluble in the plastic and are used to a much lesser extent.

Inorganic pigments are coloured solids which impart translucent or opaque colour to the plastics. Inorganic pigments are naturally occurring or synthetic and are usually metallic oxides, sulphides, lead salts, cadmium and mercury compounds and carbon black. They are very stable at high temperatures and to light.

Organic pigments are synthetic and benzenoid in nature. Organic pigments are generally more transparent and stronger in colour than inorganic pigments, however they are not as stable and fade with exposure to light and deteriorate when exposed to heat and chemicals. Organic pigments were commonly used with cellulose nitrate plastics are: phthalocyanines, vat pigments (anthraqinones, thioindigoids, perinones), azo pigments and dioxazines.

Dyes are chemical compounds which absorb certain wavelengths of light while transmitting others and scattering none, i.e. they are transparent. They are fairly unstable so are not widely used with plastics

1.4.5 The finished article

The cellulose nitrate dough is filtered under pressure then rolled on large, heated rollers to reduce the overall solvent content to around 12-15% of the plastic's total weight [22]. The sheets may either be pressed into a block form before slicing into thin sheets or chopped into small pieces for producing extrusions. The cellulose nitrate is then seasoned for a couple of days at around 50 °C to reduce the solvent content further, to around 2% (w/w).

At its zenith, 40000 tonnes of celluloid were produced every year [5]. Although this may seem insignificant compared with today's plastics production, it still represents widespread use of the plastic.
The variety of articles produced from cellulose nitrate is vast. Combs, dentures, collars, jewellery and dolls were some of the more common products [6, 9, 11]. Cellulose nitrate was also used to imitate more expensive materials. Ivory billiard balls, piano keys and cutlery handles were soon replaced with the plastic as were amber, pearl and horn articles [38]. Imitation tortoiseshell pieces were extremely common. The tortoiseshell effect was produced by preparing sheets of differing shades and thickness of the colours required (browns or greens). These were then cut and interleaved by hand to produce a variety of complex patterns.

1.5 Properties of cellulose nitrate plastics

The properties of cellulose nitrate depend on the manufacturing process. Unplasticised cellulose nitrate is very brittle and therefore cannot be used for the production of plastic articles. The degree of nitration is also very important and can be varied by changing the relative concentrations of nitric acid, sulphuric acid and water in the nitrating mixture. The final degree of nitration is related to the desired application of the cellulose nitrate, (Table 1.1).

The other main properties of cellulose nitrate can be divided into two groups: physical properties and chemical properties.

1.5.1 Physical properties

Table 1.2 summarises the main physical properties of cellulose nitrate. The process of plasticisation with camphor has the effect of reducing interchain forces, giving cellulose nitrate thermoplastic properties. It can be pressed and shaped at temperatures greater than 80 °C [39], though due to the actual cellulose molecule, the product itself is stiff and does not show rubbery properties at room temperatures [40]. The product also has a reasonable toughness and is resistant to water which are other desirable characteristics. The basic composition of cellulose nitrate has a transparent appearance, hence its application as an adhesive or lacquer. However, it is also

Table 1.1 Cellulose nitrate applications [43]

Field of Application	Mixture	Nitrogen content (%)
explosives	cellulose nitrate, plasticisers	12 - 13.5
adhesives	cellulose nitrate, plasticisers, solvents	12
film base	cellulose nitrate, plasticisers, solvents	12
lacquers, coatings	cellulose nitrate, plasticisers, solvents, dilutents, dyes	11.2 - 12
plastics	cellulose nitrate, plasticisers, solvents, fillers, dyes	10.5 - 11.2

Table 1.2 Physical properties of cellulose nitrate [24]

Softening range (°C)	80 - 90
Flow temperature (°C)	145 - 152
Ignition point in air (°C)	160
Glass Transition temperature (°C)	53
Specific Heat	0.3 - 0.4
Tensile Strength (lb $inch^{-2}$)	5000 - 10000
Refractive Index	1.5
Specific Gravity (g cm^{-3})	1.3 - 1.4

capable of forming excellent multicoloured plastics. The final attractive feature is its transparent appearance, hence its application as an adhesive or lacquer. However, it is also capable of forming excellent multicoloured plastics. The final attractive feature is its ability for after-shrinkage around inserts, a property which makes it useful even today for items such as knife handles.

1.5.2 Chemical properties

Cellulose nitrate has poor resistance to a number of chemicals and this is another reason for its limited use today. Although only slightly affected by dilute acids, concentrated acids and alkalis cause severe degradation. Contact with dilute alkali can cause some minor degradation such as surface crazing of the plastic. Cellulose nitrate may be dissolved by solvents such as acetone and tetrahydrofuran. Other solvents such as ethanol and chloroform have no immediate effect, but can extract the camphor from the plastic over time.

1.6 Degradation processes of cellulose nitrate artefacts

Cellulose nitrate has been known for some time, by manufacturers, to be intrinsically unstable [27]. Approximately two thirds of museums report some deterioration of the plastics [41], the most common being discolouration, cracking and embrittlement. The degradation processes are generally more complex in solid three dimensional objects, compared to cellulose nitrate films or lacquers [34]. The main causes of instability and deterioration for cellulose nitrate artefacts are the three primary degradation processes: thermal, hydrolytic and photochemical. The effect of the plasticiser is also important.

1.6.1 Thermal degradation

Cellulose nitrate is thermally unstable and at temperatures greater than 185 °C it will decompose violently, though when plasticised it will generally burn rapidly with no explosion [34]. At lower temperatures, including ambient, cellulose nitrate will undergo a slow degradation process whereby the nitrate groups split off from the

chain molecule to form nitrogen dioxide gas. This process is referred to as *denitration* and is exothermic and autocatalytic [22]. If the quantity of gases evolved is sufficiently low then the plastic will remain unaffected for a long time. If, however the evolution is high and the gases are unable to escape from the body of the plastic, rupturing of the object may occur.

The thermal degradation scheme outlined below as suggested by Phillips [42] and Miles [28] results in the production of aldehydes, ketones and alcohols at very high temperatures.

$$RCH_2ONO_2 \rightarrow RCH_2O^{\bullet} + {}^{\bullet}NO_2$$

$$RCH_2O^{\bullet} + RCH_2ONO_2 \rightarrow RCH_2OH + RC^{\bullet}HONO_2$$

$$RC^{\bullet}HONO_2 \rightarrow RCHO + {}^{\bullet}NO_2$$

1.6.2 Hydrolytic degradation

If nitrogenous gases, evolved during the denitration process, should come into contact with water and oxygen, then nitric acid will be formed [15]. This may occur on the surface of the plastic or even within its internal structure if water and oxygen are present. The nitric acid will cause further denitration, but also hydrolysis of the cellulose chain and destruction of the molecule. Degradation may result from acid or alkali hydrolysis. Acid hydrolysis is a slow process which results in the cleavage of the glucosidic links in the polymer molecule. Acids may be present in the cellulose nitrate from the manufacturing process or from external conditions. Sulphate ester groups, remaining from manufacture, may also slowly decompose and hydrolyse to acids. If this occurs then the rate of degradation is likely to be increased.

Alkaline hydrolysis results in the formation of a wide array of low molecular weight compounds. Inorganic nitrates, ammonia, carbon dioxide, oxalic acid, maleic acid and glycolic acid have all been reported as deterioration products [28].

1.6.3 Photochemical degradation

Exposure to light can cause severe degradation to cellulose nitrate. This is due to the ability of the molecule to absorb strongly in certain wavelengths, particularly the ultraviolet to far ultraviolet range (410-200 nm). One report suggests that short

wavelengths cause mainly viscosity and /or chain length changes in celluloid [43]. It also concludes that longer UV wavelengths cause a loss of nitrogen rather than a change in viscosity. Exposure to strong light results in yellowing of the cellulose nitrate followed by embrittlement [44]. Ultraviolet light may also decompose any light sensitive dyes and pigments causing discolouration and evolution of degradation products.

1.6.4 Plasticiser loss

During the manufacture of cellulose nitrate plastics, the amount of plasticiser added is typically 20-30% by weight. As there is such a large amount of a volatile compound present, the plasticiser will slowly volatilise out over time. Evidence for this volatilisation can be seen by the presence of surface crystalline deposits of camphor or oily droplets of phthalate plasticisers. Plasticiser loss will weaken the article causing distortion and embrittlement. Cracking may also occur which will in turn accelerate the loss of plasticiser and allow water and oxygen to penetrate the interior of the plastic, thus accelerating other degradation processes.

1.7 Recent work in this field

There has been a significant amount of research carried out on all aspects of cellulose nitrate degradation. The thermal decomposition of unplasticised cellulose nitrate has been studied by several workers. The kinetics of the thermal decomposition of cellulose nitrate has been studied by Phillips, Orlick and Steinberger [42]. Infrared spectroscopy and gravimetry were used to monitor the decomposition of thin cellulose nitrate films at temperatures greater than 140 °C. They concluded that decomposition involved a nitrate group loss with a carbonyl group growth over time. This seems to be in accordance with the previously mentioned mechanism of cellulose nitrate decomposition which involves the formation of aldehyde and ketones as a consequence of O-NO_2 fission. It was also found that the basic structure of the carbon skeleton does not change drastically during the decomposition.

In as similar study by Jutier *et al.* [45] the decomposition of cellulose nitrate films derived from wood and cotton was followed using fourier transform infrared (FTIR) spectroscopy. At 225 °C they noted the formation of carbonyl groups, in particular

formaldehyde, which indicated that some ring cleavage had occurred. They, however, suggest that even at these high temperatures there was little, if any, scission of the
C_1-O-C_4 bridge.

This is in agreement with work carried out by Wolfrom *et al.* [46]. They described the solid residue of the thermal degradation of a cellulose nitrate propellant as consisting of a central core of essentially unaltered anhydro-D-glucose units flanked at one or both ends by altered units.

Unfortunately all work examining the thermal decomposition is not directly relevant to the preservation of museum artefacts as the studies have been carried out at very high temperatures and have involved unplasticised cellulose nitrate.

Research on the photochemical degradation also provides some knowledge of deterioration mechanisms. Hon and Tang [47] studied the behaviour of cellulose nitrate lacquers in air. They found that films and solutions of the lacquers were oxidisable in air leading to the production of hydroperoxide and a reduction in the nitrogen content by 1%, and a reduction in the molecular weight by up to 10%. Ferric ions, phenol and lignin (inherent elements in wood derived cellulose nitrate) were seen to cause an increase in the degradation.

As cellulose nitrate has several applications, other than 3-dimensional plastic articles, research in these areas can provide further helpful information. The degradation of cellulose nitrate films and adhesives may offer clues to how the polymer should be stored and treated.

Edge *et al.* [48] examined a number of cellulose nitrate based cinematographic film by FTIR, ultraviolet/visible spectroscopy and viscometry. Their results indicated that films which appeared visually degraded had undergone extensive denitration and suggested that cellulosic backbone scission and ring disintegration had occurred. Archival films stored in iron cans showed greater deterioration and the iron is presumed to catalyse the degradation. They also proposed the incorporation of a stabiliser, comprising a metal deactivator and a hydroperoxide decomposer, to decelerate the degradation.

Another study of cellulose nitrate photographic film base was carried out by Louvet [49], using FTIR spectroscopy and gel permeation chromatography (GPC). His work reported that chain scission occurs before the formation of carbonyl groups and therefore a decrease in molecular weight is a primary indication of degradation. Louvet also studied the degradation products from plasticisers used with cellulose nitrate film and concluded that no degradation products are associated with camphor.

Koob [44] examined the properties and behaviour of several cellulose nitrate adhesives. He found that adhesives exposed to ultraviolet light yellowed after only eight hours and became brown and brittle after sixteen hours. He also reported that many adhesives had acid impurities remaining after manufacture. He demonstrated that the presence of acid impurities in cellulose nitrate were a source of instability as they lowered the explosion temperature of the polymer.

Shashoua, Bradley and Daniels [50] used artificial ageing experiments to study the degradation of cellulose nitrate adhesives. The effects of ageing were evaluated using FTIR spectroscopy to monitor chemical change and viscosity measurements to monitor changes in molecular weight. Their ageing experiments demonstrated that comparisons could be drawn between artificially and naturally aged cellulose nitrate adhesives.

However, plastic objects differ in size, shape, use, manufacture and composition to these materials and these factors must be considered. This inevitably makes evaluation of conservation strategies very complex. Firstly, many of the artefacts of interest were made between 50 and 150 years ago (often precise dates are not known). Therefore little is known about the exact manufacturing processes or how pure the materials used to produce the plastics were. The manufacturer's expected lifetime of the object is likely to be considerably less than the indefinite one expected by a museum or collection. It may be no fault of the object's manufacture that it is deteriorating after a period of time but simply an inherent factor of cellulose nitrate. Finally, due to the age of many of the plastic artefacts, it is usually difficult to find a comprehensive history of their age, use and exposure to certain environmental conditions. Objects may have suffered thermal and photochemical degradation prior to being added to a collections, which makes diagnosing causes of deterioration more difficult.

As well as cellulose nitrate, other polymers are susceptible to degradation, and recent research concerning these may suggest suitable ways of assessing, storing and treating collections. Cellulose acetate film has been the subject of much work, looking at ways of preventing degradation of this common photographic film.
Edge *et al.* [51] assessed a number of destructive and non-destructive physical and chemical methods of analysis for predicting the stability of cellulose triacetate based cinematographic film. Films aged naturally and artificially were examined using thermal analysis, absorption, fluorescence and nuclear magnetic resonance spectroscopic methods.

Similar studies were performed by Shinagowa, Murayama and Sakaino [52]. They again compared artificially and naturally aged cellulose acetate films, monitored using viscometry and GPC. They also used ageing experiments to investigate the effect of various additives on the stability of the polymer base.

The degradation of more modern materials, such as polyvinylchloride, in museum collections has been recently investigated by Shashoua and Ward [53]. Artificial ageing experiments were used to investigate the effectiveness of various inhibitors for the degradation of PVC. Zeolite and epoxidised soya bean oil were found to be useful conservation treatments.

Only recently have conservators come to realise that cellulose nitrate artefacts have their own intrinsic problems. Many museum and private collections have been surveyed and the extent of degradation assessed. Methods for evaluating degradation and suitable treatment and storage conditions have been proposed.

Derrick and Stulik [54] studied the processes of degradation occurring in cellulose nitrate sculptures. FTIR microscopy was used to assess the extent of degradation by monitoring changes in the nitrate group absorbance. X-ray diffraction and scanning electron microscopy were used to identify and quantify additives in the polymer. They concluded that the various states of degradation in the artefacts related to three factors; past storage and display conditions, composition of additives and impurities within the artefacts and the physical construction of the object.

Recent work by Hamrang [25] has investigated the relative rates of degradation of cellulose nitrate and cellulose acetate. The esters were subjected to various temperatures and relative humidities in the presence and absence of light. His results

demonstrated that the rate of degradation depended primarily on humidity. The role of plasticisers in the degradation was also examined. Camphor was found to exude from cellulose nitrate during degradation while phthalate plasticisers were found to be decomposed during the process.
Derrick, Daniels and Parker [55] have investigated and evaluated the comparative effects of temperature, relative humidity, oxygen and ultraviolet light on the condition of cellulose nitrate samples. Samples were placed in the various environments and changes monitored using FTIR spectroscopy and elemental analysis.

1.8 Aims of Work

Although there has been much research concerning cellulose nitrate plastics, as outlined in 1.7, there has been little tackling some of the more underlying questions concerning the artefacts.

As the result of a survey into the plastic collections of the National Museums of Scotland [56], this research project was initiated. The aim of the project was to offer fundamental scientific research into the composition and degradation of cellulose nitrate materials and to allow correct strategies to be developed for their preservation.

The study is divided into several parts.

1. To assess a select group of objects exhibiting signs of deterioration. To examine this degradation and its effects on the artefacts in detail so that the degradation processes occurring can be understood.

2. To identify the composition of the artefacts: plasticisers, fillers, colorants, other additives and any impurities. To determine the effect of these constituents on the degradation.

3. To examine other factors which may relate to the degradation of the plastics e.g. storage and treatment conditions.

4. To develop strategies for the conservation of these cellulose nitrate artefacts.

References

1. Williamson, C. in *"Polymers in Conservation"*, Allen, N. S., Edge, M. and Horie, C. V., (eds.), The Royal Society of Chemistry, Cambridge, 1992, 1-13.

2. Shashoua, Y., in *"Conservation Science in The U.K."*, Tennent, N. H., (ed.), James and James Science Publishers Ltd., London, 1993, 44-47.

3. Morgan, J., *"Conservation of Plastics, an Introduction"*, Museums and Galleries Commission, London, 1991.

4. Blank, S., *Studies in Conservation*, 1990, **35**, 53-65.

5. Friedel, R., *"Pioneer Plastic: The Making and Selling of Celluloid"*, The University of Wisconsin Press, U.S.A, 1983.

6. Kaufman, M., *"The First Century of Plastics"*, The Plastics Institute, London,
1963.

7. Dubois, J. H. and John, F. W., *"Plastics"*, Van Norstrand Reinhold Co., New York, 1974.

8. Morris, P. J. T., *"Polymer Pioneers"*, Centre for the History of Chemistry Publications, Philadelphia, 1986.

9. Katz, S., *"Plastics: Designs and Materials"*, MacMilan Publishing Co. Inc., New York, 1978.

10. Newman, T. M., *"Plastics as an Art Form"*, Pitman, London, 2nd edn., 1969.

11. *"Plastic Antiques"*, British Industrial Plastics Ltd., London, 1947.

12. Briston, J. H., *"Plastic Films"*, Longman, London, 3rd edn., 1989.

13. Daniels, R. G., *"Nitrocellulose Lacquer Manufacture"*, Leonard Hill Ltd., London, 1933.

14. Sproxton, F., *"Cellulose Ester Varnishes"*, Ernest Benn Ltd., London, 1933.

15. Barsha, S., in *"Cellulose and Cellulose Derivatives, vol. 3"*, Ott, E., (ed.), Interscience Publishers Inc., New York, 2nd edn., 1954.

16. Quinchon, J. and Tranchant, J., *"Nitrocelluloses"*, Ellis Horwood, London, 1989.

17. Elias, H. G., *"An Introduction to Plastics"*, VCH Publisher Inc., New York, 1993.

18. Corbett, W. M., in *"Methods in Carbohydrate Chemistry, vol. 3"*, Whistler, R. L., (ed.), Academic Press, London, 1963, 27-29.

19. Guthrie, R. D. and Honeyman, J., *"An Introduction to the Chemistry of Carbohydrates"*, Clarendon Press, Oxford, 1964.

20. Aspinall, G. D., *"Polysaccharides"*, Permagon Press Ltd., Oxford, 1970.

21. Wilton, A., *"The Physical and Dynamic Characterisation of Heterogeneously Acetylated Cellulose and its Interaction with Dibutylphthalate Plasticiser"*, Ph.D. Thesis, University of Strathclyde, 1992.

22. Yarsley, V. E., Flavell, W., Adamson, P. S. and Perkins, N. C., *"Cellulosic Plastics"*, Illiffe Books Ltd., London, 1964.

23. Preston, C., *"The Dyeing of Cellulosic Fibres"*, Eastern Press Ltd., London, 1986.

24. DeBussy, J. H., *"Materials and Technology, vol. 6"*, Longman, London, 1973.

25. Hamrang, A., *"Degradation and Stabilisation of Cellulose Based Plastics and Artifacts"*, Ph.D. Thesis, Manchester Metropolitan University, 1994.

26. Mascia, L., *"The Role of Additives in Plastics"*, Edward Arnold, London, 1974.

27. Worden, E. C., *"Nitrocellulose Industry"*, Constable, London, 1911.

28. Miles, F. D., *"Cellulose Nitrate"*, Oliver and Boyd, London, 1955.

29. Yin, T. P. and Brown, R. K., *Canadian Journal of Chemistry*, 1959, **37**, 444-453.

30. Green, J. W. in *"Methods in Carbohydrate Chemistry, vol. 3"*, Whistler, R. L., (ed.), Academic Press, London, 1963, 213-235.

31. Quye, A., *Chemistry in Britain*, 1995, **8**, 617-620.

32. Process Description - Nitrocellulose, produced by Royal Ordnance, Bishopton, 1994.

33. Buttrey, D. M., *"Cellulose Plastics"*, Cleaver-Hume Press Ltd., London, 1947.

34. Sirkis, L., *"The History, Deterioration and Conservation of Cellulose Nitrate and Other Early Plastic Objects"*, M.Sc. Thesis, Institute of Archaeology, London, 1982.

35. Sears, J. K. and Darby, J. R., *"The Technology of Plasticisers"*, John Wiley and Sons, New York., 1982.

36. Williams, R. S., in *"Saving the 20th Century"*, Grattan, D. W., (ed.), Canadian Conservation Institute, Ottawa, 1993, 135-152.

37. Ahmed, M., *"Colouring of Plastics: Theory and Practice"*, Van Norstrand Reinhold, New York, 1979.

38. Simpson, W. G., *"Plastics: Surface and Finish"*, The Royal Society of Chemistry, Cambridge, 2nd edn., 1993.

39. *"Modern Plastics Encyclopaedia, vol. 1"*, Plastics Catalogue Corporation, London, 1947, 64-66.

40. Brydson, J. A., *"Plastics"*, HMSO Publications, London, 1991.

41. Morgan, J. in *"Saving the 20th Century"*, Grattan, D. W., (ed.), Canadian Conservation Institute, Ottawa, 1993, 43-50.

42. Phillips, R. W., *Journal of Physical Chemistry*, 1955, **59**, 1034-1039.

43. Reilly, J. A., *Journal of the American Institute of Conservation*, 1991, **30**, 145-162.

44. Koob, S. P., *The Conservator*, 1982, **6**, 31-34.

45. Jutier, J. J., Harrison, Y., Premont, S. and Prud'homme, R. E., *Journal of Applied Polymer Science, 1987, 33, 1359-1375.*

46. Wolfrom, M. L., *Journal of the American Chemical Society*, 1955, **77**, 6573-6580.

47. Hon, D. N. S., and Tang, L., *Polymer Photochemistry*, 1986, **7**, 299-310.

48. Edge, M., Allen, N. S., Hayes, M., Riley, P. N. K., Horie, C. V. and Luc-Gardette, J., *European Polymer Journal*, 1990, **26**, 623-630.

49. Louvet, A., *"Study of the Degradation of Cellulose Nitrate Photographic Base"*, Ph.D. Thesis, Centres de Reserches sur la Conservation des Documents Graphiques, Paris, 1994.

50. Shashoua, Y., Bradley, S. M. and Daniels, V. D., *Studies in Conservation*, 1992, **37**, 113-119.

51. Edge, M., Allen, N. S., Williams, D. A. R., Thompson, F. and Horie, C.V., *Polymer Degradation and Stability*, 1992, **35**, 147-155.

52. Shinagowa, Y., Muryama, M. and Sakaino, Y., in *"Polymers in Conservation"*, Allen, N. S., Edge, M. and Horie, C. V., (eds.), The Royal Society of Chemistry, Cambridge, 1992, 68-74.

53. Shashoua, Y. and Ward, C., in *"Resins: Ancient and Modern"*, Wright, M. N. and Townsend, J. H., (eds.), The Scottish Society for Conservation and Restoration, Edinburgh, 1995, 33-37.

54. Derrick, M. and Stulik, D., in *"Saving the 20th Century"*, Grattan, D. W., (ed.), Canadian Conservation Institute, Ottawa, 1993, 169-182.

55. Derrick, M., Daniel, V. and Parker, A., in *"Preventive Conservation: Practice, Theory and Research"*, Roy, A. and Smith, P., (eds.), IIC, London, 1994, 207-211.

56. Quye, A., in *"Conservation Science in The U.K."*, Tennent, N. H., (ed.), James and James Science Publishers Ltd., London, 1993, 48.

CHAPTER TWO

ANALYTICAL TECHNIQUES

Chapter Two - Contents

2.1 Infrared spectroscopy [1-4]

2.1.1 Principles of infrared spectroscopy

The infrared region of the electromagnetic spectrum extends from the red end of the visible spectrum to the microwave region. The wavelengths of infrared radiation fall in the range 0.1 to 500 μm . For infrared spectroscopic applications, the mid infrared region from 4000 to 200 cm^{-1} is generally used.

Molecules absorb radiation when some part of the molecule vibrates at the same frequency as the incident radiation energy. The vibrating molecule must also have an alternating electric field, i.e. it must be coupled with a changing dipole moment. The atoms comprising a molecule can vibrate in several ways. Infrared spectrometry involves examination of the twisting, bending and rotational motions in a molecule. The rate at which these component atoms vibrate is quantised and can only take place at well defined frequencies. As there is a wide range of vibrations occurring simultaneously, a highly complex absorption spectrum that is uniquely characteristic of a molecule is produced. The possible vibrational modes in a polyatomic molecule, acetaldehyde, can be visualised from a mechanical model shown in Figure 2.1.

The infrared spectrum of a compound is therefore the superposition of absorption bands of specific functional groups which interact with the surrounding atoms of the molecule.

2.1.2 Fourier transform infrared (FTIR) spectroscopy

The goal of IR spectroscopic applications is to determine the chemical functional groups contained in a particular material. Each functional group absorbs characteristic frequencies of infrared radiation uniquely. Thus, a plot of radiation intensity versus frequency (the infrared spectrum) fingerprints the identifiable chemical groups in the sample.

The FTIR spectrometer consists of three basic components:

a) a source
b) a Michelson interferometer
c) a detector.

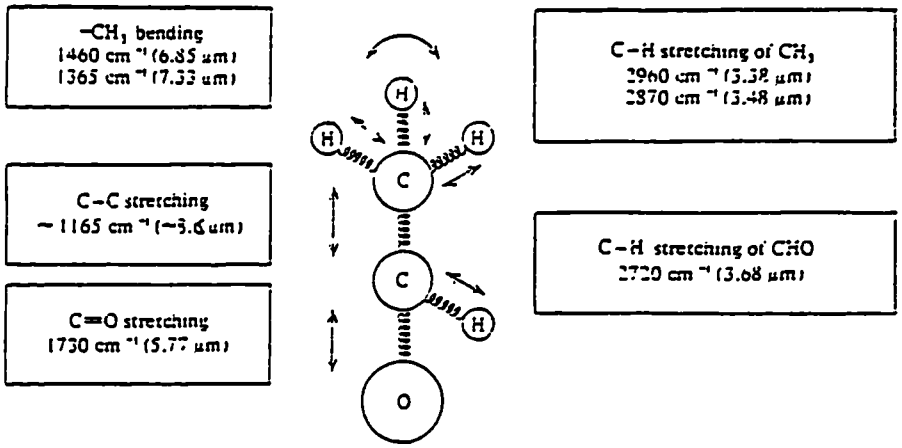

Figure 2.1 **Vibrations and characteristic frequencies of acetaldehyde [1]**

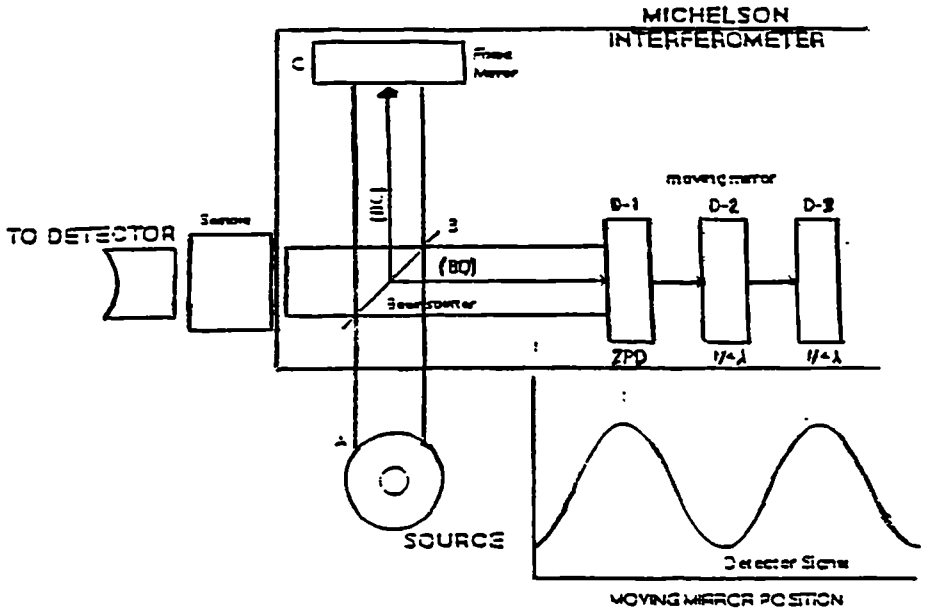

Figure 2.2 **Fourier transform infrared spectrometer [2]**

The Michelson interferometer consists of a beamsplitter, a fixed mirror and a moving mirror. Figure 2.2 shows a simplified diagram of the FTIR spectrometer.

Collimated radiation from the broadband infrared source, A, is directed into the interferometer and impinges on the beamsplitter, B (e.g. a very thin film of germanium). The beamsplitter splits the incoming beam into two beams of equal energy. Approximately 50% of the light is transmitted through the film and is directed onto the moving mirror, D. The beams reflect off the surfaces of the two mirrors and recombine at the beamsplitter. Here constructive and destructive interference occurs, depending on the position of the moving mirror relative to the fixed mirror. The resulting beam passes through the sample where selective absorption takes place, and then continues on to the detector.

When the position of the moving mirror, D, is such that the distance between the beamsplitter and the mirror, BD, is exactly the same as the distance between the beamsplitter and the fixed mirror, BC, the two reflected beams pass through exactly the same path length and consequently, are totally in phase with each other. As a result, the two beams interfere constructively and the detector observes a maximum signal intensity. The position of the moving mirror is called the Zero Path Difference, or ZPD.

As the mirror moves away from the ZPD, the distance BD increases relative to the fixed distance BC. When the distance between the beamsplitter and the moving mirror, BD, is ¼ of the wavelength of light being observed longer than BC, the total optical path (beamsplitter-mirror-beamsplitter) difference between the two beams is ½ wavelength. The two beams are now 180 degrees out of phase with each other and, at this point in the scan, interfere with each other destructively, causing a minimum in the detector response. With each ¼ wavelength displacement, this pattern of constructive and destructive interference repeats itself. Since data sampling occurs continuously, a cosine wave results.

The detector signal is sampled at precise intervals during the mirror scan. Both the sampling rate and the mirror velocity are controlled by a reference signal which is produced by modulation of the beam from the helium-neon laser. The resulting signal is known as an interferogram and contains all the information required to reconstruct the spectrum via the mathematical process known as the Fourier transformation.

Figure 2.3 shows a schematic diagram of an FTIR microscope. Most IR microscopes are based on conventional optical microscopes but with the addition of a high quality reflection (Cassegrainian) objective capable of imaging both the IR beam and an optical source. The transfer optics bring the IR beam from the interferometer to a sensitive detector (usually MCT).

The measured area of the sample must be strictly delimited so that the IR beam is only focused on the area of interest. The limit on sample size that can be analysed by FTIR microspectroscopy is essentially that of the diffraction of IR radiation. As the size of the sample approaches the radiation wavelength, some of the IR energy is bent around the defined area. This results in a blurring of the image and the detector receiving spectral information from outside the area of interest.

As well as the analysis of small samples, microscope attachments present other advantages. Relatively simple sample preparation is needed, the sample needs only to be crushed or microtomed so that the thickness is around 25-30 μm, then placed on the microscope stage. The surface of a sample can also be scanned using eyepieces so that specific areas can be analysed.

2.1.4 Diffuse reflectance fourier transform infrared spectroscopy (DRIFTS) [7-8]

For materials which are opaque, IR transmittance techniques are not applicable and a reflectance method must be used. When a beam of IR radiation hits the surface of a sample, the radiation reflected consists of a regular or specular reflection component occurring at the surface and a diffuse reflection component that has penetrated the sample before reappearing at the surface. DRIFTS is the study of this diffusely scattered component and the elimination or minimisation of specular reflection is important in the design of instruments.
The optics of a typical DRIFTS collector (SpectraTech) are shown in Figure 2.4. The accessory fits into the sample compartment of the FTIR spectrometer and the total reflectance is measured (both the specularly reflected and the diffuse reflectance components). In the SpectraTech design a post can be introduced which prevents the specularly reflected component from reaching the detector. Other instruments eliminate this component by rotating the plane of the mirrors or the sample cup.

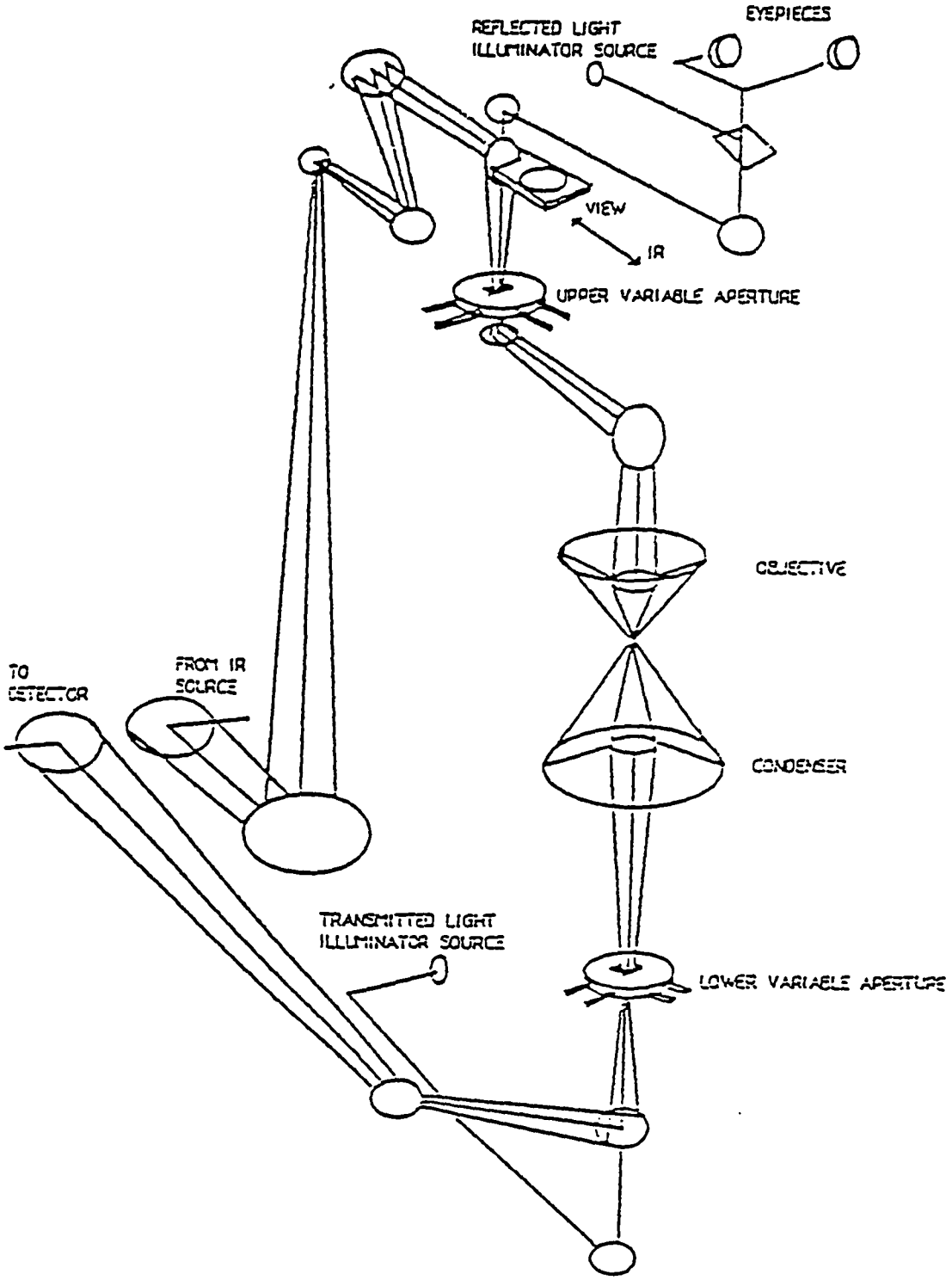

Figure 2.3 FTIR microscope [6]

reflection (Cassegrainian) objective, capable of imaging both the IR beam and an optical source. The transfer optics bring the IR beam from the interferometer to a sensitive detector (usually MCT).

The measured area of the sample must be strictly delimited so that the IR beam is only focused on the area of interest. The limit on sample size that can be analysed by FTIR microspectroscopy is essentially that of the diffraction of IR radiation. As the size of the sample approaches the radiation wavelength, some of the IR energy is bent around the defined area. This results in a blurring of the image and the detector receiving spectral information from outside the area of interest.

As well as the analysis of small samples, microscope attachments present other advantages. Relatively simple sample preparation is needed, the sample needs only to be crushed or microtomed so that the thickness is around 25-30 μm, then placed on the microscope stage. The surface of a sample can also be scanned using eyepieces so that specific areas can be analysed.

2.1.4 Diffuse reflectance infrared spectroscopy (DRIFTS) [7-8]

For materials which are opaque, IR transmittance techniques are not applicable and a reflectance method must be used. When a beam of IR radiation hits the surface of a sample, the radiation reflected consists of a regular or specular reflection component occurring at the surface and a diffuse reflection component that has penetrated the sample before reappearing at the surface. DRIFTS is the study of this diffusely scattered component and the elimination or minimisation of specular reflection is important in the design of instruments.

The optics of a typical DRIFTS collector (SpectraTech) are shown in Figure 2.4. The accessory fits into the sample compartment of the FTIR spectrometer and the total reflectance is measured (both the specularly reflected and the diffuse reflectance components). In the SpectraTech design a post can be introduced which prevents the specularly reflected component from reaching the detector. Other instruments eliminate this component by rotating the plane of the mirrors or the sample cup.
The sensitivity of the diffuse reflectance technique has improved in recent years due to the high energy throughput and signal to noise ratio of modern FTIR spectrometers.

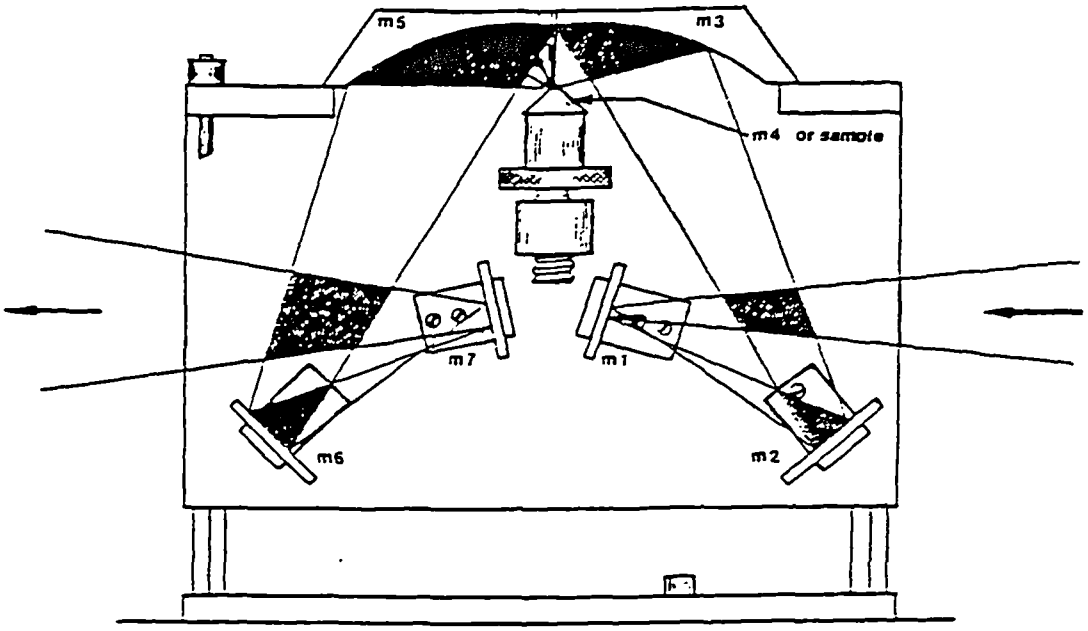

Figure 2.4 DRIFTS collector [2]

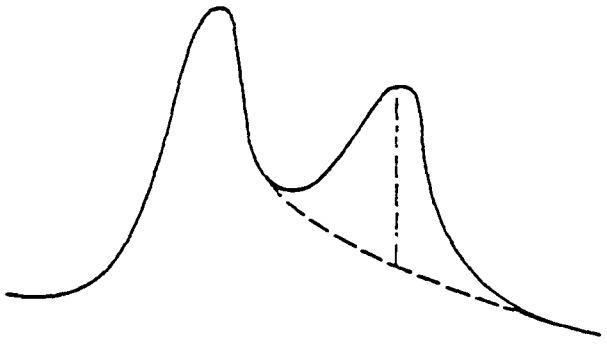

Figure 2.5 Baseline correction [1]

It is commonly used for the analysis of powders and small quantities of organic material deposited on surfaces.

2.1.5 Data processing

The initial data from the FTIR output is in the form of a single beam spectrum. In order to obtain the standard transmittance spectrum for the sample, this single beam spectrum is ratioed against a background spectrum. The background is usually a single beam spectrum collected with no sample in the holder.

Transmittance is defined as:

$$T = \left(\frac{I_s}{I_o}\right)_\upsilon \qquad \text{..... (2.1)}$$

where I_S is the instrument response function (single-beam spectrum) with the sample,
I_0 is the instrument response function without the sample, and
υ is frequency

If the instrument response is identical with and without the sample, the transmittance value will be one. If the sample absorbs light, less energy reaches the detector and the transmittance value is less than one. If the sample is totally absorbing, no energy passes to the detector and the transmittance value is zero. Most systems multiply the transmittance value by 100, defining *percentage transmittance*.

For quantitative analysis it is necessary to convert from a percentage transmittance spectrum to absorbance, where the Beer-Lambert law (2.2) states that a linear relationship exists between the measured absorbance (A) and the concentration of a sample.

$$A = \log_{10}\left(\frac{1}{T}\right) = abc \qquad \text{..... (2.2)}$$

where a is the absorptivity of the sample,
b is the internal path length of the sample cell, and
c is the concentration of the sample.

As a and b are constant, A is proportional to c.

When a compound has a strong, well-defined absorption band, the magnitude of the absorbance of the peak can be calculated. By comparison with the absorbance of a standard or series of standards of known concentration, it is possible to calculate the unknown concentration of the compound under investigation.

Often with IR spectroscopy it is not desirable to create a calibration curve from known standards, internal or external, as high errors are introduced. Quantitative analysis can be improved by establishing the blank or background absorbance in the vicinity of the band of interest and constructing a baseline for all samples (see Figure 2.5). The baseline absorbance is measured at the point where a perpendicular line from the peak maximum intersects the baseline. This absorbance is subtracted from the peak absorbance. Using the baseline correction method, all measurements are made at points defined by the spectrum itself, i.e. there is no dependence on wavelength. Changes in the instrument sensitivity or optical set-up are also eliminated.

The most general theory relating to diffuse reflection is that developed by Kubelka and Munk. For an infinitely thick opaque specimen, the Kubelka-Munk equation is

$$\frac{(1-R_\infty)^2}{2R_\infty} = \frac{K}{s} \qquad \text{..... (2.3)}$$

where K is an absorption coefficient
s is a scattering coefficient, and
R_∞ is the diffuse reflectance from an infinitely thick sample.

The factor $(1 - R_\infty)^2 / 2R_\infty$ is defined as the Kubelka-Munk unit, and spectra collected are expressed in these units. In theory the spectra should be linear with concentration, but this is rarely achieved in practice and DRIFTS is generally only useful over a limited range.

2.2 Ion chromatography (IC) [9-12]

2.2.1 General principles of ion chromatography

Ion chromatography is a term used to describe the analysis of dissolved ions by ion-exchange chromatography, using HPLC equipment. The technique therefore follows the principles of ion exchange chromatography. Separation of ionic materials is achieved by passage of a solution through a column consisting of an ion exchanger or stationary phase. This stationary phase consists of a porous resinous material containing fixed charge bearing functional groups and oppositely charged mobile counterions. Transport of analytes through the column is performed by an eluent. The analytes are separated due to variation in affinity for the stationary phase, with components of lowest affinity eluted first.

The primary process of ion-exchange chromatography involves interaction of charged ionic materials in the sample, in the mobile phase, with permanently charged counter ions on the stationary phase. This interaction between the sample and the stationary phase is an equilibrium process. For example, the exchange between a resin initially with acidic hydrogen attached and a solution containing K^+ ions, can be written as.

$$\text{Resin}-H^+ \;+\; K^+ \;\Leftrightarrow\; \text{Resin}-K^+ \;+\; H^+$$

If the affinity of the resin for K^+ is greater than for H^+ then an exchange will take place.

The equilibrium constant or selectivity coefficient $K_{k/H}$ can also be determined.

$$K_{K/H} = \frac{[K^+]_R \; [H^+]}{[H^+]_R \; [K^+]} \qquad \text{..... (2.4)}$$

where $[K^+]_R$ and $[H^+]_R$ are the equilibrium concentrations of the ions within the resin structure and $[K^+]$ and $[H^+]$ are the equilibrium concentrations in the mobile phase.

The greater the affinity for a particular ion relative to hydrogen, the greater the value of K. In the above example, if $K_{K/H} < 1$ then H^+ has a greater affinity for the

stationary phase than K^+. The affinity of ions for the stationary phase determines the retention of the analytes and is governed by the physical properties of the ions. The stationary phase has a greater affinity for and hence, the retention will be longer for:

a) the ion with higher charge,

b) the ion with the smaller ionic radii in the hydrated state,

c) the ion with the greater polarisability.

The partitioning of each ion between the stationary and mobile phase can be defined by the concentration distribution ratio, D_C.

$$(D_C)_K = \frac{[K^+]_R}{[K^+]} \qquad \text{..... (2.5)}$$

by combining equations 2.4 and 2.5 we get

$$(D_C)_K = K_{K/H} \frac{[H^+]_R}{[H^+]} \qquad \text{..... (2.6)}$$

The larger the value of D_C, the slower the progress of the solute through the system and hence, analytes in a solution will elute from the column in order of increasing values of D_C.

Figure 2.6 shows a typical chromatogram for a solution containing three components and the parameters used to characterise the peaks.

A number of other quantitative measurements can be made to describe the quality of a chromatographic separation. As well as being able to state where on chromatograms solute peaks are eluted, it is necessary to determine whether or not they are separated from one another and if so, how efficiently.

Selectivity

Although a peak in a chromatogram can be identified by its retention time, this varies with column length and mobile phase flow rate. Peaks are commonly identified using the capacity factor, k′ which is directly proportional to D_C but takes account the volume of each phase. For component A in Figure 2.6,

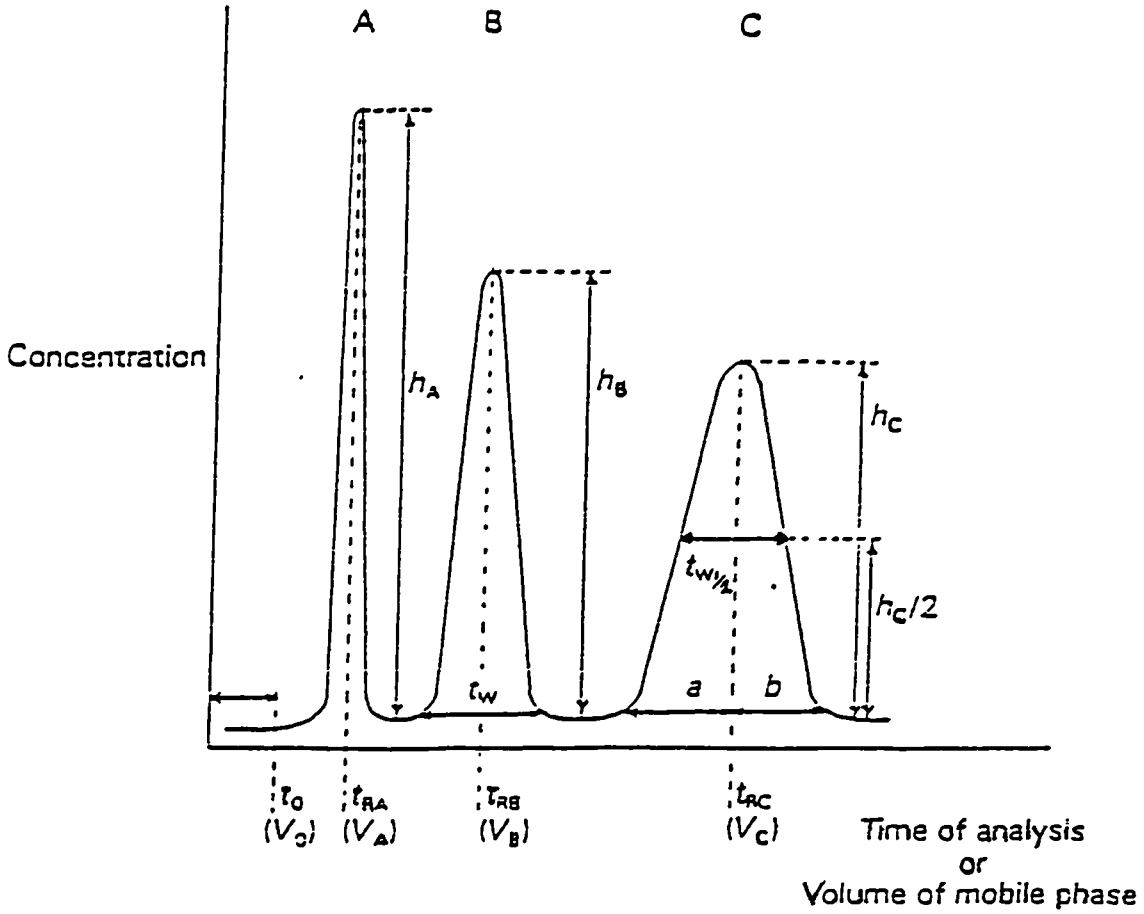

Figure 2.6 Chromatographic separation [1]

t_0 = time for the solvent or mobile phase to pass through the system

t_{RA} = retention time of component A, that is the time for A to pass through the system; V_A is the retention volume

t_{RB} = retention time of B, V_B = retention volume

t_{RC} = retention time of C, V_C = retention volume

h = peak height, h_A for component A, h_B for B, h_C for C

t_w = width at the base of peak

$t_{w1/2}$ = width of a peak at half height

$$k'_A = \frac{t_{RA} - t_o}{t_o} = \frac{V_A - V_o}{V_o} \quad \text{..... (2.7)}$$

If k' = 0, then the solute is eluted without being retarded by the stationary phase. To achieve separation of analytes during chromatography it is necessary that they are taken up by the resin in distinct preferences.

Selectivity describes the separation of two peaks relative to each other in a chromatogram and is defined by the selectivity or separation factor.

$$\alpha_{A/B} = \frac{k'_B}{k'_A} = \frac{(D_C)_B}{(D_C)_A} \quad \text{..... (2.8)}$$

Resolution

The resolution, R_S, is a measure of the degree to which peaks in a chromatogram are resolved or separated. R_S for component A in Figure 2.6, relative to B, is defined by the equation

$$R_S = \frac{t_{RB} - t_{RA}}{0.5(t_{WA} + t_{WB})} \quad \text{..... (2.9)}$$

For peaks to be completely resolved at the baseline, a value of $R_S \geq 1.5$ is required. If the resolution is significantly greater than 1.5, the longer elution time would be undesirable, and in practice a compromise is obtained.

Efficiency

The narrowness of a peak is a measure of the efficiency of a chromatographic column. To separate the components, it is necessary that they do not spread out in the column and overlap one another. Efficiency of a chromatographic column is expressed by the number of theoretical plates, N. The total number for a column is calculated using one of the alternative forms.

$$N = 16\left(\frac{V}{t_o}\right)^2 \quad \text{..... (2.10)}$$

$$\text{or} \qquad N = 5.54\left(\frac{V}{t_{w\frac{1}{2}}}\right)^2 \qquad \text{..... (2.11)}$$

Where $t_{w½}$ is the width of the peak at half height.

Generally the efficiency of a column increases as the particle size of the resin decreases. In practice, values of N >1000 are desired.

For a good separation of components in a mixture, three conditions have to be met:

a) the peaks must be retained on the column ($k'>0$),

b) the peaks must be separated from one another ($\alpha>1$),

c) the column must have a minimum number of theoretical plates.

2.2.2 The ion chromatograph

Throughout the course of this research, Dionex ion chromatographs were employed. The following description concerning the operation of the ion chromatograph, is therefore specific to Dionex instrumentation.

Ion chromatography incorporates HPLC equipment although the nature of the exchange resin and the method of detection differ. The system is basically a two column set up as shown in Figure 2.7. The system has four modes: delivery, separation, detection and data collection.

Delivery mode

At this stage the sample is injected at the head of the analytical column where it mixes with the eluent from the reservoir. The eluent used must have an affinity with the sample ion for the stationary phase. It must also provide a low background conductivity to allow sensitive detection of the sample ions, ideally down to the µg/L range. Eluents used for anion analysis will commonly contain borate, bicarbonate, hydroxide or salicylate. HCl is the usual eluent for cation analysis although newer columns use methane sulphonic acid.

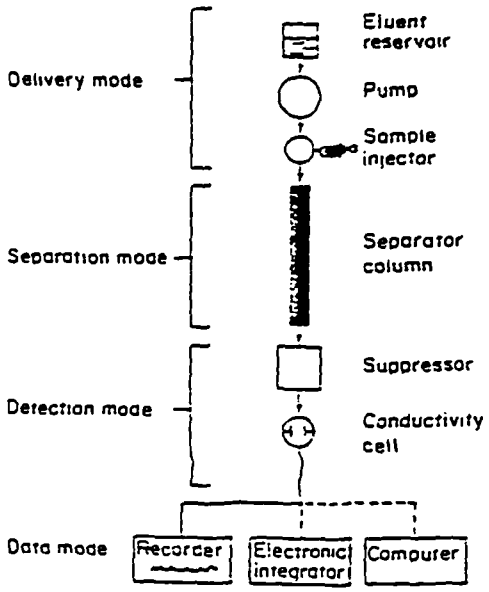

Figure 2.7 Schematic diagram of ion chromatograph [9]

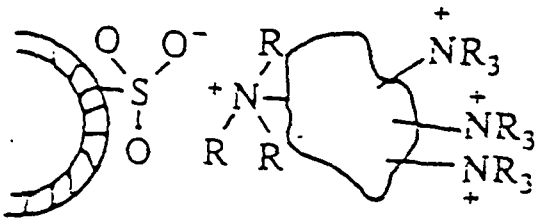

Figure 2.8 Structure of stationary phase [1]

Separation mode

Chromatographic columns used in IC contain an inert resinous support, prepared by polymerising styrene and divinylbenzene. The copolymerisation of PS/DVB contains significant crosslinking, which makes the resin more mechanically stable.

In anion exchange columns , the resin core is sulphonated to provide an intermediate layer. In addition a thin layer of latex particles are incorporated around this core which are usually aminated. These particles provide the groups necessary for anion exchange. Figure 2.8 shows the structure of the ion-exchange packing.

The exchange of Y^- ions in a sodium hydroxide eluent will be as follows.

$$\text{Resin}-NR_3^+OH^- + Y^- \rightarrow \text{Resin}-NR_3^+Y^- + OH^-$$
$$Y^- + Na^+ \rightarrow Na^+Y^-$$

The eluent converts the anions to dissolved sodium salts.

In traditional cation exchange chromatography, the column matrix is based on a PS / DVB core which is again surface sulphonated. Unlike anion exchange columns, however, there are no latex particles. With modern analytical columns, the stationary phase is a polyethylvinylbenzene / divinylbenzene resin, functionalised with carboxylic acid.

The exchange of X^+ ions in a HCl eluent will be as follows.

$$\text{Resin}-SO_3^-H^+ + X^+ \rightarrow \text{Resin}-SO_3^-X^+ + H^+$$
$$X^+ + Cl^- \rightarrow X^+Cl^-$$

The separation mode of the ion chromatograph may also consist of a guard column. This is a smaller version of the analytical column used for anion or cation exchange. It is placed before the main analytical column to remove possible contaminants in the solution

Detection mode

The eluents used in ion chromatographic separations have a high conductivity. As conductivity detectors are generally used for measuring ions in solution, the sensitivity is greatly reduced due to the low signal to noise ratio. The use of chemical suppression with ion chromatography greatly enhances signal to noise ratios by: 1)

decreasing the background eluent conductivity and 2) increasing the analyte conductivity. Two types of suppressor devices are used, the micromembrane suppressor and the self-regenerating suppressor.

In anion ion chromatography, analytes elute from the analytical column with their sodium counterions and enter the suppressor. The micromembrane suppressor consists of two cation exchange membranes, containing fixed sulphonic acid groups, through which the eluent flows. On the other side of the membranes there are sulphuric acid regenerant chambers. There is a flow of positive ions through the membrane which results in the eluent being neutralised and the conductivity of the analytes being enhanced.

eluent: $Na^+HCO_3^- + RSO_3^-H^+ \rightarrow RSO_3^-Na^+ + CO_2 + H_2O$

analyte: $RSO_3^-H^+ + Na^+Y^- \rightarrow RSO_3^-Na^- + H^+Y^-$

regenerent: $RSO_3^-Na^+ + H^+{}_2SO_4^- \rightarrow RSO_3^-H^+ + Na^-HSO_4^-$

In cation ion chromatography the suppressor membranes are anion exchange plates and tetrabutylammonium hydroxide is used as the external regenerant. The regenerant provides hydroxide ions which pass into the eluent chamber as anions pass out.

eluent: $RNR_3^+OH^- + H^+Cl^- \rightarrow RNR_3^+Cl^- + H_2O$

analyte: $RNR_3^+OH^- + X^+Cl^- \rightarrow RNR_3^+Cl^- + XOH$

regenerant: $RNR_3^+Cl^- + TBA^+OH^- \rightarrow RNR_3^+OH^- + TBA^+Cl^-$

In recent years, a new type of suppressor has been introduced, the self-regenerating suppressor (SRS). The SRS consists of alternating layers of high capacity ion exchange membranes separating a cathode and anode. The screens create a low volume flow path for the eluent and provide an ion transport path for the ion exchange process.

Two versions of the SRS are available - the anion self-regenerating suppressor (ASRS) for the determination of anions, and the cation self-regenerating suppressor (CSRS) for the determination of cations (see Figure 2.9).

The water regenerant undergoes electrolysis to form oxygen gas and hydronium ions in the anode chamber and hydrogen gas and hydroxide ions in the cathode chamber.

ASRS

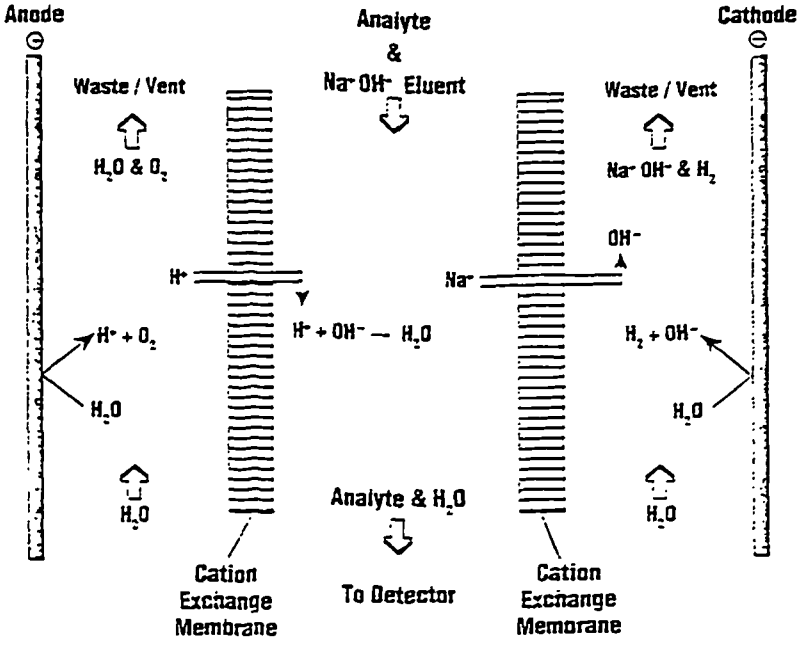

CSRS

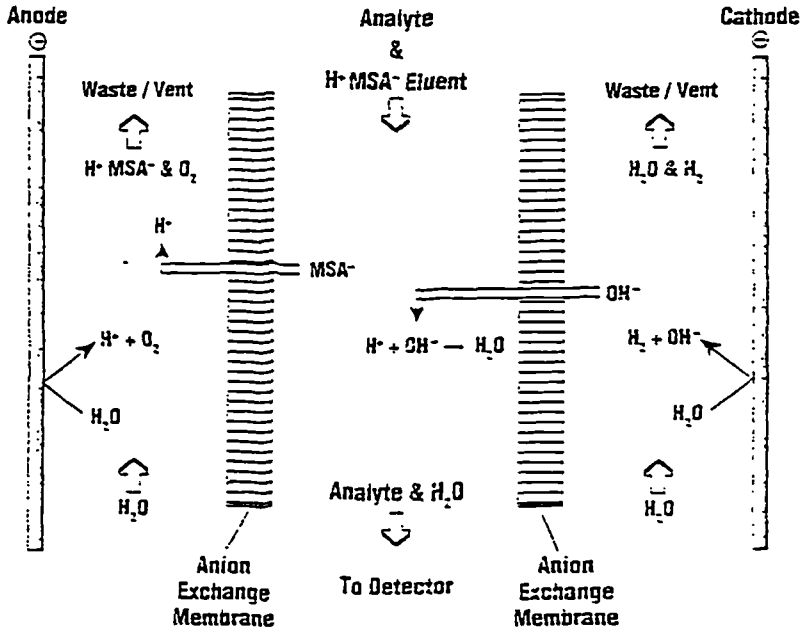

Figure 2.9 Autosuppression with the anion and cation self regenerating suppressor [13]

In ASRS, the hydroxide ions generated at the cathode are excluded from the eluent chamber by Donnan exclusion. Cation exchange membranes allow hydronium ions to move from the anode chamber into the eluent chamber to neutralise hydroxide eluent. The sodium ions in the eluent move across the membrane into the cathode chamber, maintaining the charge balance.

In CSRS, the hydronium ions generated at the anode are excluded from the eluent chamber by Donnan exclusion. Anion exchange membranes allow the hydroxide ions to move from the cathode chamber into the eluent chamber to neutralise hydronium ions in the eluent. Eluent counter ions (e.g. MSA^-) move across the membrane into the anode chamber, maintaining the charge balance.

Conductivity detection

The analyte solution flows through a cell containing a pair of electrodes which are fixed in position. When a potential is applied to the two electrodes, immersed in a solution of electrolytes, an electric current begins to flow through the solution which has a certain electrical conductance. The resistance of the cell is measured using a Wheatstone bridge. *Modern conductivity detectors are designed with wide signal* suppression ranges, i.e., extensive zero offset capability.

2.3 X-ray fluorescence (XRF) spectroscopy [3,9,14,15]

2.3.1 General

When a sample is placed in a beam of high energy photons, such as x-rays or fast moving electrons, the energy of the x-rays can be transferred to the sample atoms. If the x-ray has sufficient energy, the absorbing atoms become excited and are lost from the inner shells (K, L, M, etc.) and the atom becomes ionised. An electron from an outer shell then falls into the position vacated by the dislodged inner electron and an x-ray photon is given off in the process. The energy or the wavelength of the emitted x-ray is characteristic of the element being bombarded and can be used to identify it.

The energy of the radiation is given by:

$$\Delta E = \frac{hc}{\lambda} \qquad \text{..... (2.12)}$$

where h is Plank's constant,
c is the velocity of light and
λ is the wavelength of the x-ray.

The fluorescent x-rays emitted can be analysed by passing them through a crystal, which resolves the x-rays into individual wavelengths according to Bragg's law:

$$n\lambda = 2d \sin\theta \qquad \text{..... (2.13)}$$

where d is the plane spacing,
n is an integer, and
θ is the angle of dispersion.

The resolved x-rays are then detected by an appropriate system such as a scintillation counter. Such a system is referred to as a *wavelength dispersive system (WDXRF)*, and has good resolution for multi-element analysis.

For *energy dispersive x-ray fluorescence (EDXRF)* systems, as opposed to WDXRF ones, the crystal analyser is eliminated and the undispersed x-rays are sorted into energy groups by means of a semiconductor detector coupled to a multichannel analyser.

2.3.2 Instrumental aspects of EDXRF

The components of a typical energy dispersive x-ray fluorescence spectrometer are shown in Figure 2.10.

The x-ray source is achieved by the use of an x-ray tube (Figure 2.11). The tube uses a hot cathode, typically a tungsten filament, which emits electrons by thermionic emission. The electrons are accelerated by a potential onto a target anode made or plated with an element of choice, such as rhodium. The collisions convert kinetic energy mainly to heat, but a small amount of x-rays are also produced. The generated x-rays pass through a window of beryllium and fall onto the sample.

The fluorescent x-rays from the sample are detected by means of a semiconductor detector, e.g. lithium "drifted" silicon, cooled in liquid nitrogen to produce stability.

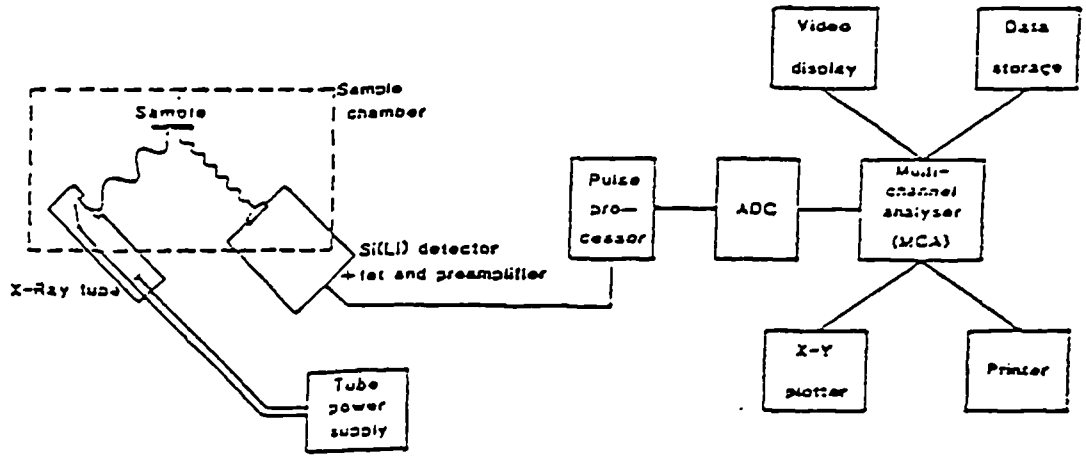

Figure 2.10 **Diagram showing the components of a typical energy dispersive x-ray fluorescence spectrometer**

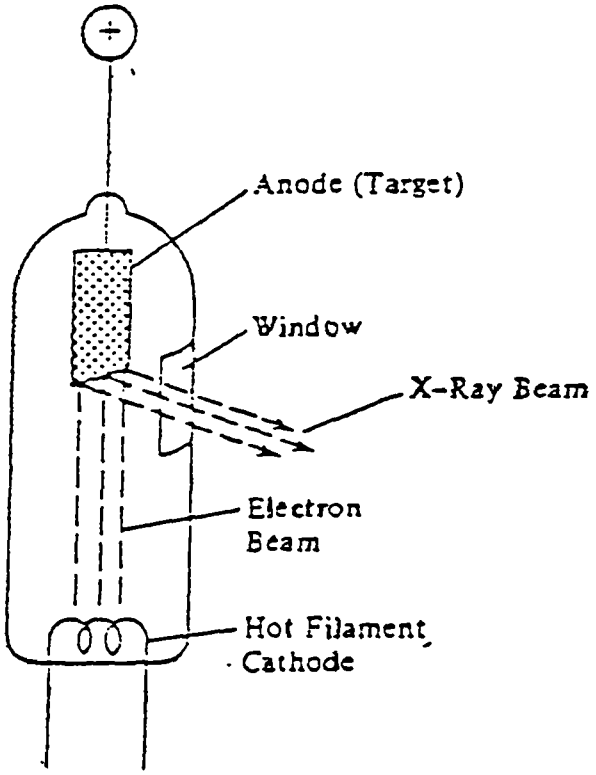

Figure 2.11 **Schematic diagram of high vacuum x-ray tube** [14]

Semiconductor detectors are fabricated with the semiconductor material deposited on glass in a sealed, evacuated envelope. When radiation, such as x-rays, falls on the semiconductor material, it becomes a conductor and hence, a very rapid change in electrical resistance can be detected. The response time for a semiconductor is the time required to change from an insulator to a conductor and can be as short as 1 nsec.

The x-rays entering the detector produce voltage pulses proportional to their energies. These pulses are then amplified and sorted according to energy by means of a multichannel analyser. A spectrum showing the elemental composition of the sample is then produced.

EDXRF is very fast and sensitive and can detect elements as low as 5 $\mu g\ g^{-1}$. The resolution of an EDXRF instrument is however much less than a WDXRF spectrometer, for low atomic number elements, but is better at higher atomic numbers.

2.4 Atomic absorption spectroscopy (AAS) [1,15,]

2.4.1 Principles of atomic absorption

Atomic absorption is a physical process involving the absorption, by free atoms of an element, of light at a wavelength specific to that element. It is a means by which the concentration of metals, in solutions of samples, can be measured.

The absorption of energy by atoms follows physical laws which provide the basis for quantitative analysis. When a sample or sample solution is burned in a flame or heated in a tube, the individual atoms of the sample are released to form a cloud inside the flame or tube. Each atom consists of a nucleus surrounded by a number of electrons in rapid motion around the nucleus, occupying discrete energy levels. If an atom is excited, by photons or by collisions due to heat, then electrons can be raised from their ground states to higher energy levels. The energy required for this transition between ground state and higher energy level (E_1-E_0) can be supplied by a photon of light with an energy given by equation 2.12.

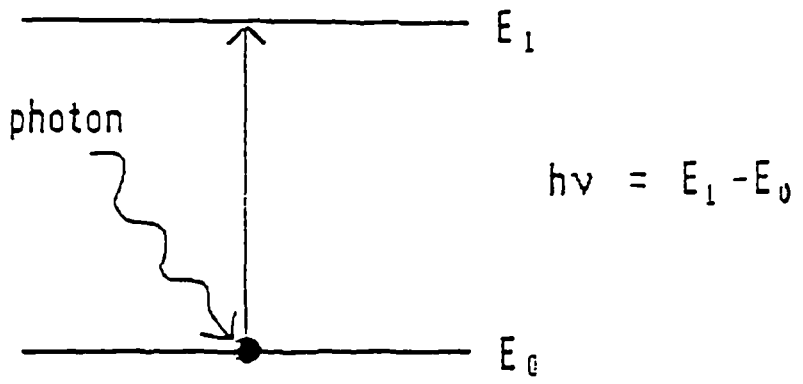

Figure 2.12 Absorption process [15]

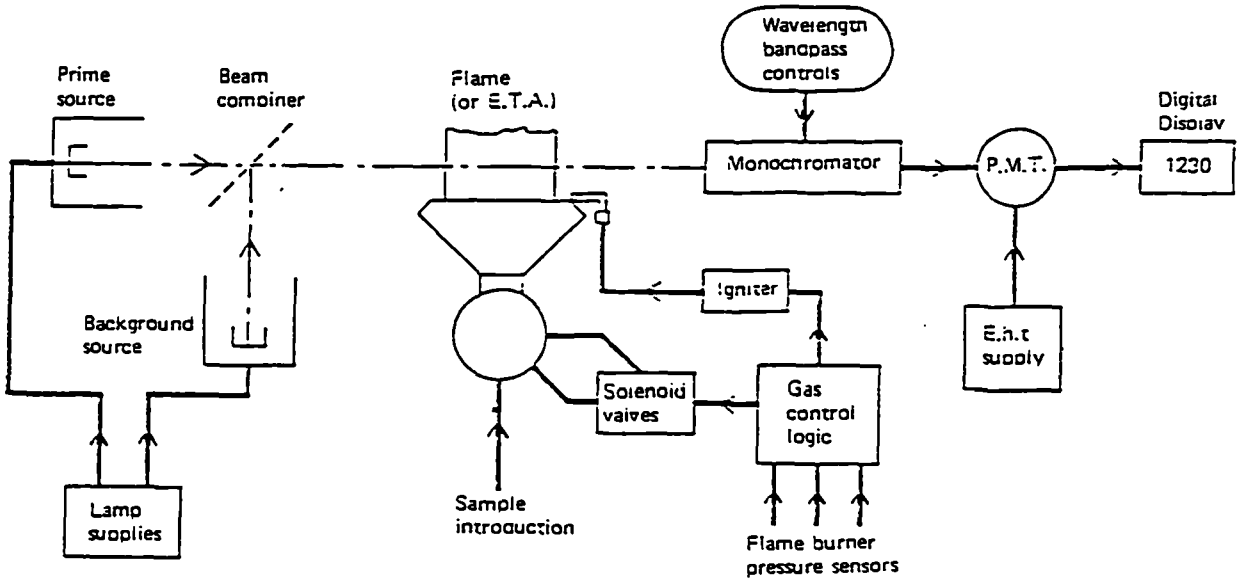

Figure 2.13 Schematic diagram of an atomic absorption spectrometer [15]

The absorption process is shown in Figure 2.12. The energy gap (E_1-E_0) is large and an energetic photon in the ultraviolet region is required to excite the atom. For each element, energy gaps for particular electrons are identical. This energy gap is not found in any other element. Therefore, if light of sufficiently narrow wavelength is sent through a cloud of various atoms, only atoms of one particular element will absorb photons. Hence, atomic absorption is a very selective technique.

2.4.1.2 Production of free atoms

To generate free atoms the atomiser must supply energy to break the chemical bonds between atoms of a molecule. An atomiser, such as a flame or electrothermal atomiser must supply sufficient energy, and the ability to produce uncombined and un-ionised atoms determines the success of an atomic absorption procedure.

A fine spray of droplets containing molecules in solution, is passed into a flame, at a temperature of around 2000-2800 °C. The solvent evaporates, leaving behind small solid particles. For some materials, these particles melt, vaporise and form dissociate to free atoms which enables atomic spectra to be observed. The individual metal atoms absorb energy and become either excited or ionised, e.g. for sodium chloride.

atomisation	$NaCl \Leftrightarrow Na + Cl$
excitation	$Na + h\upsilon \rightarrow Na^*$
ionisation	$Na \Leftrightarrow Na^+ + e^-$

The flame atomises the sample as shown by the first reaction . The atom is excited by the energy from the light source in the second reaction and if excessive heat is applied, ionisation occurs which removes the atoms as well. Atomisation may also occur by reducing radical attack of particles' surface.

Three main mechanisms of atomisation are thought to occur in the graphite furnace: a) the reduction of metal oxides by carbon to produce atoms in the gas phase; b) thermal decomposition of metal oxides or halides in the condensed or vapour phases, and c) thermal decomposition of metal carbides, formed by reaction of oxides with carbon on the atomiser surface [17].

2.4.2 Quantitative analysis

The Beer-Lambert law (eqn. 2.2) is the fundamental law which relates absorption in a solution to the concentration of individual components in a solution. It is not however possible to directly relate the Beer-lambert law to AAS. This is because solutions (molecular concentrations) are homogeneous throughout the sample absorption path and the free atoms in the flame are not constant throughout the light path. The total absorption is therefore proportional to the number of free atoms in the light path which is proportional to the concentration of the element in the solution. By using a series of standards solutions, a calibration graph can be constructed which relates concentration with absorption.

2.4.3 Instrumentation and operation of AAS

2.4.3.1 Flame AAS

The basic layout of a flame atomic absorption spectrometer is shown in Figure 2.13. In order to make measurements in AAS it is necessary to produce a population of ground state atoms as efficiently as possible and pass resonance radiation of the element to be measured through the population of atoms. In an ideal system, the detector should only measure at the wavelength being absorbed, as any other radiation sensed will decrease the sensitivity of the measurement. Light from a line source of characteristic wavelength for the element being determined passes through the flame into which has been sprayed a fine mist of the sample solution. The region of the spectrum to be measured is selected by the monochromator. The isolated spectral line falls on the photomultiplier or optical detector and the output is amplified and data processed. The intensity of the resonance line is measured twice, once with the sample in the flame (I) and once without (I_o). The logarithimic ratio of the two readings is the absorbance, which is proportional to the concentration of the atoms in the flame, which in turn, it is assumed is proportional to the concentration of the element in the sample.

Hollow cathode lamp (HCL)

The most common source for AAS is the hollow cathode lamp, shown in Figure 2.14. It consists of a tungsten anode and a cathode made from, or containing, the element

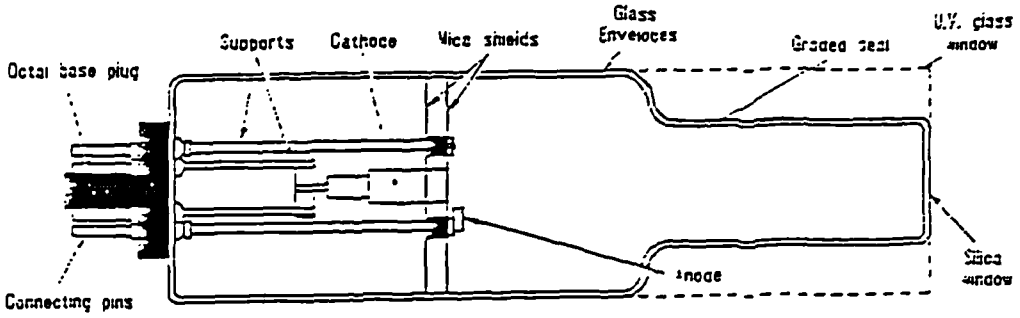

Figure 2.14 Hollow cathode lamp [15]

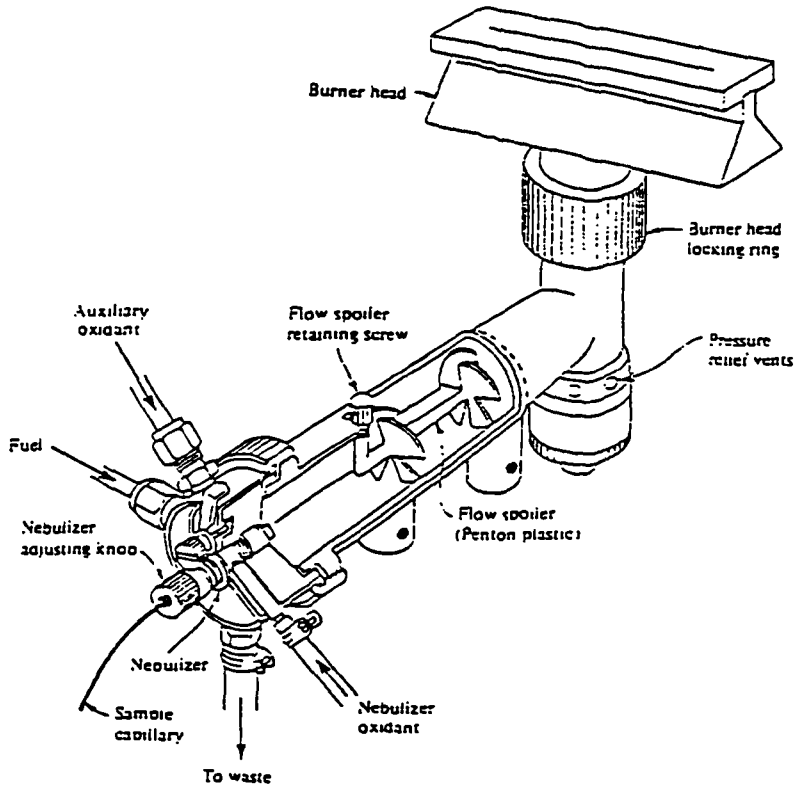

Figure 2.15 Burner for Flame AAS [1]

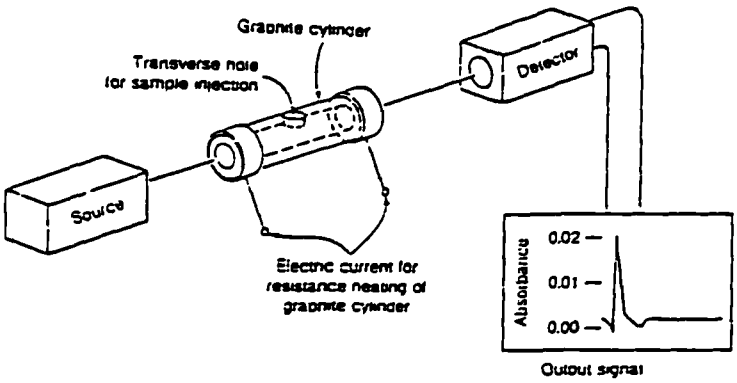

Figure 2.16 Furnace for Electrothermal AAS [3]

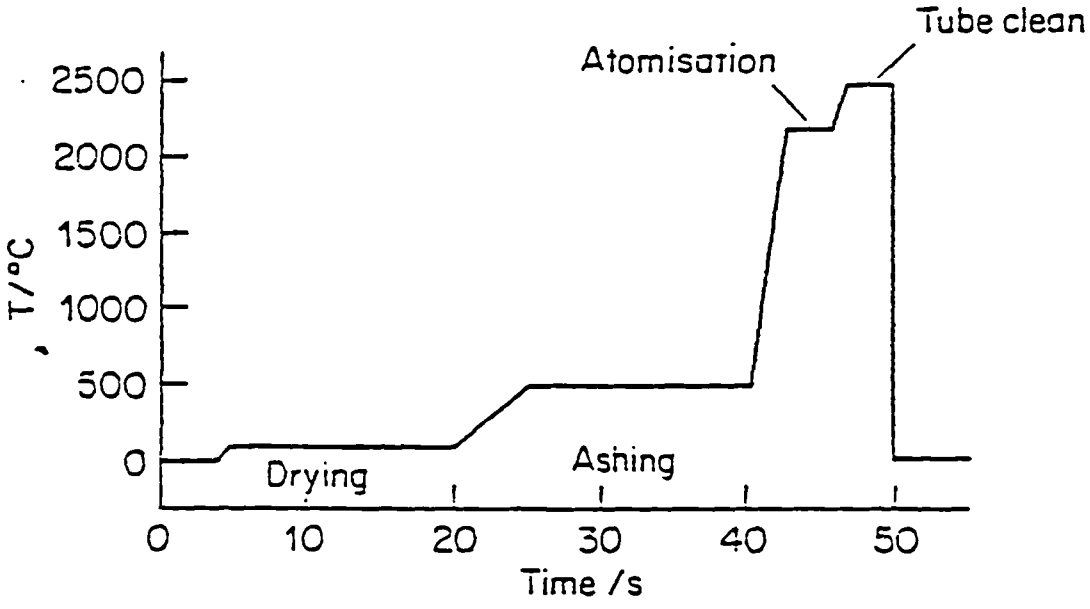

Figure 2.17 Typical furnace program

to be measured. The lamp is filled with an inert gas, usually argon, at a pressure of 1-10 Torr. A potential is applied across the electrodes causing ionisation of the argon. If the potential is sufficiently large, the cations of the gas strike the cathode with sufficient energy to dislodge some of the metal atoms, a process known as sputtering, and an atomic cloud is produced. A fraction of the metal atoms are in, or are elavated to, an excited state and emit a characteristic photon as they return to the ground state.

Burner

Figure 2.15 shows a typical burner for flame AAS. The sample solution is dispersed, or nebulised, into an aerosol of small droplets which are then mixed with a gaseous fuel and oxidant and swept into the burner. The droplets are then carried into the flame where atomisation occurs. An air - acetylene flame is commonly used or alternatively a nitrous oxide - acetylene flame can be used for more refractory elements. The sensitivity of atomic absorption procedures is dependent on the flame conditions. For each element it is necessary to optimise: a) the fuel flow, which determines the temperature, concentration of oxygen and concentration of carbon based radicals, and b) the observation height in the flame.

2.4.3.2 Electrothermal ETAAS

All commercially available electrothermal atomisers are based on the principle of resistance heating. A schematic diagram showing a typical furnace is shown in Figure 2.15. An electrothermal atomiser is normally a small cylindrical furnace, cuvette or cell made from graphite which can be heated to a high temperature by resistive heating. In order to atomise samples, the atomiser must be heated to 2000 °C for most elements and up to 3000 °C for more refractory elements. Typically, 10 or 20 μL of a sample solution are deposited on the graphite tube. The temperature of the atomiser is then increased through a series of stages which cause volatilisation of the solvent, pyrolysis of the residue to remove contaminant species, atomisation of the analyte and, finally, a high temperature tube clean. A typical furnace program is shown in Figure 2.17.

2.4.4 Comparison of FAAS and ETAAS

Flame AAS is a relatively simple and well established technique. However, it does have a number of disadvantages associated with it. As the flame is a dynamic system,

atoms have a very short residence time in the flame (10-100 ms) and therefore little time to absorb the radiation. The analyte is also diluted by the gases of the flame. These problems lead to a decrease in sensitivity, which leads to a high limit of detection, normally in the order of 0.1-1 $\mu g\ mL^{-1}$. FAAS usually requires large amounts of sample, around 10 mL. The large volume required is due to the uptake rate being 5 $mL\ min^{-1}$, and the efficiency of the nebuliser. Only 5-10 % of the volume will actually reach the flame. Solid samples cannot be analysed easily by FAAS.

ETAAS can analyse both solid and liquid samples and only requires approximately 20 µL volume per injection. Detection limits are in the order of $\mu g\ L^{-1}$ as atoms are more efficiently produced, and have a longer residence time in the graphite furnace, typically 0.2-1 s, as the gas flow is reduced to zero in the atomisation stage. This allows for many more repeat excitations of an atom.

ETAAS does have some disadvantages, one of which is interferences. Line spectral interferences are relatively rare but molecular absorption or light scattering are more common. Chemical interferences can also cause problems. Graphite furnace instruments can also be more difficult to operate than flame instruments.

2.5 Gel permeation chromatography (GPC) [18,19]

Gel permeation chromatography, or size exclusion chromatography, is a technique for separating materials according to their molecular size and shape by passage of a solution through a column consisting of a polymeric gel.

The stationary phases used in GPC are porous particles with a closely controlled pore size. Depending on their size and shape, sample molecules may be able to enter the pores of the stationary phase particles. The pores of the gel exclude molecules greater than a certain critical size whilst smaller molecules can permeate the gel structure by diffusion. Excluded molecules pass through the system more rapidly than smaller ones that can diffuse into the gel. Diffusion within the gel also varies with molecular size and shape because pores of different dimensions are distributed throughout the gel structure in a random manner. These smaller molecules are eluted at rates dependent upon their degree of permeation into the gel, and components of a sample mixture therefore elute in order of decreasing size or molecular weight.

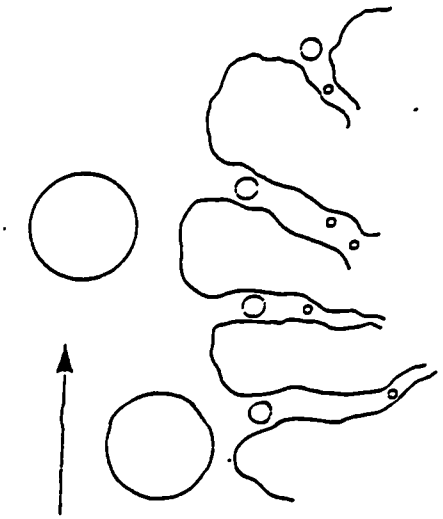

Figure 2.18 GPC process [10]

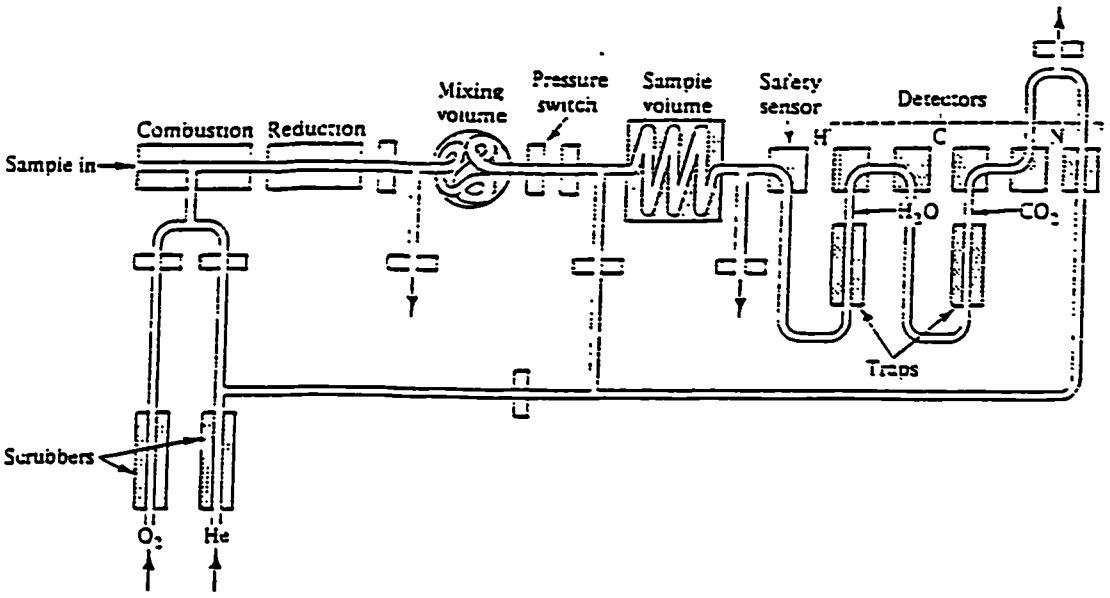

2.19 Schematic diagram of an elemental analyser [1]

Unlike other chromatographic processes, in GPC there is no interaction between the solute and the surface of the stationary phase. The process is illustrated in Figure 2.18.

Column packings

Packings for GPC are semirigid, cross-linked macromolecular polymers. The gels can be hydrophilic, for separations in aqueous and other polar solvents, or hydrophobic, for use in non-polar or weakly polar solvents. The gels are chemically stable at pH values less than 10 and can be used routinely and indefinitely.

Detectors

The most widely used detector is the differential refractometer. This monitors the difference in refractive index between the mobile phase (reference) and the column eluent. It responds to any solute whose refractive index is significantly different from that of the mobile phase.

Column calibration

To determine molecular weights or molecular weight distributions for the sample species, the columns must be calibrated. This is achieved by eluting the appropriate calibration standards and monitoring the elution volume. Polystyrene or polyisoprene standards are commonly used with organic solvents. Polyethylene glycols, polystyrene sulfonates and proteins are used with hydrophilic solvents [1]. The hydrodynamic radius of the molecule is proportional to the relative molecular mass. A graph of log M_R versus the elution volume provides a relationship for determining the molecular weight of the sample species.

2.6 Elemental analysis [1, 20]

Instrumentation for carbon, hydrogen and nitrogen (CHN) analysers is based on one of two general procedures. One involves the separation of the combustion products, carbon dioxide, nitrogen and water using specific absorbents, with the resulting change in the composition of the gas mixture being measured. The other involves separation by gas liquid chromatography. Thermal conductivity is the detection method in both cases.

The sample (<3 mg) is combusted in pure oxygen at temperatures of up to 1800 °C. Carbon in the sample is converted to carbon dioxide and carbon monoxide, hydrogen is converted to water. Nitrogen is released as the free gas along with some oxides. A schematic diagram of an elemental analyser is shown in Figure 2.19. The combustion gases are carried by a stream of helium gas into a secondary furnace where simultaneous reduction and oxidation of the gases occurs. Nitrogen oxides are reduced to nitrogen, carbon monoxides are converted to carbon dioxide and oxygen is removed. Any interferences are also removed from the gases if needed, e.g. a magnesium oxide layer in the furnace to remove fluorine or a silver wool plug to remove chlorine, bromine and iodine.

For this study, separation of the gases was achieved by means of specific adsorbents for carbon dioxide and water. Three pairs of thermal conductivity cells (glass coated platinum filaments) are used in series for detection: one pair each for water, carbon dioxide and nitrogen. A magnesium perchlorate trap between the first pair of cells absorbs any water from the gas mixture before it enters the second pair of cells. The differential signal, measured before and after the trap, is proportional to the amount of hydrogen (measured as water removed) in the sample. A soda-asbestos trap between the second and third pair of cells results in a signal proportional to the carbon (carbon dioxide) in the sample. The last pair of cells measures nitrogen by comparing the helium-nitrogen mixture with pure helium.

Results are reported as a percentage for each element and are calculated by analysing standard samples and occasional blanks.

2.7 Use of the techniques in this study

FTIR spectroscopy was employed to characterise all the historical artefacts used in this study, to identify constituents and to monitor changes which had occurred as a result of the deterioration processes. The technique was also used to study changes in cellulose nitrate samples which were artificially aged.

Ion chromatographic techniques were used to identify the constituents of the samples including residual acids and impurities from manufacturing. Degradation products arising from ageing processes were also studied in both cellulose nitrate artefacts and artificially aged samples.

X-ray fluorescence spectroscopy was used to analyse the plastic artefacts and determine qualitatively their metal content. The technique allowed the identification of fillers and dyes contained in the artefacts.

Flame AAS and electrothermal AAS were employed to identify and quantitatively determine any trace levels of elements from fillers, colourants and any other possible additives in the artefacts.

The nitrogen content of the samples was quantified using microanalytical techniques. Changes over time as samples aged were also monitored.

Gel permeation chromatography was used to study the molecular weight distribution of the cellulose nitrate plastics. Comparisons between deteriorated samples and samples in good condition were made.

References

1. Willard, H. H., Merritt, L. L., Dean, J. A. and Settle, F. A., *"Instrumental Methods of Analysis"*, Wadsworth Publishing Company, California, 7th edn., 1988.

2. Griffiths, P. R. and De Haseth, J. A., *"Fourier Transform Infrared Spectrometry"*, John Wiley and Sons, New York, 1986.

3. Svehla, G., *"Comprehensive Analytical Chemistry, vol. 4"*, Elsevier Scientific Publishing Company, Amsterdam, 1975.

4. Christian, G. D. and Callis, J. B., *"Trace Analysis - Spectroscopic Methods for Molecules"*, John Wiley and Sons, New York, 1986.

5. Gardette, J. L., *Spectroscopy Europe*, 1993, **5**, 28-32.

6. Humecki, H. J., *"Practical Guide to Infrared Microspectroscopy"*, Marcel Dekker Inc., New York, 1995.

7. Frei, R. W. and MacNeil, J. D., *"Diffuse Reflectance Spectroscopy in Environmental Problem Solving"*, The Chemical Rubber Company, Cleveland, U.S.A., 1973.

8. Garton, A., *"Infrared Spectroscopy of Polymer Blends, Composites and Surfaces"*, Hanser Publishers, Munich, 1992.

9. Robinson, J. W., *"Undergraduate Instrumental Analysis"*, Marcel Dekker Inc., New York, 3rd edn., 1982.

10. Lindsay, S., *"High Performance Liquid Chromatography"*, John Wiley and Sons, Chichester, 2nd edn., 1992.

11. Hamilton, R. S. and Sewell, P. A., *"Introduction to High Performance Liquid Chromatography"*, Chapman and Hall, London, 2nd edn., 1986.

12. Smith, R. E., *"Ion Chromatography Applications"*, CRC Press Inc., Florida, 1988.

13. Gibson, L. T., *"Analytical Studies of the Degradation of Calcareous Artefacts in Museum Environments"*, Ph.D. Thesis, University of Strathclyde, 1995.

14. Braun, R. D., *"Introduction to Instrumental Analysis"*, McGraw-Hill Inc., Singapore, 1987.

15. Salmon, M. E., in *"X-ray Analysis"*, Henke, B. L., (ed.), Plenum Press, New York, 1970, 94-104.

16. Milner, B. A. and Whiteside, P. J., *"Introduction to Atomic Absorption Spectrophotometry"*, Pye Unicam Ltd., 3rd edn., 1994.

17. Littlejohn, D., *Analytical Proceedings*, 1992, **29**, 203-205.

18. Ravindranath, B., *"Principles and Practice of Chromatography"*, Ellis Horwood Ltd., West Sussex, 1989.

19. Kremmer, T. and Boross, L., *"Gel Chromatography"*, Wiley-Interscience, Chichester, U.K., 1979.

20. Skoog, D. A. and West, D. M., *"Analytical Chemistry: an Introduction"*, Saunders College Publishing, New York, 4th edn., 1986.

CHAPTER THREE

SURVEY OF PLASTICS

Chapter Three - Contents

3.1 Introduction

There were several reasons for carrying out a general survey of plastic artefacts for the initial part of this research. The first was to locate as many relevant artefacts as possible for the study. Secondly, to assess the condition of the artefacts gathered and to identify which showed signs of degradation. Finally, it was hoped that it would be possible to define the type and the extent of degradation in these objects.

Several surveys of collections containing modern materials such as plastics and rubbers had been carried out by museums, prior to this study [1, 2]. These had generally found that a high proportion of plastic artefacts showed some signs of visible degradation. It was decided, therefore, that a comprehensive visual examination of the artefacts would provide the best starting point for assessing and understanding the problems of degradation. Examination by microscopy was also undertaken to study the degradation in more detail.

The technique of FTIR spectroscopy is widely used in museums for analysing organic materials. It has also been used to study polymers in collections by several workers [3, 4]. In recent years FTIR microspectroscopy has become recognised as an efficient tool for studying the ageing of polymers. The technique was used initially, in this work, to identify the plastic in the artefacts. It was also hoped that FTIR microspectroscopy could be used qualitatively to identify the constituents of the plastics, and quantitatively, to assess the extent of degradation.

3.2 Experimental

3.2.1 Artefacts

Plastic artefacts were gathered from various sources for the purpose of this research project. The majority were donated from museum collections: The National Museums of Scotland, he Science Museum in London, the Musee d'Oyonnax in France, the British Museum and the Museum of London. Other pieces were donated from private collections or other researchers.

Very little or no information was available regarding the history of the production, storage or treatment of the samples. This, however, reflects the situation for many conservators and curators. The ages of the samples were also unknown.
Around 40 - 50 artefacts were gathered which showed various signs of degradation. The objects used in this project are described in Table 3.1. A glossary of terms used to define chemical and physical degradation is given in Table 3.2.

3.2.2 Preparation of cellulose nitrate films for IR standards

A procedure was developed for the preparation of cellulose nitrate films. This involved dissolving cellulose nitrate in a suitable solvent. Various solvents were tried, with acetone giving the best results.

A 1% (w:v) solution of cellulose nitrate, 10.7 - 11.2% nitrogen content (BDH Chemicals Ltd.), in acetone was prepared (0.5 g cellulose nitrate in 50 mL acetone). The solution was then cast onto glass microscope slides and left for the solvent to evaporate.

Films were also produced containing various levels of camphor (Fisons), 1 - 50% (w:w). The camphor was added to the mixture before casting. Films with camphor levels <2% were hard and brittle. Films with levels >50% were cloudy and soft and could not be lifted from the glass plates.

3.2.3 Microscopy

Analysis of the artefacts was carried out using a PM-10 automatic photomicrographic system. This consisted of a PM-PBK exposure body, mounted onto the FTIR microscope. A PM-D 35A adapter connected an Olympus C35 AD4 camera onto the exposure body. Photographs were taken on 35 mm film. A 15x magnification objective lens was used.

Table 3.1 Description of artefacts studied

Sample	Description
1. Tortoiseshell box	Extremely degraded. Discoloured, opaque with loss of tortoiseshell effect. Embrittled throughout. Cracked and in many pieces. Sugary deposit on surface.
2. Tortoiseshell handbag handle	See Figure 3.2. Extremely degraded. Discoloured and embritted in most areas. Severe crazing and distorted surface. In several pieces.
3. Boothook	See Figure 3.5. Handle originally tortoiseshell effect but now completely degraded. Handle cracked and extremely brittle. Surface is distorted. Object contains steel hook.
4. Green box	See Figure 3.1. Very degraded. Severe cracking and crazing throughout. Sides extremely distorted and collapsing inwards. In several pieces.
5. Set square	Plastic has a cloudy yellow colour. Cracked and in several pieces. Extensive areas with clear, bubbled effect at surface.
6. Pink lid	See Figure 3.4. Base of lid is opaque and appears undegraded. Lacquer coating is breaking off in many pieces and is very brittle.
7. Station pointer	Extremely degraded. Plastic has dull opaque appearance and is very brittle.
8. Sun compass	Extremely degraded and in several pieces. Very brittle and discoloured.
9. Fan	Part of handle sealed in plastic bag is cracked and is sweating. Part of handle not sealed in bag is not degraded.
10. Pink jewellery box	See Figure 3.3. Relatively undegraded. Interior of box is darker than outer surface. Lid is slightly distorted.
11. Blue mirror	Back of mirror is paler in colour to front. Some blistering on the surface.

Table 3.1 (cont.) **Description of artefacts studied**

Sample	Description
12. Tortoiseshell lid	Relatively undegraded. Some cracking and crazing on the surface.
13. Yellow jewellery box	In good condition. Slightly discoloured brown in areas
14. Yellowed container	Clear box has become yellow/brown in appearance. Sides are slightly distorted
15. Tortoiseshell jewellery box	Very good condition.
16. Tortoiseshell handle	Very good condition
17. Napkin ring	Very good condition. Very slight blistering in inside.
18. Tortoiseshell hair clips (6)	All in very good condition. Metal clasps in some showed signs of corrosion

Table 3.2 **Glossary of terms used to describe the condition of artefacts**

Sweating	Stickiness or presence of beads of liquid on objects surface.
Chalkiness	Grainy deposits on object's surface
Crack	Line of failure which does not penetrate entire thickness of plastic.
Scratch	Indentation made by mechanical means over a few millimetres.
Craze	Series of interconnecting cracks on surface or within body of object.
Blistering	Surface of object appears raised or flaking

3.2.4 FTIR microspectroscopy

3.2.4.1 Apparatus

A Nic-Plan IR microscope was used, coupled to a Nicolet 510P spectrometer. A Nicolet 0.25 mm MCT-A detector was used with the microscope, cooled by liquid nitrogen. A SpectraTech Cassegrain infrared lens (Reflechromat) of x15 magnification was used

3.2.4.2 Sample preparation

Particles for analysis were removed from the solid object using a scalpel. To prepare the samples for the microscope, a SpectraTech μ Sample-Plan - sample compression cell was used. This is a device used to hold and flatten samples for analysis by FTIR microscopy. The cell consists of a metal holder with a screw assembly, that holds two diamond windows. The sample was placed between the two windows and the screwcap tightened down, flattening and thinning the samples. One diamond window was then removed leaving the sample in place on the second window. This was then placed on the microscope stage.

3.2.4.3 Recording of spectra

Using upper illumination only, the sample was focused with the visible light objective. The measured area of the sample was delimited by bringing the area of interest into the centre of the field of view which was then reduced by means of adjustable knife-edge apertures, to around 200 μm^2. The visible beam was then switched to the IR beam and the spectrum recorded using the following parameters.
Number of scans = 128
Resolution = 4 cm^{-1}
MCT scanning velocity = fast
Electronic gain = 1

The spectrum was recorded between 4000 and 600 cm^{-1}. For each spectrum, a background spectrum was first recorded (diamond window only), which was subtracted from the sample spectrum. All data manipulation was carried out using PCIR software. For quantitative analysis, all spectra were recorded so that the

absorbance was less than 1 and in the linear absorption region, typically between 0.2 and 1.0 abs units.

3.3 Results and discussion

3.3.1 Visual inspection of artefacts

Initial examination of all the plastic artefacts revealed that the majority showed some effects of deterioration. Although the artefacts differed considerably in respect to size
and shape, the signs of degradation were consistent throughout.

Nearly all the artefacts showed some form of mechanical damage. The objects had scratches on their surface caused by handling over the years. In more serious cases, objects had been chipped or broken into fragments. Areas of the artefacts which had been damaged tended to show greater degradation than other areas of the same object. The pale yellow jewellery box, for example, was chipped on its surface and the plastic had become brown and brittle.

Several objects exhibited signs of distortion or dimensional change, in particular the thin sides and lids of boxes. The absorption of moisture, or the loss of plasticiser from the objects, resulted in dimensional changes and consequently stresses were formed. If an object had been subjected to varying external conditions, such as changes in humidity, the damage would be accelerated.

The surfaces of nearly all the objects had tiny cracks. These cracks were signs of the failure in the polymer, caused by stresses in the artefact. In many cases the cracks were widespread throughout the object and interconnecting, so that the phenomenon of crazing was seen. This can be see clearly in the pale green box shown in Figure 3.1.
The cracks in the artefacts were also the areas where other signs of degradation were seen. White, chalky deposits were noted in some objects beside cracks, presumably due to the plasticiser exuding from the interior of the object (The deposits were later analysed by FTIR and found to be crystals of camphor). Sticky deposits were also found on the surface where the plastic was cracked and these were often acidic. This is often referred to as sweating. This is probably due to plasticiser loss and also

Figure 3.1 **Green cellulose nitrate box (sample no. 4) showing severe cracking and crazing.**

Figure 3.2 **Tortoiseshell handbag handle (2). Plastic is extremely degraded and is showing discolouration and embrittlement.**

Figure 3.3 **Pink jewellery box (10) in good condition. Top of box has faded in colour.**

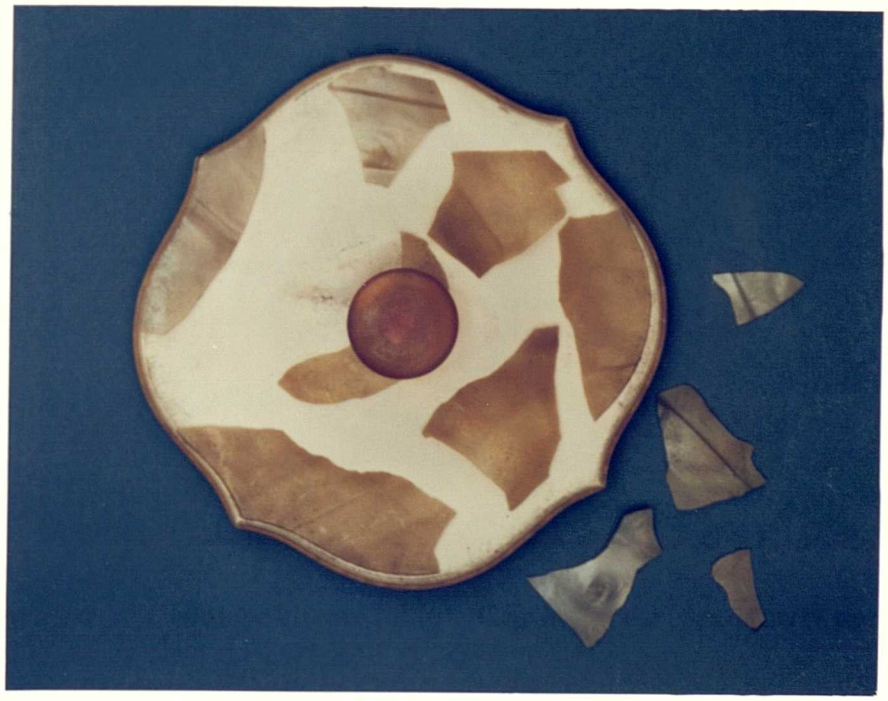

Figure 3.4 **Cellulose nitrate lid (6). Coating of lid is extremely degraded.**

Figure 3.5 **Boothook (3). Plastic handle is extremely degraded and is very brittle.**

the evolution of degradation products, such as nitrogenous gases, from the cellulose nitrate.

Other evidence for degradation, on an artefact's surface, is the presence of blisters or surface blooms. These were seen on several objects, e.g. the back of the blue mirror and the inner surface of the yellow napkin ring.

In several artefacts, the cracking and crazing was to such a great extent that the objects were either very fragile or had broken into several pieces. The artefacts were usually extremely brittle, from the loss of plasticiser, and sections that were removed could be crushed to powder very easily. Figure 3.2 shows a section from a cellulose nitrate tortoiseshell effect handle which is severely degraded and is now brittle and broken.

The other main effects of deterioration, seen on examination of the artefacts, were associated with colour change. Objects which were brightly coloured, generally had areas which were faded compared to other areas. The pink jewellery box and the yellow jewellery box were both more faded on their outer surfaces compared to the interior. The pink jewellery box is shown in Figure 3.3. Similarly, the back of the blue mirror was quite markedly more faded than the front face. This fading of colour is associated with exposure to sunlight

Many of the artefacts were designed as imitation tortoiseshell, and many of these pieces were now experiencing degradation. The tortoiseshell handle shown in Figure 3.2 had areas which had deteriorated to different extents and the stages of degradation could be seen. The original dark brown tortoiseshell effect had faded over time, becoming a pale yellow/brown colour. The plastic, which was originally translucent, has become cloudy. In other areas, the artefact's colour had deteriorated to an opaque yellow colour, the tortoiseshell effect being completely lost. Some areas, particularly on large cracks or broken edges, had lost all colour and had a shiny, clear, bubbled appearance. Over the surface of the plastic there were also many dark brown spots.

Other artefacts, which were originally clear cellulose nitrate, had become yellow/brown in colour. This general darkening is due to degradation products forming within the plastic.

It was also found that many artefacts contained fillers to opacify the cellulose nitrate, for example, the pink jewellery box in Figure 3.3. These artefacts were all in reasonably good condition, none exhibiting severe signs of degradation. The pink lid showed this clearly (see Figure 3.4). The base and the lacquer coating are both cellulose nitrate. The base contains a filler and appears undegraded, however the lacquer, which does not contain a filler, is very brittle and has become yellow/brown in areas.

During this initial examination of plastic artefacts, some of the items gathered were contained in plastic bags. On opening the bags, there was often a notable acidic smell, associated with a build up of gases. The fan with the cellulose nitrate handle had been stored in a sealed plastic bag prior to this study. Inside the bag the pink feather of the fan had been bleached near the handle, and the handle itself was sticky and exhibiting blistering and cracking. However, part of the plastic handle had not been stored inside the bag and was in very good condition. Obviously all the acidic degradation products had built up within the bag and had accelerated the deterioration, and on opening there was a strong acidic smell.

It was also noted that some objects contained metal inserts. There was often localised corrosion of the metal in areas where the deteriorated cellulose nitrate contacts the metal, such as the hinge in the tortoiseshell jewellery box, or the steel hook in the cellulose nitrate boothook (see Figure 3.5). In the case of the boothook, the plastic handle was more degraded around the metal insert than in other parts of the handle. It may be, that the iron is catalysing the degradation of the plastic.

When evaluating the amount of degradation each artefact has undergone during its history, it would be useful if conservators were able to compare the extent of degradation between samples. This would allow a quick diagnosis so that artefacts showing the first signs of degradation could be treated early on, resulting in limited damage. From the point of view of this study, it is important that the different techniques used to assess the degradation can be compared.
A scheme for quantifying the degradation of the artefacts by visual observation was therefore devised. The scheme provides a quantitative value, for each artefact, which increases with the amount of degradation. Typical results from using this scheme are shown in Figure 3.6.

Sample	1	Tortoiseshell box
	3	Boothook
	5	Set square
	10	Pink jewellery box
	14	Yellowed container
	17	Napkin ring

Degradation seen	**sample**					
	1	3	5	10	14	17
Colour						
Fading of colour				2		
Yellow/brown					2	
Opaque appearance	4	4				
Bubbled effect			4			
Surface						
Cracking						
Sweating						
Blistering						1
Chalkiness	4	4	3			
Crazing						
Overall						
Distortion				1		
Brittleness			5			
Disintegrating	5	5				
TOTAL	13	13	12	3	2	1

Figure 3.6 Scheme proposed for assessing the visual degradation of an artefact.

For, each artefact, marks are assigned for each type of degradation seen and then summed to produce a total. The classes of degradation are divided into three sections

(a) colour changes
(b) surface effects
(c) overall

Each section is further divided into the different effects of degradation seen. The more severe the effect and the more widespread throughout the artefact, then the greater the value attributed (1 to 5). Only one value, the highest, is given for each of the three classes of degradation (i.e. one for colour, surface and overall degradation)

Although the scheme is rather crude and seems to oversimplify the whole problem, it can provide a very simple but effective way of assessing the artefacts.

values from scheme

0-2	Artefact requires no treatment.
3-5	Artefact is showing early signs of degradation and will require treatment.
6-10	Artefact is exhibiting advanced signs of degradation and requires immediate treatment. Object should be separated from other artefacts.
11-15	Artefact is severely deteriorated and should be separated from other artefacts.

3.3.2 Microscopy

Sections of artefacts were examined in more detail using the photomicrographic system, to assemble more information concerning degradation. All samples had some form of surface erosion, even artefacts which appeared to be in very good condition. Tiny cracks, unable to be seen by eye, were evident on all artefacts. Cross sections of artefacts were also examined and again these revealed that most artefacts showed some surface deterioration. Figure 3.7 is a photograph taken of a section of the tortoiseshell lid. It can be seen that there is a noticeable amount of surface pitting. Tiny cracks also penetrate from the surface to the interior of the plastic.

Figure 3.8 is a cross section of a more degraded artefact, the set square. Again there is surface erosion as with the tortoiseshell lid, but there are much larger cracks

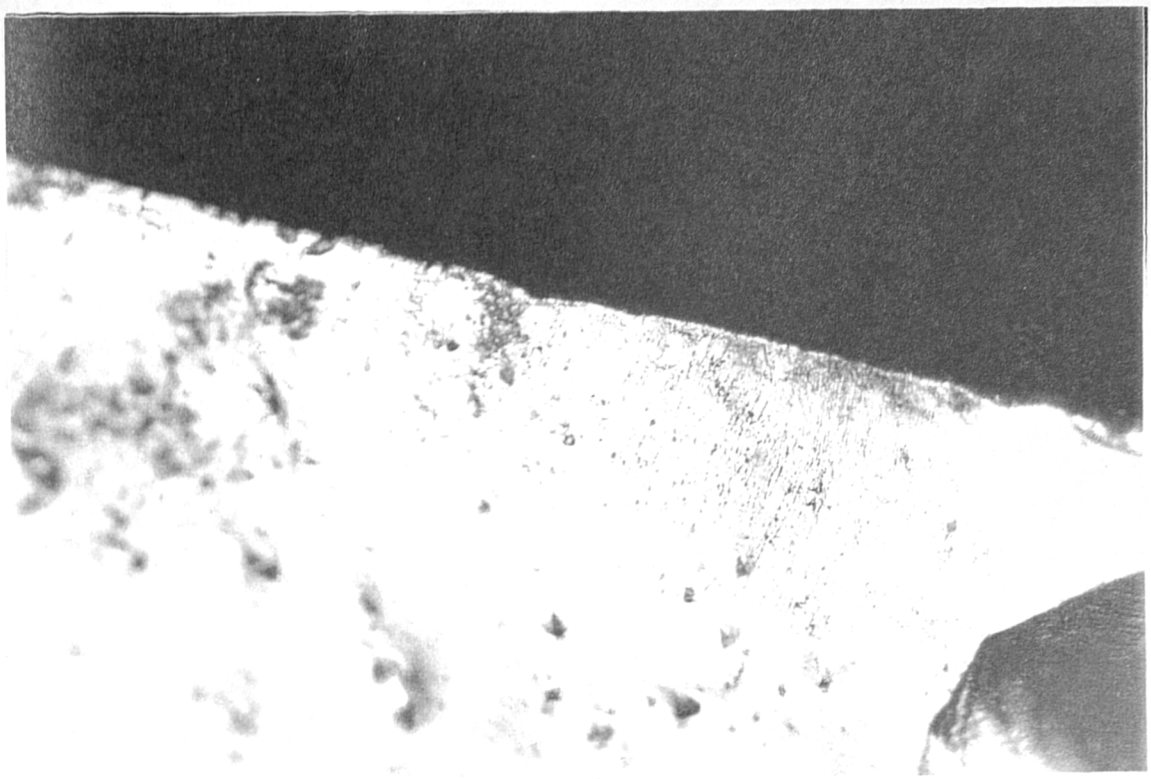

Figure 3.7 Photograph of section of tortoiseshell lid (x15 magnification)

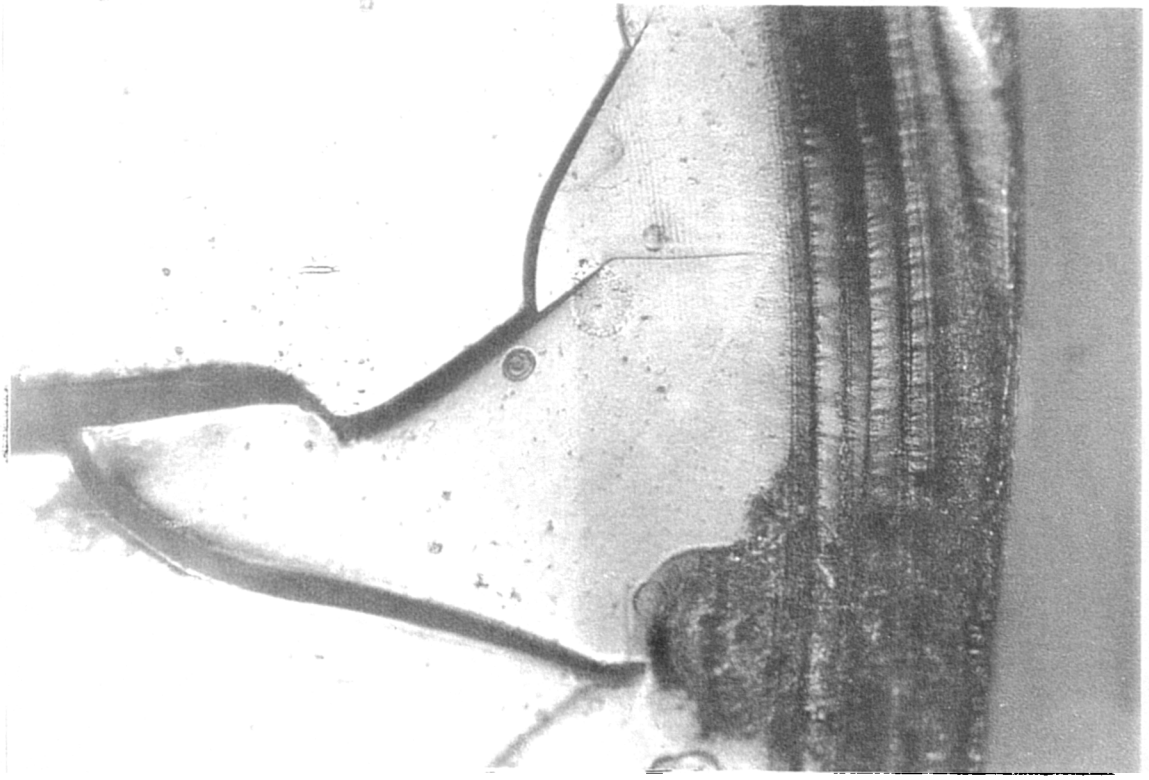

Figure 3.8 Photograph of section of set square (x15 magnification)

extending to the core of the sample. This is seen with all of the more degraded artefacts. The surface erosion is most likely due to hydrolytic degradation of the artefact. The more degraded samples have obviously been subjected to further stresses, from loss of plasticiser of evolution of degradation gases. The large cracks that have opened up in these samples will simply hasten the degradation process, allowing water and oxygen to permeate the plastic.

It is clear from microscopic analysis that even samples which appear visibly undegraded, may already be undergoing some form of degradation. Although a visual inspection will provide a quick assessment, a more detailed analysis may be required to predict deterioration in the artefacts.

3.3.3 Characterisation of artefacts

FTIR spectra were initially recorded for all of the artefacts, to identify the plastic. All the samples were found to be cellulose nitrate with the exception of two (a piece of cellulose acetate film and a cellulose acetate box, not mentioned previously), so the work was therefore continued solely with cellulose nitrate objects.

Figure 3.9 shows a typical spectrum for a cellulose nitrate artefact, the tortoiseshell jewellery box. Table 3.4 lists the peak frequencies and assignments in the unplasticised cellulose nitrate spectrum [5]. Spectra for a cellulose nitrate standard (unplasticised), a cellulose nitrate artefact in good condition, the pink jewellery box and a degraded artefact, the tortoiseshell box, are shown in Figure 3.10.

For the three spectra, principal absorptions for the NO_3 groups occur at approximately 1650, 1280 and 840 cm^{-1}. The ether group on the cellulose nitrate chain has an absorption at approximately 1070 cm^{-1}. The broad band around 3500 cm^{-1} is attributed to OH groups on the cellulose chain (the cellulose nitrate sample has a degree of nitration of 2-2.5 nitrate groups per glucose unit so some OH groups will not be esterified). The spectra for the two artefacts also show a peak at approximately 1730 cm^{-1} which is attributed to the plasticiser present in these samples.

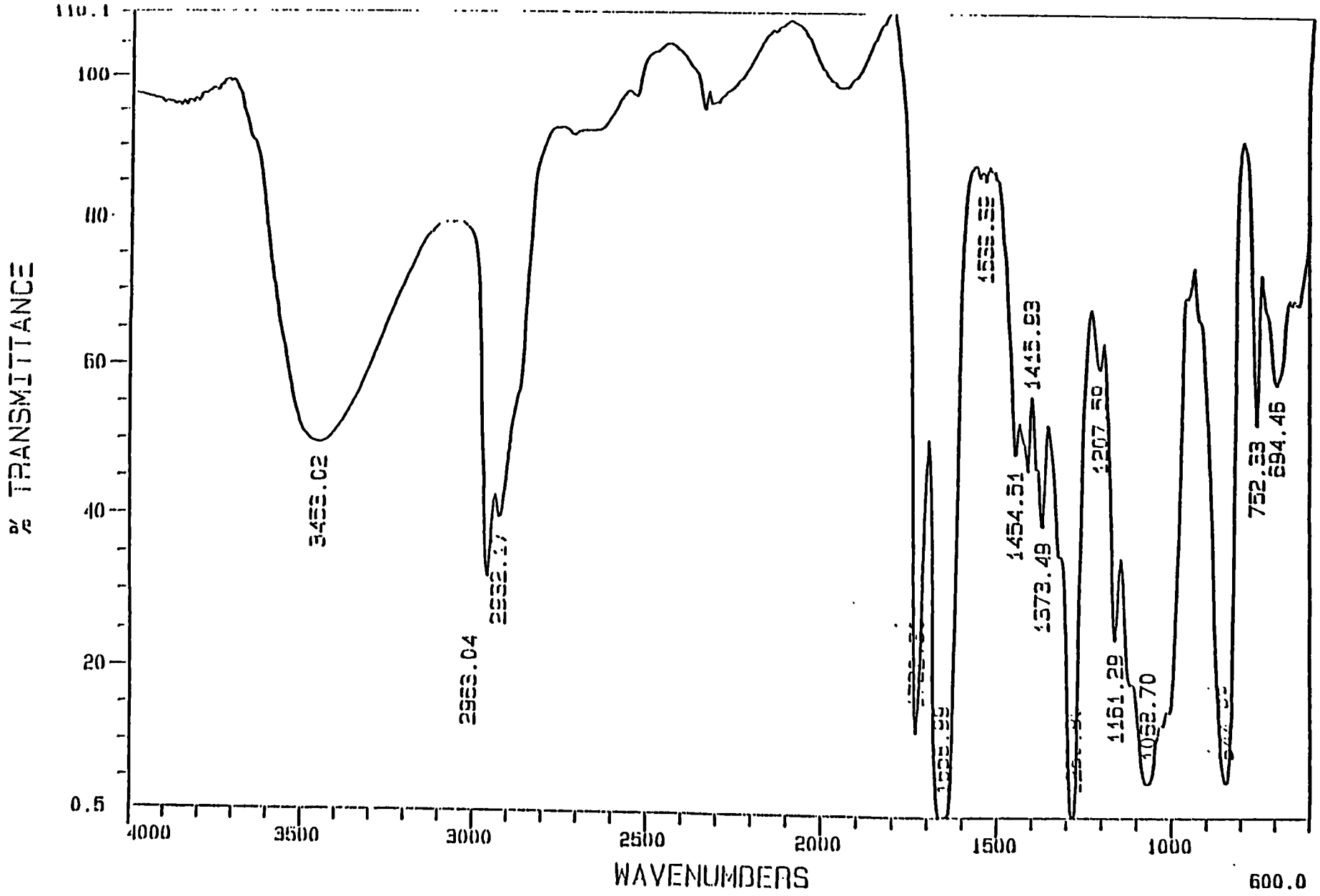

Figure 3.10 Spectrum for cellulose nitrate tortoiseshell jewellery box

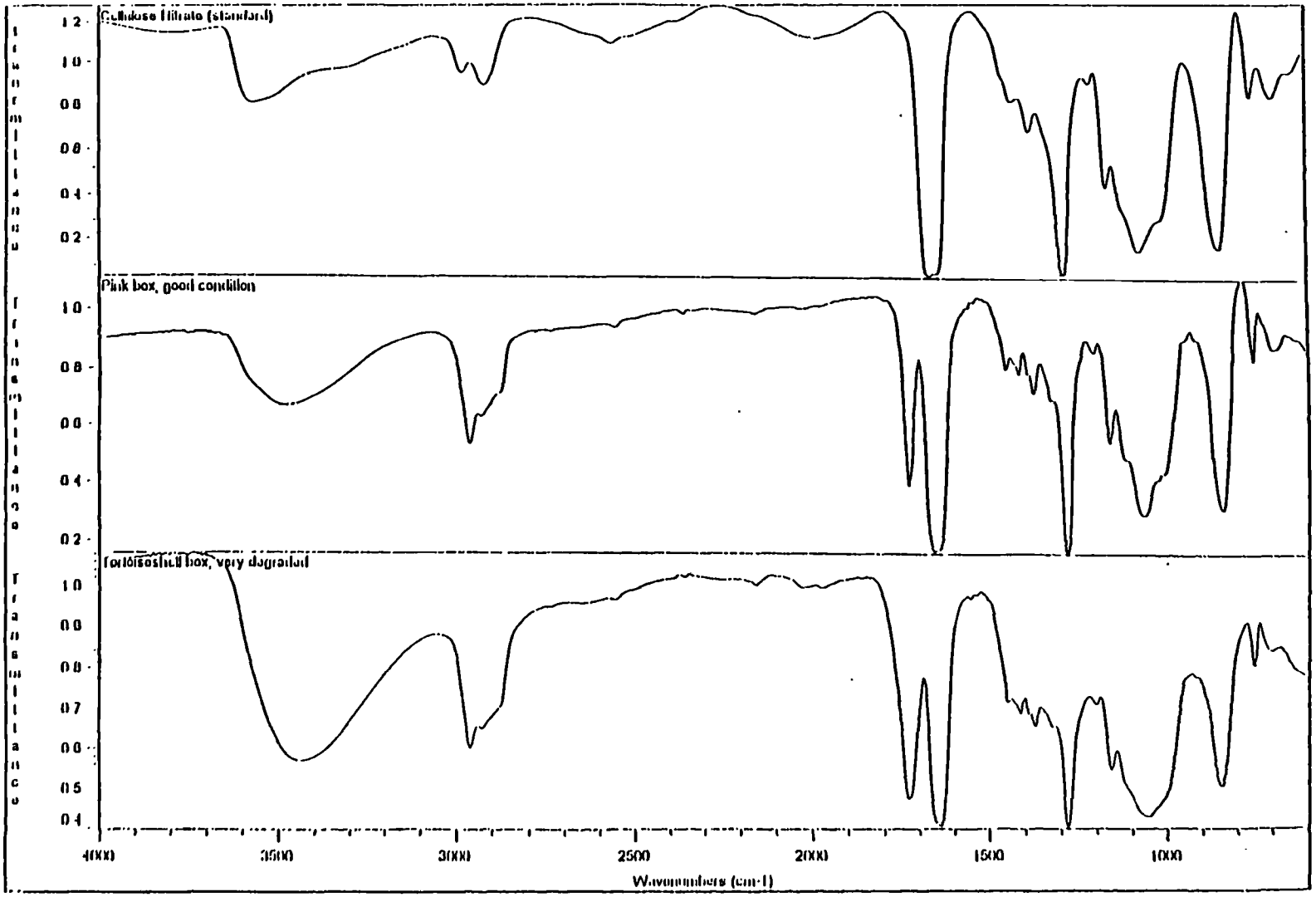

Figure 3.10 Spectra for cellulose nitrate standard (top), pink jewellery box (10) and the tortoiseshell box (1).

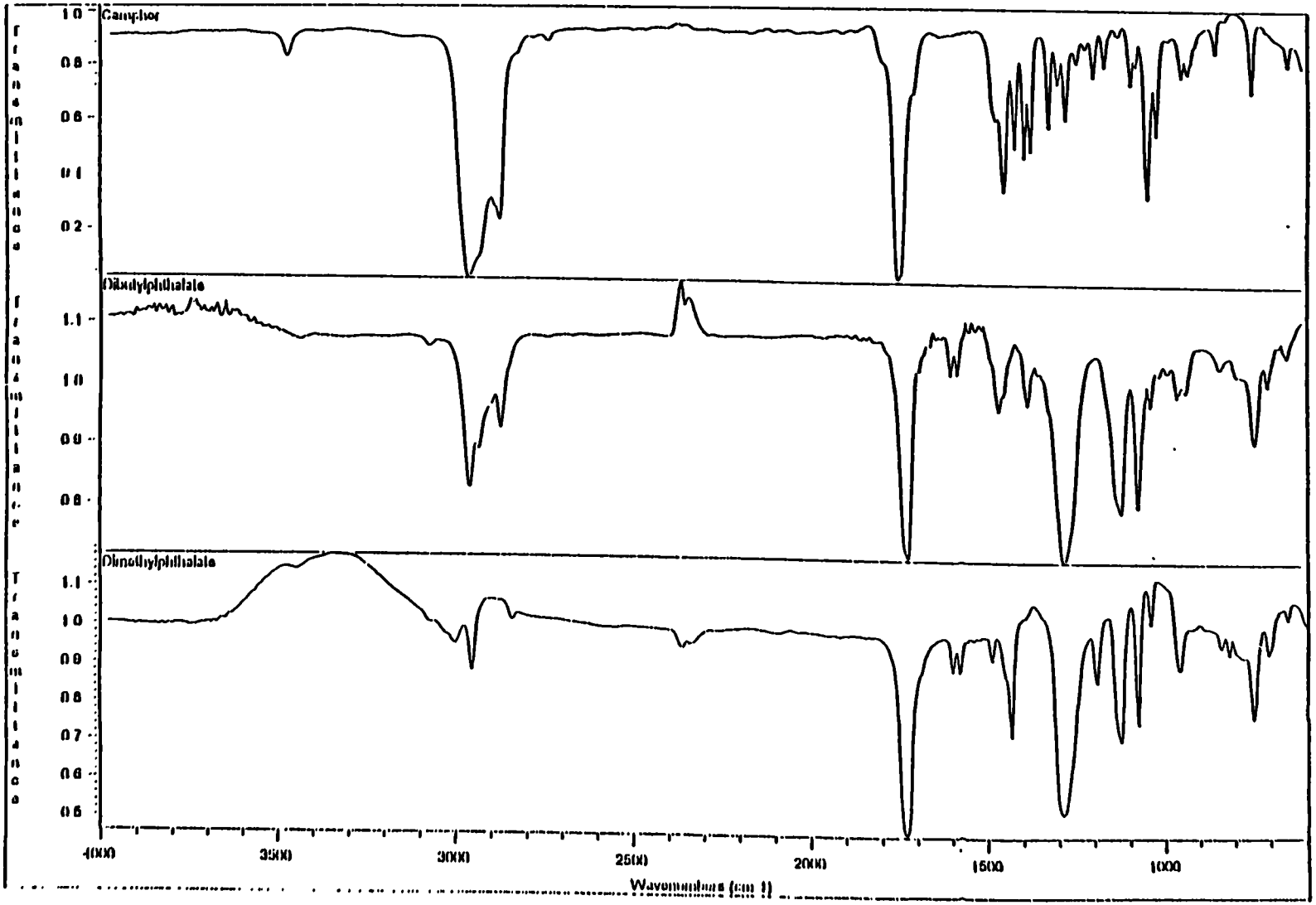

Figure 3.11 Spectra for camphor, dibutylphthalate and dimethyl phthalate

Table 3.3 Principal peak frequencies in cellulose nitrate spectrum (unplasticised) [5].

Frequency (cm^{-1})	Assignment
3300 - 3500	OH stretching
2970	CH_2 asymmetric stretching
2930	CH stretching
1650	NO_2 asymmetric stretching
1415	CH_2 bending
1380	CH bending
1280	NO_2 symmetric stretching
1160	asymmetric ring stretching
1118	asymmetric ring stretching
1070	C-O stretching in C_1-O-C_4
840	O-NO_2 stretching
750	O-NO_2 deformation
694	O-NO_2 deformation

FTIR was also used to identify the plasticiser (and if possible any other constituents), used in the manufacture of the artefacts. Spectra for three possible plasticisers, camphor, dibutylphthalate and dimethylphthalate are shown in Figure 3.11. Camphor was identified as the plasticiser in all of the artefacts. It has principal peaks at 1733 cm^{-1} (the carbonyl group in the molecule), 2963 cm^{-1} and 2874 cm^{-1}.

Phthalate esters were commonly used in the manufacture of cellulose nitrate artefacts after 1940 [6]. They also have a principal peak at approximately 1735 cm^{-1} , and peaks at 1286, 1130 and 1074 cm^{-1}. These latter three peaks could not be seen in the spectra of the artefacts, but they could be masked by cellulose nitrate absorbances. It is possible that phthalate esters are present in a few of the artefacts.

Additives such as dyes or colourants could not be identified from the spectra because of their low concentrations (typically $\mu g\ g^{-1}$) in the plastics.

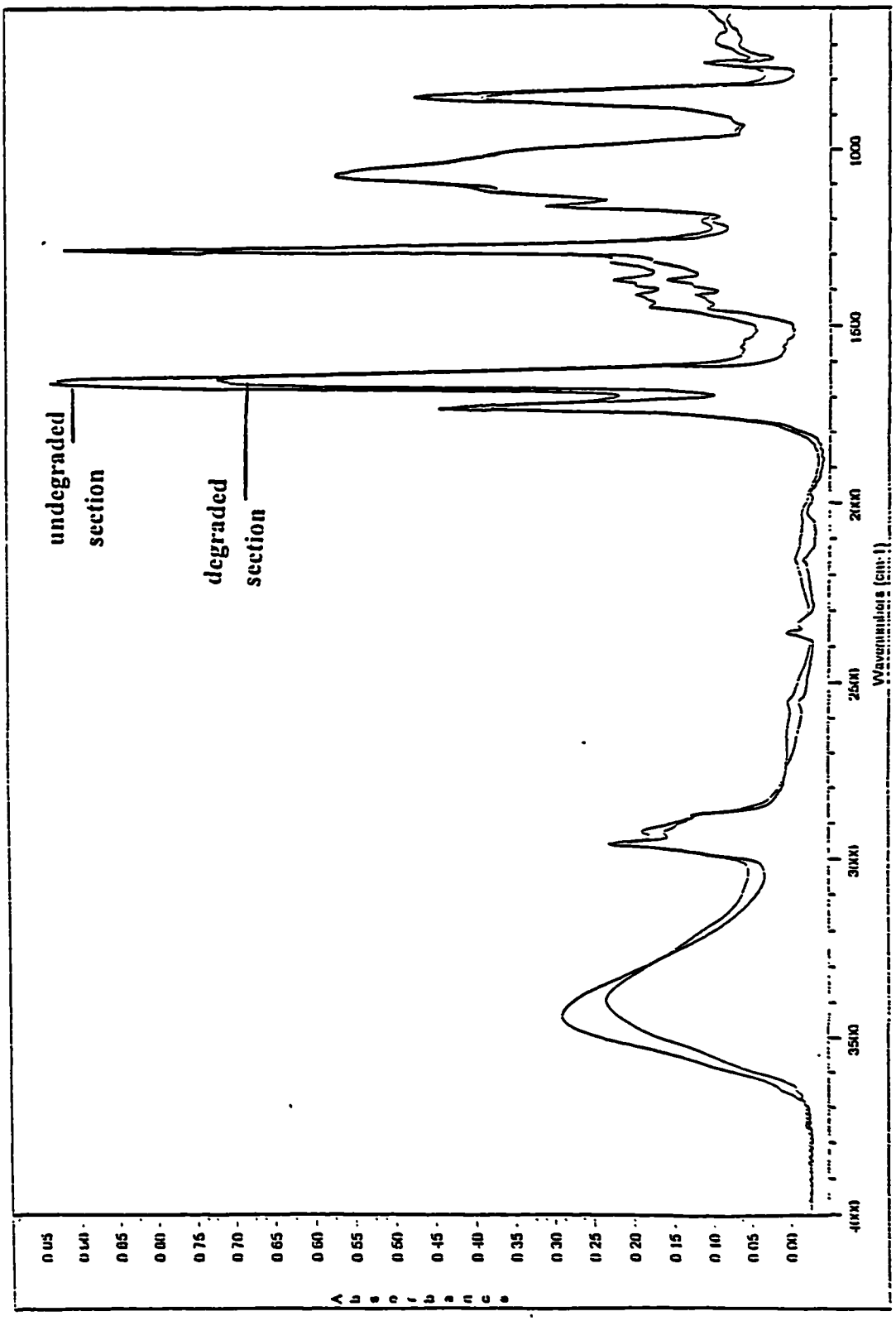

Figure 3.12 Spectra for degraded and undegraded sections of tortoiseshell handbag handle (2).

3.3.4 Assessment of degradation

Spectra were compared between artefacts which were visibly degraded and artefacts which appeared to be in very good condition. In addition, spectra were recorded for degraded and undegraded sections of the same artefact. It was hoped that any differences noted in the spectra might give an indication to the processes of degradation that were occurring in the artefacts. Figure 3.12 compares two spectra taken from an undegraded and a degraded section of the tortoiseshell handbag handle.

A couple of observations could be made from the initial comparison of spectra. The nitrate groups in the cellulose nitrate spectra, principally at 1650 cm^{-1}, showed appreciable differences between samples. There seemed to be a definite reduction in the absorbance for degraded samples compared to samples from undegraded cellulose nitrate. This decrease in absorbance for the nitrate group would correlate with loss of nitrogen as cellulose nitrate degrades to form nitrogen oxide and nitrogen dioxide.

The carbonyl group absorption at approximately 1733 cm^{-1} also appeared to be reduced for the more degraded samples, presumably as plasticiser has been lost.

It was necessary to develop a method that could be used to quantify the extent of degradation in the cellulose nitrate artefacts. A method of calculating the ratio of heights of peaks which appear in the spectra was adopted to study the degradation. The extent of degradation was quantified by ratioing the peak height absorbance of a functional group which was affected by degradation, against one which was unaffected. It had been suggested by Jutier [5] that the ether absorption, at 1070 cm^{-1}, remained relatively unchanged for cellulose nitrate samples showing varying extents of degradation. Although some of these ether bonds may have been broken, from hydrolytic degradation of the cellulose nitrate chain, it was presumed that insufficient chain destruction had occurred to significantly alter this peak. Therefore, the absorbance of the peaks of interest, i.e. the nitrate group (1650 cm^{-1}) and the plasticiser carbonyl group (1733 cm^{-1}) were ratioed against the absorbance of the ether group (1070 cm^{-1}) for every sample.

Other authors, [7-9] have used ratios of peaks at 1650 cm^{-1} : 1733 cm^{-1} to monitor the loss of nitrogen during degradation. Here, they attribute the peak at 1733 cm^{-1} simply to carbonyl impurities in cellulose nitrate, formed during degradation.

Table 3.4 **IR ratios for a selection of cellulose nitrate artefacts showing varying extents of degradation. Peak absorbances ratioed against ether peak absorbance (1070 cm^{-1}).**

a) Undegraded artefacts

Sample	IR ratio nitrate peak (1650:1070 cm^{-1})	IR ratio carbonyl peak (1733:1070 cm^{-1})
Pink jewellery box (10)	2.1 ± 0.1	1.4 ± 0.1
Yellow jewellery box (13)	2.0 ± 0.1	1.3 ± 0.1
Napkin ring (17)	1.8 ± 0.1	1.3 ± 0.2
Tshell jewellery. box (15)	1.9 ± 0.1	1.3 ± 0.1
Yellowed container (14)	1.7 ± 0.1	1.4 ± 0.1
Hair clip (18)	1.9 ± 0.1	1.2 ± 0.1

b) Degraded artefacts

Sample	IR ratio nitrate peak (1650:1070 cm^{-1})	IR ratio carbonyl peak (1733:1070 cm^{-1})
Tortoiseshell box (1)	1.3 ± 0.1	0.7 ± 0.2
Tshell handbag handle (2)	1.2 ± 0.1	1.1 ± 0.2
Station pointer (7)	1.2 ± 0.1	0.9 ± 0.2
Sun compass (8)	1.2 ± 0.05	0.8 ± 0.1
Set square (5)	1.6 ± 0.05	1.2 ± 0.1
Green box (4)	1.4 ± 0.1	1.0 ± 0.2

For each artefact, two samples were taken and two spectra recorded for each sample (i.e. n = 4).

Mean and standard deviation reported above.

Absorbance measurements between 0.2 and 1.0.

Table 3.5 **IR ratios for a selection of cellulose nitrate artefacts showing varying extents of degradation within the artefact. Peak absorbances ratioed against ether peak absorbance (1070 cm^{-1}).**

Sample		IR ratio nitrate peak (1650:1070 cm^{-1})	IR ratio carbonyl peak (1733:1070 cm^{-1})
Tortoiseshell box (1)	undegraded section	1.4 ± 0.05	0.7 ± 0.1
	degraded section	1.2 ± 0.05	0.7 ± 0.05
Handbag handle (2)	undegraded section	1.4 ± 0.1	1.2 ± 0.1
	degraded section	1.2 ± 0.1	1.1 ± 0.2
Boothook (3)	undegraded section	1.7 ± 0.05	1.1 ± 0.1
	degraded section	1.2 ± 0.1	0.9 ± 0.1
Pink lid (6)	undegraded base	1.8 ± 0.1	1.3 ± 0.05
	degraded coating	1.2 ± 0.1	0.8 ± 0.05
Set square (5)	undegraded section	1.5 ± 0.2	1.2 ± 0.2
	degraded section	1.5 ± 0.1	0.9 ± 0.2

For each artefact, two samples were taken and two spectra recorded for each sample (i.e. n = 4).
Mean and standard deviation reported above.
Absorbance measurements between 0.2 and 1.0.

However, this ratio cannot be used with artefacts containing camphor or phthalate esters, as the peak does not remain constant between samples.

Table 3.4 compares the ratios of absorption peaks in cellulose nitrate artefacts exhibiting varying extents of degradation. The peak ratio for 1650 : 1070 cm^{-1} shows a definite decrease for artefacts in very good condition to those showing severe effects of degradation. It may be assumed that, generally, all artefacts were manufactured with more or less the same nitrogen content (10-11%). This trend therefore confirms that significant denitration has occurred in the deteriorated artefacts.

Similarly the peak ratios for 1733 : 1070 cm^{-1} show a decrease from undegraded artefacts to degraded ones. This decrease in the carbonyl group is not as distinct when compared to the loss of nitrate. This is probably due to three reasons. First, the loss of plasticiser as an artefact degrades is an unsystematic process which is dependent on many factors. Therefore correlations with degradation are very difficult to predict. Secondly, it has been suggested by Edge [7], that as cellulose nitrate degrades, carbonyl groups are formed on the cellulose nitrate chain. Carbonyl formation would only slightly affect the absorbance at 1733 cm^{-1}, if at all, as the concentration of camphor in the artefacts is significantly higher. Finally, the sampling technique used to record the spectra may cause inaccurate results. Camphor is a volatile compound, and as the sample is crushed between diamond windows, some losses will probably occur.

Table 3.5 compares IR ratios of nitrate/plasticiser absorption groups in degraded sections of artefacts when compared to sections that appear less degraded. Again a reduction in the absorbance for nitrate and plasticiser is seen. However, differences between sections of the same objects are not as great as those seen when comparing different artefacts. The results do suggest though, that some areas of an artefact have undergone greater denitration and loss of plasticiser than other areas.

Later work in this project involving molecular weight analysis of the artefacts (described in Chapter 6) indicated that some chain scission may have occurred in the degraded artefacts. Although this probably has very little effect on the ether absorption in the FTIR spectra, it cannot be assumed that the absorbance is completely constant for all the artefacts. The peaks at 1118 cm^{-1} and 1160 cm^{-1} are

both associated with the ring structure of cellulose nitrate and degradation should affect them to a lesser extent. Both these peaks have a medium intensity in the cellulose nitrate spectrum, however in some spectra, the peak at 1118 cm^{-1} is not fully resolved from the ether peak at 1070 cm^{-1}. Quantitative analysis is therefore easier to perform using the peak at 1160 cm^{-1}.

Tables 3.6 and 3.7 show the IR ratios for the same samples as before, this time using the peak at 1160 cm^{-1} to calculate the ratios. The results again show a definite decrease in the absorption of the nitrate and carbonyl peaks between undegraded and degraded samples. However, because of the poor precision for the results, it is impossible to determine whether using this peak to calculate IR ratios, has any benefits.

Precision of FTIR microspectroscopic technique

For the IR ratios reported in Tables 3.4 to 3.7, each artefact was sampled two times from the same area. For each sample, two IR spectra were recorded, the average result reported in the tables. It can be seen that there is considerable variation in the results. It was decided therefore to determine the precision of both the FTIR measurement and the sampling procedure.

In the first case a sample was prepared and placed on the microscope stage. The background spectrum was recorded, followed by the sample. This was then repeated a further seven times so that eight spectra were produced for the same sample; the IR ratios were then calculated. Three different artefacts were sampled, the pink jewellery box, the tortoiseshell jewellery box and the tortoiseshell box. The relative standard deviations are shown in Table 3.8. The precision is fair for the three artefacts, approximately 5%.

The precision of the sampling procedure was also determined. Eight samples were taken from the same area of an artefact and the IR spectrum recorded. This was carried out for the same three artefacts. The relative standard deviations are shown in Table 3.9. The precision is extremely poor for all the artefacts. The precision is worse for the tortoiseshell box, compared to the other artefacts, presumably because the extent of denitration and plasticiser loss is not constant throughout the artefact. The IR ratios for the carbonyl peak generally show poorer precision than the nitrate peak due to the reasons stated earlier, i.e. carbonyl impurity formation and loss of camphor through crushing the samples.

Table 3.6 **IR ratios for a selection of cellulose nitrate artefacts showing varying extents of degradation. Peak absorbances ratioed against ring stretching peak absorbance (1160 cm^{-1}).**

a) Undegraded artefacts

Sample	IR ratio nitrate peak (1650:1160 cm^{-1})	IR ratio carbonyl peak (1733:1160 cm^{-1})
Pink jewellery box (10)	4.6 ± 0.1	3.3 ± 0.1
Yellow jewellery box (13)	4.3 ± 0.1	3.0 ± 0.2
Napkin ring (17)	4.1 ± 0.1	3.3 ± 0.3
Tshell jewellery. box (15)	4.2 ± 0.1	3.0 ± 0.2
Yellowed container (14)	4.2 ± 0.1	3.4 ± 0.2
Hair clip (18)	3.8 ± 0.2	2.8 ± 0.3

b) Degraded artefacts

Sample	IR ratio nitrate peak (1650:1160 cm^{-1})	IR ratio carbonyl peak (1733:1160 cm^{-1})
Tortoiseshell box (1)	3.0 ± 0.2	1.8 ± 0.1
Tshell handbag handle (2)	2.9 ± 0.1	2.6 ± 0.4
Station pointer (7)	2.8 ± 0.2	2.2 ± 0.3
Sun compass (8)	2.8 ± 0.1	2.0 ± 0.1
Set square (5)	3.7 ± 0.1	2.9 ± 0.3
Green box (4)	3.4 ± 0.2	2.4 ± 0.4

For each artefact, two samples were taken and two spectra recorded for each sample (i.e. four spectra per artefact)

Mean and standard deviation reported above.

Absorbance measurements between 0.2 and 1.0.

Table 3.7 **IR ratios for a selection of cellulose nitrate artefacts showing varying extents of degradation within the artefact. Peak absorbances ratioed against ring stretching peak absorbance (1160 cm^{-1}).**

Sample		IR ratio nitrate peak (1650:1160 cm^{-1})	IR ratio carbonyl peak (1733:1160 cm^{-1})
Tortoiseshell box (1)	undegraded section	3.4 ± 0.1	1.9 ± 0.1
	degraded section	2.9 ± 0.2	1.8 ± 0.1
Handbag handle (2)	undegraded section	3.0 ± 0.1	2.9 ± 0.3
	degraded section	2.9 ± 0.3	2.9 ± 0.3
Boothook (3)	undegraded section	3.9 ± 0.2	2.6 ± 0.1
	degraded section	2.9 ± 0.2	2.2 ± 0.2
Pink lid (6)	undegraded base	4.2 ± 0.1	3.3 ± 0.1
	degraded coating	2.9 ± 0.3	1.9 ± 0.1
Set square (5)	undegraded section	3.7 ± 0.3	3.0 ± 0.4
	degraded section	3.5 ± 0.1	2.0 ± 0.2

For each artefact, two samples were taken and two spectra recorded for each sample (i.e. n = 4).
Mean and standard deviation reported above.
Absorbance measurements between 0.2 and 1.0.

Table 3.8 Relative standard deviations (%) for IR measurements

Sample	1650:1070 (cm^{-1})	1733:1070 (cm^{-1})	1650:1160 (cm^{-1})	1733:1160 (cm^{-1})
Pink jewellery box (10)	4	6	5	7
Tshell jewellery box (15)	4	6	4	6
Tortoiseshell box (2)	6	8	6	7

8 spectra recorded for each sample

Table 3.9 Relative standard deviations (%) for IR sampling procedure

Sample	1650:1070 (cm^{-1})	1733:1070 (cm^{-1})	1650:1160 (cm^{-1})	1733:1160 (cm^{-1})
Pink jewellery box (10)	15	21	18	20
Tshell jewellery box (15)	12	23	10	22
Tortoiseshell box (2)	24	30	25	30

8 samples taken from each artefact and spectra recorded

Determination of camphor in artefacts

An attempt was made to determine the concentration of camphor in the artefacts by preparing a series of external standards. Cellulose nitrate films were prepared containing 0-50% camphor (w:w) and spectra recorded. Unfortunately, the films prepared were unusable as standards as the absorbance did not increase linearly with concentration. This was probably due to the extremely non-homogeneous nature of the standards; the camphor may not have been evenly mixed throughout the films during preparation. The films did however show that there is a significant shift in the position of the carbonyl peak to lower wavenumbers as the concentration of camphor decreases.

The spectrum for pure camphor has a carbonyl peak at 1744 cm^{-1} (see Figure 3.11). For films containing 40-50% camphor, the peak is shifted to 1736 cm^{-1}. For films containing 5-35% camphor, the peak is shifted further to 1732 cm^{-1} and films containing <5% camphor show a carbonyl peak at 1728 cm^{-1}. This shift may indicate that, in high concentrations, the camphor forms discrete pockets within the plastic framework, but at lower concentrations hydrogen bonding occurs between the cellulose nitrate and camphor.

3.4 Conclusions

A thorough visual examination can be used to spot the very initial symptoms of degradation in cellulose nitrate artefacts, i.e. discolouration, surface blooming and blistering, or cracking. However, this will require regular, time-consuming examinations of collections, which are usually not practicable. The technique of FTIR microspectroscopy is well suited for identifying the composition of historical cellulose nitrate plastics and has potential for the quantitative assessment of their degradation. This could prove particularly useful for evaluating visibly undegraded materials which may be starting to deteriorate.

The cellulose nitrate artefacts seemed to degrade through two main mechanisms, a denitration process resulting in loss of $O\text{-}NO_2$ groups on the polymer chain, and a

general loss of plasticiser. Both these mechanisms could be assessed and monitored using FTIR microspectroscopy, although poor precision indicated that the procedure had its limitations.

References

1. Shashoua, Y., Bradley, S. M. and Daniels, V. D., *Studies in Conservation*, 1992, 37, 113-119.

2. Morgan, J. in *"Saving the 20th Century"*, Grattan, D. W., (ed.), Canadian Conservation Institute, Ottawa, 1993, 43-50.

3. Derrick, M. and Stulik, D., in *"Saving the 20th Century"*, Grattan, D. W., (ed.), Canadian Conservation Institute, Ottawa, 1993, 169-182.

4. Kozloski, L. D., Baker, M. T. and McManus, E., Preprints from ICOM committee for conservation, 1993, 308-313.

5. Jutier, J. J., Harrison, Y., Premont, S. and Prud'homme, R. E., *Journal of Applied Polymer Science*, 1987, 33, 1359-1375.

6. Reilly, J. A., *Journal of the American Institute of Conservation*, 1991, 30, 145-162.

7. Edge, M., Allen, N. S., Hayes, M., Riley, P. N. K., Horie, C. V. and Luc-Gardette, J., *European Polymer Journal*, 1990, 26, 623-630.

8. Hon, D. N. S., and Tang, L., *Polymer Photochemistry*, 1986, 7, 299-310.

9. Shashoua, Y., Bradley, S. M. and Daniels, V. D., *Studies in Conservation*, 1992, 37, 113-119.

CHAPTER FOUR

ANALYSIS OF ARTEFACTS

Chapter Four - Contents

4.1 Introduction

A more thorough analysis of the artefacts was required to identify compositional differences between samples, which may relate to degradation. The presence of additives, trace impurities or residual acids in the plastics may offer clues as to why certain artefacts have degraded. If degradation products were also detected in the artefacts, information regarding the processes of deterioration could be provided.

Ion chromatography was used for the simultaneous detection of a number of individual components in a sample. A number of inorganic and organic anions can be detected, including; fluoride, chloride, nitrate, nitrite, phosphate, bromide, sulphate, oxalate, acetate and formate. Similarly, mono and di-valent cations can be measured including; sodium, potassium, ammonium, magnesium and calcium. The technique is widely used where the capability to detect very low concentrations of ions is required and has previously found applications in conservation science [1, 2].

X-ray fluorescence spectroscopy and atomic absorption spectroscopy were used as complementary techniques for metal analysis of the artefacts. XRF allowed the simultaneous analysis of artefacts to assess qualitatively their metal content. AAS was selected as it can provide quantitative analysis of solutions for trace metals.

Elemental analysis of the artefacts was used to determine their total nitrogen content.

4.2 Experimental

4.2.1 Sample preparation

Aqueous extracts of artefacts

Samples were removed from the artefacts using a scalpel and were crushed or chopped as thoroughly as was possible. Aqueous extracts were obtained from each of the artefacts, by steeping approximately 50 mg of plastic in 20 mL distilled water for 24 hours. This period of 24 hours was found to be the shortest time required to extract all the material. Samples were then filtered before analysis.

Ashing of artefacts

Samples were also prepared by ashing the plastic in a muffle furnace and then dissolving the residual ash for analysis. Approximately 0.1 g of plastic was removed from the artefact, crushed and placed in a clean silica crucible. 3g of magnesium oxide (AnalaR, BDH Chemicals Ltd.) was added and mixed with the sample. The samples were than placed in a Gallenkamp furnace and heated very gradually to 200 °C, over 1 hour. The temperature was then raised to 500 °C and maintained for 4 hours. The crucibles were then allowed to cool. Upon ignition, the magnesium oxide fused with the polymer and provided a matrix in which all the components being determined were retained - only the organic material was lost. The residual ash and crucible washings were dissolved in 5% nitric acid for analysis.

Initial work suggested that losses were occurring due to the cellulose nitrate combusting too quickly and compounds of interest being lost in a gaseous form. To overcome this, 0.5 g sucrose (Fisons) was added to the mixture in the crucible, to slow the combustion process. Furthermore, to obtain intimate contact between the sample and the ashing mixture, acetone was added to the crucible and left for 5 hours before ashing.

For analysis using ion chromatography or atomic absorption spectroscopy, two samples were prepared from each artefact. Each sample was then analysed in duplicate. This gave a total of four measurements for each artefact. Blank solutions were prepared throughout and the concentrations reported are blank corrected. For elemental microanalysis, two samples were removed from an artefact and analysed, giving a total of two measurements.

4.2.2 Ion chromatography

Initial work was carried out using a Dionex 4000i ion chomatograph to determine the quantity of anions present in samples. The 4000i comprised an EDM 2 Dionex eluent degas module, Dionex gradient pump and Dionex conductivity detector. The main analytical column was the Dionex Chromatography IONPAC® AS4 with an AG4A guard column. A 0.75 mM sodium carbonate - 2.2 mM sodium bicarbonate eluent (AR-Fisons) was used, with a flow rate of 2 mL min^{-1}. Suppression was performed using a Dionex anion micromembrane suppressor, model AMMS-I. The

external regenerant source was provided using 10 mM sulphuric acid (AR- BDH Chemicals Ltd.). A Trio Trivector integrator was used to collect the results.

For later work, a Dionex DX 100 ion chromatograph was used. It comprised a Dionex single piston pump and Dionex conductivity detector. For anion analysis, Dionex Chromatography IONPAC® AS5 analytical and guard columns were used with a 0.75 mM sodium carbonate - 2.2 mM sodium bicarbonate eluent (AR-Fisons), delivered at 2 mL min^{-1}. Suppression was performed using a Dionex anion self-regenerating suppressor, ASRS-I. A Dionex integrator was used to collect the data. For cation analysis, Dionex Chromatography IONPAC® CS12 analytical and guard columns were used with 18 mM methane sulphonic acid eluent (>99% pure- Fluka Chemicals Ltd.), delivered at 1 mL min^{-1}. Suppression was performed using a Dionex cation self-regenerating suppressor, CSRS-I.

Solutions containing different ion concentrations were prepared by diluting stock solutions of analytes (1000 μg mL^{-1}) with distilled water. Calibration graphs for each analyte were prepared by injecting increasing concentrations of ions.

4.2.3 X-ray fluorescence spectroscopy

The samples were analysed directly using a Canberra Energy Dispersive XRF system. No sample preparation was required. The area of the artefact to be analysed was placed in the Xray beam. A rhodium source was incorporated, operating at 0.3 mA and 46 kV. The spectra were recorded over 100 seconds.

4.2.4 Atomic absorption spectroscopy

Electrothemal AAS

A Perkin Elmer (PE) 3030 atomic absorption spectrometer was used, with a PE HGA 500 furnace and a PE AS40 autosampler. Pye Unicam hollow cathode lamps were used throughout. The conditions for the char and atomisation steps were based on conditions recommended by the manufacturer. These were slightly altered to obtain the maximum signal (see Table 4.1).

Table 4.1 Instrumental conditions for analysis by electrothermal AAS

element	wavelength (nm)	bandpass (nm)	char temp, ramp, hold			atomisation temp, ramp, hold		
			(°C)	(s)	(s)	(°C)	(s)	(s)
Cu	324.8	0.5	850	5	30	2100	0	5
Fe	248.3	0.2	1200	5	25	2000	1	5
Pb	217.0	0.5	500	5	25	2000	0	4
Zn	213.9	0.5	500	5	30	1600	0	5

Table 4.2 Instrumental conditions for analysis by flame AAS

element	wavelength (nm)	bandpass (nm)	lamp current mA	fuel flow rate	burner height (cm)
Cu	324.8	0.5	4	21	5
Fe	248.3	0.5	12	24	10
Pb	217.0	0.5	5	21	5
Zn	213.9	0.5	8	22	5

For each sample analysis, 20 μL of sample solution was injected into a pyrolytically coated graphite tube. The tube was then heated to a dry stage at 150 °C for 25 secs to remove the solvent, followed by the char and atomisation stages. The tube was then heated to a clean stage at 2500 °C for 5 secs, to remove any residual salts, before the next injection.

Flame AAS

Analyses were carried out using a Philips PU 9100 atomic absorption spectrometer, incorporating Pye Unicam hollow cathode lamps. An air-acetylene flame was used for all analyses. The instrumental conditions were first optimised for each element by varying the fuel flow rate and the observation height in the flame so that the maximum signal was achieved. The conditions used for the analyses are given in Table 4.2. A small injection volume of 50 μL was needed because of the limited sample volume remaining after analysis by ion chromatography. This was introduced by using a micropipette to inject the sample solution into the nebuliser.

Solutions containing different metal concentrations were prepared by diluting stock solutions of analytes (1000 μg mL^{-1}) with distilled water. Calibration graphs for each analyte were prepared by injecting increasing concentrations of metals.

4.2.5 Elemental microanalysis

The microanalysis department at the university was able to provide total nitrogen concentrations for the samples. The analysis of the samples was performed using a Perkin Elmer 2400 analyser (as described in 2.6). Approximately 20 mg of sample was required for each analysis.

4.3 Results and discussion

4.3.1 Analysis of artefacts using XRF spectroscopy

All the artefacts were examined by XRF to assess their metal content. Artefacts which had an opaque appearance gave a strong signal for zinc; e.g. the pink jewellery

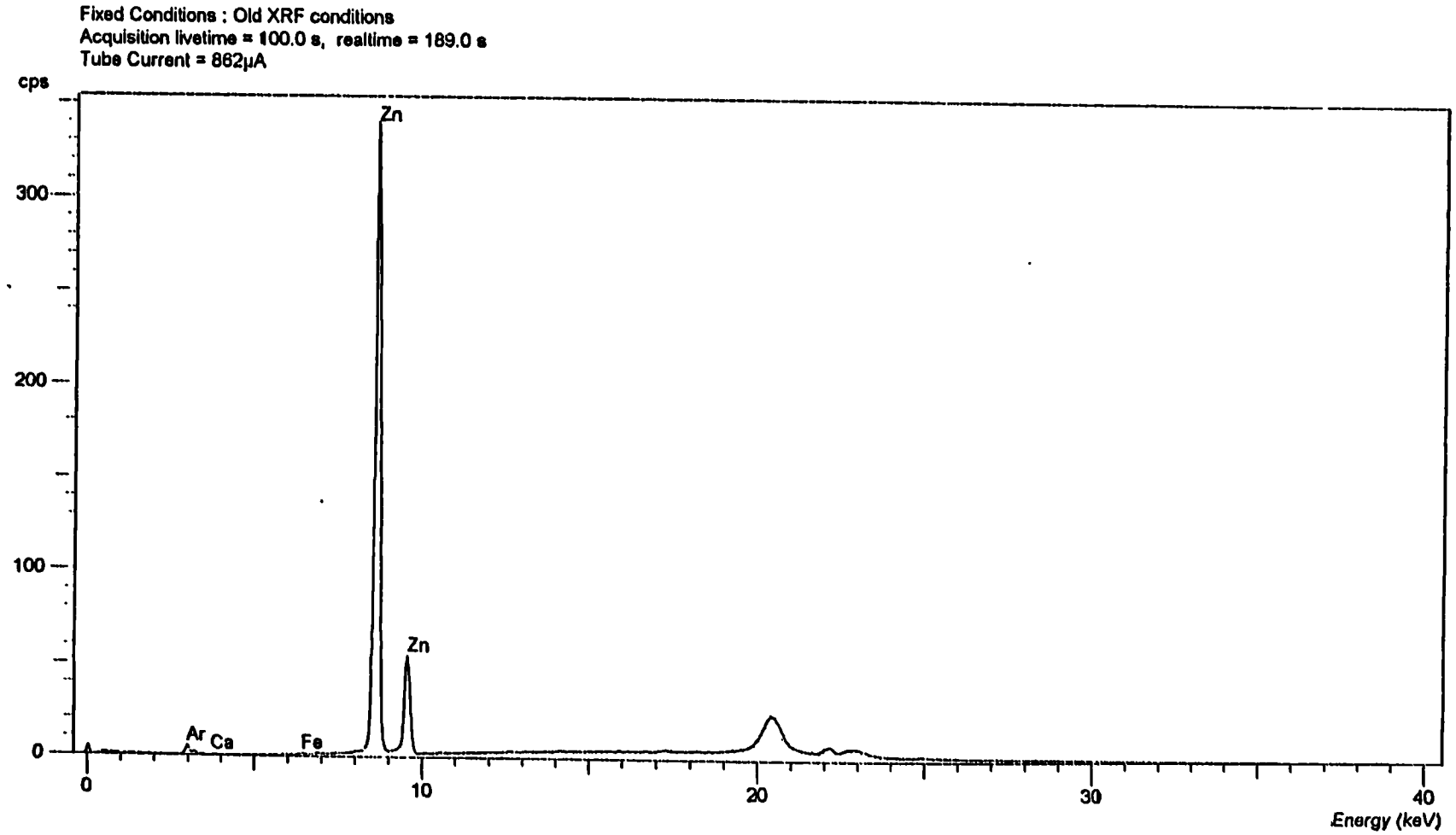

Figure 4.1 XRF spectrum for the napkin ring (sample number 17).

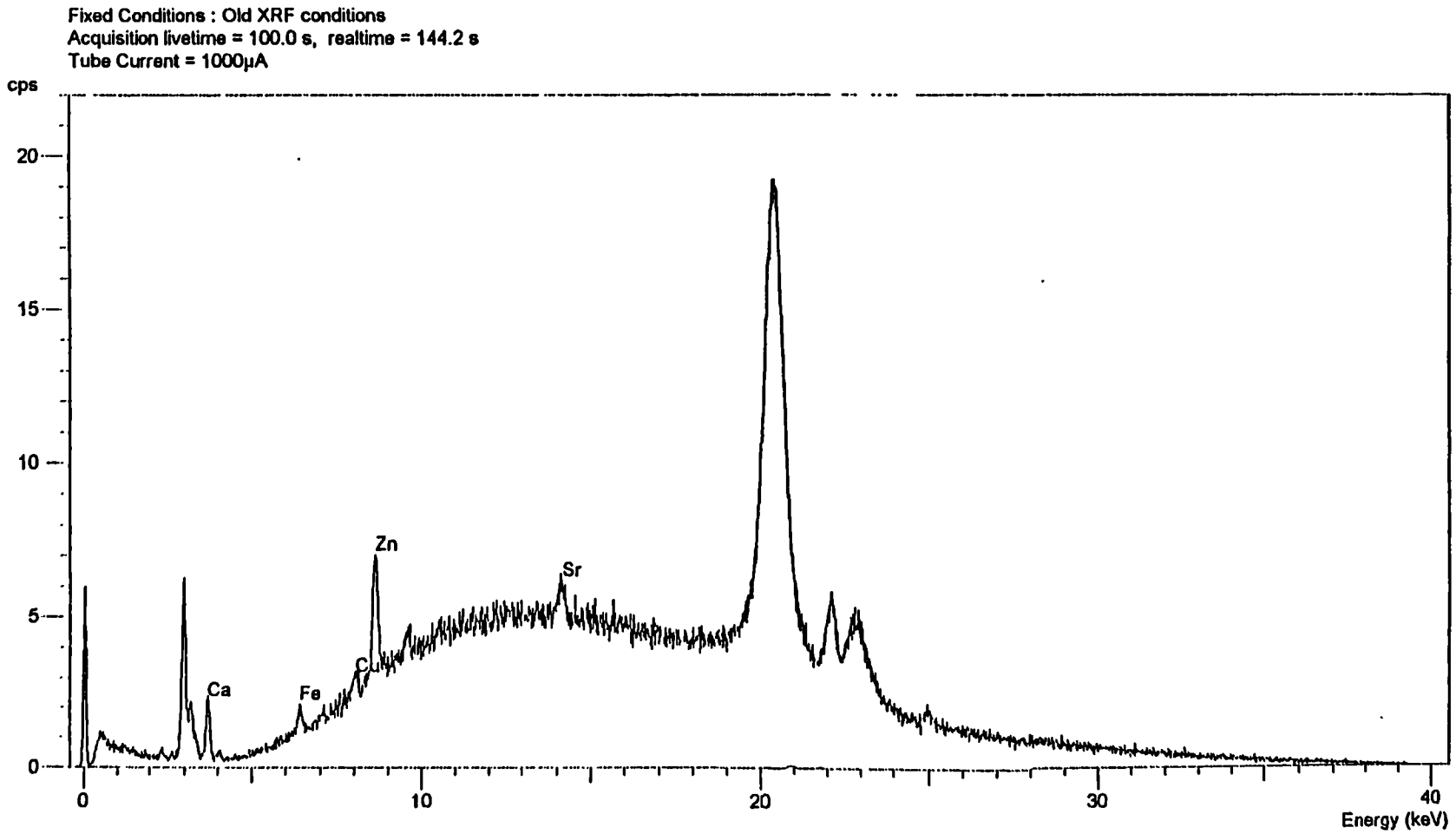

Figure 4.2 **XRF spectrum for the cellulose nitrate handbag handle (sample number 2)**

Table 4.3 Major and minor/trace elements found in artefacts by XRF spectroscopy

sample	major elements	trace elements
(1) tortoiseshell box		zinc, copper, iron, lead
(2) handbag handle		copper, zinc
(3) boothook		iron
(4) green box		
(5) set square		
(6) pink lid base coating	zinc	titanium iron, zinc
(7) station pointer		zinc
(8) sun compass		zinc, iron
(9) fan handle		iron, zinc
(10)pink jewellery box	zinc	titanium
(11) blue mirror		calcium, zinc, lead
(12) tortoiseshell lid		zinc, copper, iron
(13) yellow jewellery box	zinc	
(14) yellowed container		calcium, lead
(15) tort. jewellerey box		
(16) tortoiseshell handle		copper,iron, calcium, lead
(17) napkin ring	zinc	lead, iron
(18) hair clips		zinc, iron

box, the yellow jewellery box and the base of the pink lid. The XRF spectrum for the napkin ring is shown in Figure 4.1. The peak at 9.6 keV corresponds to the Zn Kα1 line and the peak at 8.7 keV corresponds to the Zn Kα2. The peaks at 20.6, 22.1 and 23.0 keV are attributed to scatter radiation from the rhodium tube and not the sample. The scatter peaks should be constant for all analyses. The strong zinc signal for these artefacts is probably due to zinc oxide being used as a filler in their manufacture.

Other elements were detected in the artefacts, e.g. copper, iron, calcium, lead and titanium (see Table 4.3). Figure 4.2 shows the XRF spectrum for the tortoiseshell handle, in which these metals are identified. These elements gave very weak signals and are present in only trace concentrations.

The artefacts containing high levels of zinc were in better condition than those without. No other differences relating inorganic composition to condition of the artefacts, could be determined. Likewise, XRF spectra from artefacts showing varying degrees of deterioration appeared identical.

4.3.2 Analysis of aqueous extracts of artefacts

Determination of anions by ion chromatography

Analysis revealed that many anions were present in the aqueous extracts of the objects studied. Acetate, formate, chloride, nitrate, sulphate and oxalate were all detected. Quantitative analysis of the solutions was carried out (Table 4.4). The overall anion content was considerably higher in the more degraded artefacts. This may be partially explained by the fact that these artefacts are embrittled and cracked and are generally crushed to smaller particles during sample preparation, compared to samples in good condition. During extraction, the water will have more contact with these samples and also an increased accessibility to the ions for hydrolysis.

The sulphate levels were generally greater for the more degraded samples. The sulphate may be due to residual acid left over from the manufacturing process or sulphate ester groups, present in the polymer, that have been hydrolysed by the water during steeping. The presence of sulphate is, therefore, the result of an inadequate stabilisation stage during the cellulose nitrate manufacture. As high sulphate levels are only seen in the artefacts which are degraded, it is probable that the sulphate has

initiated or accelerated the deterioration. As mentioned in 1.4.3, residual sulphuric acid in the artefacts will severely degrade the polymer as will sulphate groups which are hydrolysed to acids in the presence of water.

Oxalate levels were similarly higher for the more degraded samples. The oxalate may be present for a number of reasons. Oxalic acid was commonly used as a bleaching agent in the manufacture of cellulose nitrate [3]. It may also be a product from the purification treatment of the original cellulose using sodium hydroxide as alkaline degradation of cellulose results in the product of oxalic acid [4]. The most probable explanation is that oxalate is produced by normal degradation processes of cellulose nitrate [5]. For this to be possible, severe deterioration of the cellulose nitrate chain must occur. If it does, then this probably also explains the presence of acetate and formate in the samples. The exact degradation mechanism is unknown and is likely to be very complex. Joutier *et al* [6] have reported a possible degradation scheme that may result in the production of small, organic compounds such as oxalate, acetate and formate.

The levels of nitrate were often higher in extracts from deteriorated artefacts. Nitrogenous gases trapped within these artefacts could have been hydrolysed by the steeping in water. Nitric acid may also be present in these artefacts as a result of hydrolytic degradation. Some of the artefacts in very good condition were also found to have high nitrate levels, i.e. the pink jewellery box and the tortoiseshell lid. This may indicate that nitrogenous gases are forming in artefacts, before any visible deterioration is seen. The comparatively low values for some degraded artefacts may indicate that nitrogenous gases have been lost from the artefact during degradation.

Similar differences were seen between extracts from very degraded sections of artefacts and sections which were in better condition (Table 4.5). Oxalate, acetate and formate levels were generally higher in the more deteriorated samples, indicating that they are products of degradation. Nitrate levels were similar throughout the artefacts except for the pink lid. The coating of the lid was extremely degraded compared to the base which was in very good condition. Sulphate levels did not show great differences between sections of an artefact. As sulphate is most likely a residual component from the manufacturing process, it should be constant throughout an artefact.

Table 4.4 Concentration of anions in plastics, removed after steeping in distilled water.

Undegraded artefacts

sample	acetate mg g^{-1}	formate mg g^{-1}	nitrate mg g^{-1}	sulphate mg g^{-1}	oxalate mg g^{-1}
pink jewellery box (10)	<0.05	<0.05	4.2 ± 0.4	0.2 ±0.01	<0.05
yellow jewel. box (13)	<0.05	<0.05	0.5 ±0.05	0.4 ±0.02	<0.05
napkin ring (17)	<0.05	<0.05	<0.1	<0.05	<0.05
tort. jewellery box (15)	<0.05	<0.05	0.4± 0.05	<0.05	<0.05
yellowed container (14)	<0.05	<0.05	1.2 ± 0.3	0.2 ±0.01	<0.05
tortoiseshell lid (12)	<0.05	<0.05	4.0 ± 0.4	<0.05	<0.05

Degraded artefacts

sample	acetate mg g^{-1}	formate mg g^{-1}	nitrate mg g^{-1}	sulphate mg g^{-1}	oxalate mg g^{-1}
tortoiseshell box (1)	1.3 ± 0.3	0.7 ± 0.1	7.6 ± 0.9	8.1 ± 0.4	5.8 ± 0.2
handbag handle (2)	1.0 ± 0.2	0.3 ± 0.1	2.0 ± 0.3	4.0 ± 0.2	5.3 ± 0.2
station pointer (7)	1.2 ± 0.1	0.4 ±0.05	5.3 ± 0.1	6.3 ± 0.2	6.4 ± 0.5
boothook (3)	1.4 ± 0.3	0.5 ±0.05	1.8 ± 0.2	6.6 ± 0.4	1.7 ± 0.2
green box (4)	0.8 ± 0.2	0.3 ±0.05	1.6 ± 0.1	0.8 ± 0.1	1.1 ± 0.3
set square (5)	0.6 ± 0.1	0.2 ±0.05	5.2 ± 0.4	0.7 ± 0.1	5.4 ± 0.3

For each artefact, two samples were taken and two measurements taken for each sample (i.e. n= 4)

Mean and standard deviation reported above

Table 4.5 **Concentration of anions in plastics, removed after steeping in distilled water, from sections of artefacts showing varying degradation.**

sample		acetate mg g^{-1}	formate mg g^{-1}	nitrate mg g^{-1}	sulphate mg g^{-1}	oxalate mg g^{-1}
tortoiseshell box (1)	A	1.0 ± 0.2	0.5 ± 0.1	5.3 ± 0.8	8.0 ± 0.5	4.8 ± 0.2
	B	1.3 ± 0.3	0.7 ± 0.1	7.6 ± 0.9	8.1 ± 0.4	5.8 ± 0.2
handbag handle (2)	A	0.3 ±0.05	0.2 ±0.05	2.7 ± 0.3	4.0 ± 0.3	3.6 ± 0.3
	B	1.0 ± 0.2	0.3 ± 0.1	2.0 ± 0.3	4.0 ± 0.2	5.3 ± 0.2
boothook (3)	A	1.2 ± 0.2	0.2 ±0.05	1.0 ± 0.1	6.4 ± 0.3	1.3 ± 0.2
	B	1.4 ± 0.3	0.5 ±0.05	1.8 ± 0.2	6.6 ± 0.4	1.7 ± 0.2
pink lid (6)	A	<0.05	<0.05	0.5 ±0.05	<0.05	<0.05
	B	0.2 ±0.05	0.1 ±0.02	6.3 ± 0.5	0.4 ±0.05	0.9 ±0.01
set square (5)	A	<0.05	<0.05	4.8 ±0.02	0.7 ± 0.1	1.3 ± 0.1
	B	0.6 ± 0.1	0.2 ±0.05	5.2 ± 0.4	0.7 ± 0.1	5.4 ± 0.3

A = sample taken from least degraded section of artefact

B = sample taken from most degraded section of artefact

For each artefact, two samples were taken and two measurements taken for each sample (i.e. n= 4)

Mean and standard deviation reported above

Table 4.6 Concentration of cations in plastics, removed after steeping in distilled water.

sample	Na mg g^{-1}	NH_4 mg g^{-1}	K mg g^{-1}	Mg mg g^{-1}	Ca mg g^{-1}
pink jewellery box (10)	0.1 ±0.01	<0.1	<0.05	<0.05	<0.05
tortoiseshell lid (12)	0.2 ±0.01	0.5 ± 0.1	0.1 ±0.02	<0.05	<0.05
blue mirror (11)	0.7 ±0.03	<0.1	0.5 ±0.02	0.4 ±0.03	4.0 ± 0.3
green box (4)	0.1 ±0.02	0.2 ± 0.1	<0.05	<0.05	0.2 ±0.05
handbag handle (2)	0.2 ±0.03	0.7 ±0.05	0.1 ±0.05	<0.05	0.3 ±0.05
tortoiseshell box (1)	0.9 ±0.04	1.0 ± 0.1	0.6 ±0.03	0.2 ±0.05	0.4 ±0.05

For each artefact, two samples were taken and two measurements taken for each sample (i.e. n= 4)
Mean and standard deviation reported above

Determination of cations by ion chromatography

The aqueous extracts of the artefacts were also analysed by ion chromatography for the determination of cations. Sodium, ammonium, potassium, magnesium and calcium ions were identified and their concentrations measured for several artefacts (see Table 4.6). Cations were not detected for the other artefacts. It is likely that the cations present were not deliberately included chemicals, but were contaminant levels in the manufacturing materials. Their presence does not apparently influence the state of degradation.

Determination of metals by ETAAS

The extracts were analysed by ETAAS to determine what metals were being taken into solution and whether they seemed to be related to the extent of degradation (Table 4.7). The metal concentrations were generally at levels equivalent to concentration in the plastic of less than 50 μg g^{-1} and these were likely to be close to contaminant levels for the materials of manufacture. Higher levels of zinc in some samples were likely to be due to zinc filler in the plastic.

Calculation of ion balances for aqueous extracts

It was clear that in most artefacts there was a high concentration of anions in the wash solutions and a very low metal content (e.g. the tortoiseshell box). The pH of the plastic washes were determined using a pH meter (Table 4.8) and it was found

that many of the samples had a low pH value. This H^+ ion concentration may account for the ion imbalance in many of the samples.
Ion balances were therefore calculated for the artefacts using the following equations.

Total ions (anions + cations) = $\Sigma Z_i W_i$ = Σion equivalences

where Z_i is the charge on the ion and W_i is the number of moles.

Example Calculation of ion balance for tortoiseshell box (sample number 1)

Ion equivalence, NO_3^- = $Z_i W_i$

$$W_i = \frac{\textit{concentration of nitrate in sample } (mg\ g^{-1})}{\textit{atomic weight } NO_3^-}$$

$$W_i = \frac{7.6 \times 10^{-3}}{62.003}$$

= 1.2 x 10-4 moles

Z_i = 1 (charge = -1)

∴ Ion Equivalence (NO_3^-) = 120 μmoles ($\mu Eq\ g^{-1}$)

Anions ($\mu Eq\ g^{-1}$)

Cl	NO_3	SO_4	C_2O_4	Total
8	120	210	132	468 ± 25

Cations ($\mu Eq\ g^{-1}$)

Cu	Zn	Fe	Pb	H	Na	NH_4	K	Mg	Ca	Total
1	2	2	0	624	39	53	14	20	20	775 ± 160

Table 4.7 Concentration of metals in plastics, removed after steeping in distilled water, by Electrothermal AAS.

Undegraded artefacts

sample	copper $\mu g\ g^{-1}$	lead $\mu g\ g^{-1}$	iron $\mu g\ g^{-1}$	zinc $\mu g\ g^{-1}$
pink jewellery box (10)	<20	39 ± 5	<20	270 ± 30
yellow jewel. box (13)	<20	<10	<20	140 ± 25
napkin ring (17)	<20	24 ± 5	<20	120 ± 14
tort. jewellery box (15)	<20	<10	<20	<10
yellowed container (14)	<20	750 ± 50	<20	130 ± 37
tortoiseshell lid (12)	<20	45 ± 5	31 ± 4	220 ± 30

Degraded artefacts

sample	copper $\mu g\ g^{-1}$	lead $\mu g\ g^{-1}$	iron $\mu g\ g^{-1}$	zinc $\mu g\ g^{-1}$
tortoiseshell box (1)	25 ± 5	12 ± 3	54 ± 10	60 ± 8
handbag handle (2)	120 ± 24	<10	21 ± 3	95 ± 11
boothook (3)	<20	<10	56 ± 16	<10
green box (4)	<20	<10	<20	52 ± 7
set square (5)	<20	<10	<20	43 ± 15

For each artefact, two samples were taken and two measurements taken for each sample (i.e. n= 4)

Mean and standard deviation reported above

Table 4.8 pH measurements of aqueous extracts. Single measurement for each sample

sample	pH
pink jewellery box (10)	4.0
tortoiseshell lid (12)	3.6
blue mirror (11)	4.9
green box (4)	3.4
handbag handle (2)	3.7
tortoiseshell box (1)	2.9

The total concentrations of anions and cations were still not in balance for the majority of the samples (see Table 4.9). It is difficult to interpret these results as the cation concentration was dominated by the hydrogen ion concentration.

4.3.3 Analysis of artefacts after ashing

As all the organic material is lost during the ashing procedure, this experiment was only applicable to the determination of sulphate and metals in the artefacts. The concentration of nitrate could not be determined because nitric acid was used for the sample preparation. The sulphate levels are shown in Table 4.10, compared to the levels determined by aqueous extraction. The sulphate concentrations for the ashed samples correlated well with the aqueous concentrations. For the degraded artefacts it was clear that steeping extracts nearly all of the sulphate ions. The yellow jewellery box and yellowed container all showed appreciably higher sulphate levels in the ashed samples. For these samples, steeping did not release all the sulphate ions, presumably because the water was not able to access the bulk of the plastic.

The ash solutions were also analysed by Flame AAS (Table 4.11). Copper, lead, iron and zinc were identified as present in many of the samples. Zinc concentrations were considerable for the opaque artefacts containing filler; the pink jewellery box, yellow jewellery box and napkin ring, with levels similar to those expected for fillers (1 to 5%) [5]. The detection limits for this procedure were high, due to high blank levels and hence ETAAS analysis was not performed.

4.3.4 Investigation of simple swabbing procedure for analysing artefacts

The need for a simple, non-destructive procedure for analysing artefacts is very important. This would allow conservators to assess quickly and easily the condition of large numbers of artefacts in a collection. The applicability of analysing a swab taken from an artefact was therefore carried out. A damp cotton bud was wiped over a small area of the artefact (2 cm x 2 cm) approximately twenty times, then steeped in 5 mL water for 10 minutes. The water was then analysed by ion chromatography as before (Table 4.12).

Table 4.9 Calculation of ion balances of artefacts

sample	total anions $\mu Eq\ g^{-1}$	total cations $\mu Eq\ g^{-1}$
pink jewellery box (10)	222 ± 15	72 ± 22
tortoiseshell lid (12)	209 ± 28	186 ± 54
blue mirror (11)	407 ± 45	289 ± 85
green box (4)	93 ± 16	230 ± 57
handbag handle (2)	142 ± 10	176 ± 53
tortoiseshell box (1)	468 ± 25	775 ± 160

Table 4.10 Concentration of sulphate in artefacts by ashing procedure compared to levels determined by aqueous extraction.

Undegraded artefacts

sample	sulphate (ashing) $mg\ g^{-1}$	sulphate (steeping) $mg\ g^{-1}$
pink jewellery box (10)	0.2 ± 0.06	0.2 ± 0.01
yellow jewel. box (13)	2.5 ± 0.3	0.4 ± 0.02
napkin ring (17)	<0.1	<0.05
tort. jewellery box (15)	<0.1	<0.05
yellowed container (14)	0.5 ± 0.1	0.2 ± 0.01
tortoiseshell lid (12)	<0.1	<0.05

Degraded artefacts

sample	sulphate (ashing) $mg\ g^{-1}$	sulphate (steeping) $mg\ g^{-1}$
tortoiseshell box (1)	9.2 ± 0.8	8.1 ± 0.4
handbag handle (2)	4.8 ± 0.6	4.0 ± 0.2
station pointer (7)	6.5 ± 0.6	6.3 ± 0.2
boothook (3)	6.5 ± 0.3	6.6 ± 0.4
green box (4)	0.6 ± 0.2	0.8 ± 0.1
set square (5)	0.6 ± 0.1	0.7 ± 0.1

For each artefact, two samples were taken and two measurements taken for each sample (i.e. n= 4)

Mean and standard deviation reported above

Table 4.11 Concentration of metals in artefacts after ashing by FAAS.

Undegraded artefacts

sample	zinc mg g^{-1}	copper mg g^{-1}	lead mg g^{-1}
pink jewellery box (10)	54 ± 4	<0.1	<0.1
yellow jewel. box (13)	16 ± 2	<0.1	<0.1
napkin ring (17)	17 ± 2	<0.1	<0.1
tort. jewellery box (15)	<0.1	<0.1	<0.1
yellowed container (14)	<0.1	<0.1	0.9 ± 0.05

Degraded artefacts

sample	zinc mg g^{-1}	copper mg g^{-1}	lead mg g^{-1}
tortoiseshell box (1)	0.2 ± 0.03	<0.1	<0.1
handbag handle (2)	<0.1	0.2 ± 0.02	0.3 ± 0.02
station pointer (7)	0.5 ± 0.01	<0.1	<0.1
green box (4)	<0.1	<0.1	<0.1
set square (5)	0.2 ± 0.02	<0.1	<0.1

For each artefact, two samples were taken and two measurements taken for each sample (i.e. n= 4)

Mean and standard deviation reported above

Iron was not detected in any of the samples

Table 4.12 Concentation of anions in swabs taken from artefact's surface.

Undegraded artefacts

sample	nitrate mg L^{-1}	sulphate mg L^{-1}	oxalate mg L^{-1}
pink jewellery box (10)	1.4 ± 0.6	0.3 ± 0.07	<0.01
yellow jewel. box (13)	0.3 ± 0.1	0.8 ± 0.04	<0.01
napkin ring (17)	<0.05	<0.01	<0.01
tort. jewellery box (15)	0.3 ± 0.1	<0.01	<0.01
yellowed container (14)	1.0 ± 0.1	0.3 ± 0.05	<0.01
tortoiseshell lid (12)	1.3 ± 0.3	0.3 ± 0.03	<0.01

Degraded artefacts

sample	nitrate mg L^{-1}	sulphate mg L^{-1}	oxalate mg L^{-1}
tortoiseshell box (1)	5.1 ± 1.2	6.1 ± 0.5	4.9 ± 0.04
handbag handle (2)	2.5 ± 1.1	4.3 ± 0.3	5.9 ± 0.5
station pointer (7)	5.5 ± 0.8	6.7 ± 0.5	6.5 ± 0.6
green box (4)	4.3 ± 2.1	3.8 ± 0.4	1.7 ± 0.2
set square (5)	1.2 ± 0.2	1.3 ± 0.2	4.2 ± 0.7

For each artefact, two samples were taken and two measurements taken for each sample (i.e. n= 4)
Mean and standard deviation reported above

The swabbed samples correlated well with the analysis of aqueous extracts from the artefacts (see Table 4.4), with similar anion concentrations seen. The values could not be directly compared as the anion levels reported for the aqueous extracts are given as the equivalent concentration in the plastic, mg g^{-1}. The more degraded artefacts again had higher concentrations of nitrate, sulphate and oxalate.

Repeatability of swabbing experiment

For three artefacts; the blue mirror, pink lid and sun compass, swabs were taken from eight areas (each 2 cm x 2 cm) and analysed (Table 4.13). The repeatability was poor for the procedure, as expected, due to differences in the area swabbed and swabbing time. RSD values for nitrate levels were worse than for sulphate and oxalate, resulting from large differences throughout an artefacts surface. This followed the

Table 4.13 Calculation of relative standard deviations (%) for swabbing procedure.

sample	nitrate	sulphate	oxalate
blue mirror (11)	36	8	17
pink lid (6)	31	4	17
sun compass (8)	45	8	14

Eight measurements taken for each sample (n=8)

Table 4.14 Nitrogen content of artefacts

Undegraded artefacts

sample	%	
pink jewellery box (10)	6.7	6.8
yellow jewellery box (13)	7.8	8.1
napkin ring (17)	8.3	8.6
tortoiseshell. jewellery box (15)	9.5	9.3
yellowed container (14)	8.4	8.4
tortoiseshell lid (12)	7.8	8.0

Degraded artefacts

sample	%	
tortoiseshell box (1)	5.0	4.4
handbag handle (2)	6.3	6.7
station pointer (7)	3.8	4.0
boothook (3)	4.2	4.5
green box (4)	6.5	6.8
set square (5)	4.6	4.9

For each artefact, two measurements taken (i.e. n= 2)

trend seen in the FTIR analysis (see 3.3.4) due to the unsystematic loss of nitrogen from the artefacts as they degrade. Swabbing does however give a relative indication of anion levels.

4.3.5 Nitrogen content of artefacts

The nitrogen content of an artefact may correlate with the extent of deterioration as denitration is one of the main degradation processes. The artefacts were analysed by the microanalysis department of the university (Table 4.14). The artefacts which were degraded had lower nitrogen contents as expected, as low as 3.8% for the station pointer, compared to the undegraded artefacts. The artefacts in visibly good condition had nitrogen contents of generally 7 - 9%. This was low compared to expected values for cellulose nitrate artefacts (10 - 11% nitrogen) and indicated that these artefacts have undergone some denitration over time.

4.4 Conclusions

The results suggest that the deterioration of a cellulose nitrate artefact over a period of time may relate to its trace sulphate levels. These are likely to result from poor manufacture. Predicting the likelihood of degradation may therefore be possible by measuring the levels of leachable sulphate in an object. Levels of oxalate may also give a clear indication of how much deterioration has occurred. Oxalate results from degradation of the cellulose nitrate polymer structure.

The presence of sulphate, oxalate and other ions is important, for if they should come into contact with water they will be hydrolysed to acids, which will severely degrade the polymer. A simple measurement of the pH of an object's surface, can give a very general gauge to its stability. The analysis of a swab taken from an artefact's surface will also determine what ions are present. If either sulphate or oxalate are identified, then the artefact should be separated from other objects to minimise damage to collections. However, by the time oxalate is detectable, degradation may be already visually obvious.

Artefacts containing 1-5% of a zinc filler do not show severe degradation, even with samples containing appreciable sulphate levels. It is likely that the filler acts as a

buffer in the cellulose nitrate, neutralising any acids that form and hence slowing degradation. Other metals identified are in very low concentrations and do not appear to be associated with degradation.

The nitrogen content of artefacts, as determined by microanalysis, also correlates with the extent of degradation. This technique may prove useful for monitoring samples and determining whether denitration is occurring over time.

References

1. Tennent, N. H., Cooksey, B. G., Littlejohn, D., Ottaway, B. J., Tarling, S. T. and Vickers, M., in *"Conservation Science in the U.K."*, Tennent, N. H., (ed.), James and James Science Publishers Ltd., London, 1993, 60-66.

2. Gibson, L. T., *"Analytical Studies of the Degradation of Calcareous Artefacts in Museum Environments"*, Ph.D. Thesis, University of Strathclyde, 1995.

3. Worden, E. C., *"Nitrocellulose Industry"*, Constable, London, 1911.

4. Richards, G. N., in *"Methods in Carbohydrate Chemistry, vol. 3"*, Whistler, R. L., (ed.), Academic Press, London, 1963, 154-164.

5. Miles, F. D., *"Cellulose Nitrate"*, Oliver and Boyd, London, 1955.

6. Jutier, J. J., Harrison, Y., Premont, S. and Prud'homme, R. E., *Journal of Applied Polymer Science*, 1987, **33**, 1359-1375.

CHAPTER FIVE

THE USE OF ACCELERATED AGEING TESTS FOR STUDYING THE DEGRADATION OF CELLULOSE NITRATE

Chapter Five - Contents

5.1 Introduction

Accelerated ageing tests are now commonly used to understand and predict the long term behaviour of artefacts. Hamrang [1] and Derrick [2] examined the influence of temperature and light exposure on cellulose nitrate artefacts by using simulated environments. The structural changes in artificially aged cellulose nitrate photographic base have been studied by Louvet [3] and in cellulose nitrate adhesive by Shashoua [4].

Accelerated ageing tests are used, in the laboratory, so that the chemical and physical changes in a material can be monitored in a conveniently short time. There are several objectives of these tests [5]. First, to determine whether a material is chemically stable and physically durable, in a range of conditions. Second, to predict the long term serviceability of a material under expected conditions. Thirdly, the processes of deterioration are speeded up in order to elucidate the chemical reactions involved in the degradation and the physical consequences for the material. Finally, the ultimate objectives for conservators, is to develop techniques that can monitor the extent of degradation and methods by which the lifetime of materials can be extended.

The objective of using accelerated ageing tests in this study, was to examine the changes occurring in cellulose nitrate as it was aged artificially and to monitor these changes by chemical analysis. The importance of certain factors was also studied. As earlier work had shown that high concentrations of sulphate are associated with degradation, the influence of sulphate was examined. The apparent ability of zinc fillers to counteract the onset of degradation was also investigated. The influence of iron was studied, as other researchers [6] have suggested that very low levels (<10 parts per million) may accelerate degradation. Other factors such as humidity and temperature were studied, as these are important when appropriate storage or display conditions are being considered.

In planning ageing tests, it is first necessary to decide what chemical or physical measurements are to be taken as the samples age. As chemical changes are usually the underlying cause of the physical changes that occur in materials during deterioration, and because such changes can usually be measured with greater ease and precision, accelerated ageing tests commonly involve studies of chemical change. In cellulose nitrate, physical changes such as discolouration or embrittlement are

difficult to measure and, as they are subjective judgements, will be very imprecise. Therefore, chemical changes in cellulose nitrate, nitrate and oxalate levels and the total nitrogen content were chosen, as they are relatively easy to measure precisely. However, these measurements are only concerned with changes in single components in the samples. As the artefacts are complex systems, containing plasticisers, colourants, e.t.c., other possible factors must be considered such as chain scission and plasticiser loss. Further studies therefore involved measuring the change in weight of samples as they degraded, to gain information regarding the degradation processes.

5.2 Experimental

5.2.1 Samples

Preparation of cellulose nitrate

Much of the work involved examining the influence of certain factors in the cellulose nitrate plastics, e.g. sulphate, zinc and iron. In order to create samples with these constituents added, it was necessary to prepare the plastic in the laboratory from its starting material, i.e. cotton.

As mentioned in Chapter 1, the nitration of cellulose is relatively straightforward. An preparative procedure as described by Green [7] was adopted for the experiment.

Materials:
cotton linters (supplied by Royal Ordnance, Bishopton)
nitric acid, 69% (BDH Chemicals Ltd.)
sulphuric acid, 98% (Fisons)
camphor flowers (Fisons)
zinc oxide (Fisons)
iron, 1000 mg L^{-1} standard solution (BDH Chemicals Ltd.)

Cellulose nitrate was prepared by immersing 5 g of dried cotton linters in a 200 mL bath of 5:16:4 (v:v:v) nitric acid:sulphuric acid:water, for 30 minutes at room temperature. The mixture was stirred throughout. The esterified cellulose was then removed and the bulk of the acid drained off by placing the mixture on a porcelain Buchner funnel (no suction or paper) and pressed with a glass stopper. The cellulose nitrate was then washed thoroughly with 3 x 500 mL distilled water and 3 x 15 mL

boiling ethanol. The ethanol wet mixture was then placed in a bowl and 0.5 g camphor was added. The mixture was kneaded thoroughly, then allowed to dry for 24 hours.

The resultant cellulose nitrate contained approximately 5 mg g^{-1} sulphate as determined by ion chromatography. Cellulose nitrate containing lower levels of sulphate was prepared by extending the earlier washing stage. Samples containing approximately 2 mg g^{-1} sulphate were prepared by washing the cellulose nitrate with 5 x 500 mL water and 3 x 15 mL boiling ethanol. Washing with 10 x 500 mL water and 100 mL boiling ethanol resulted in levels of <0.1 mg g^{-1} sulphate.

Other samples were prepared by adding either zinc oxide or iron to the ethanol wet mixture during the kneading stage.

Initial studies involved the use of thin films, approximately 200 μm thick. A 1 % (w:v) solution of the dried mixture in acetone was prepared (0.5 g in 50 mL acetone). Films were cast in glass petri dishes 10 cm in diameter. The films were then cut into 2 x 2 cm squares for ageing. Later studies involved thicker samples. The dried mix was pressed into disks, 2 cm in diameter and 3 mm thick, between stainless steel dies using a hand pump.

Artefacts

Samples were also taken from artefacts for ageing experiments. Small sections, similar in size and shape to the cellulose nitrate disks (2 x 2 x 0.3 cm) were removed using a scalpel.

5.2.2 Ageing of samples

Samples were placed in glass tanks (5 L) in an oven maintained at the temperature required, initially 70 °C. The relative humidity (R.H.) in the tanks was controlled by the use of saturated salt solutions. The salt solutions (in 100 mL distilled water) used, were as follows :

75 % R.H. (at 70 °C) sodium chloride (Sigma Chemical Company Ltd.)
55% R.H. (at 70 °C) magnesium nitrate (BDH Chemicals Ltd.)
12% R.H. (at 70 °C) lithium chloride (May & Baker Ltd.)

5.2.3 Sample analysis

Samples were removed from the glass tanks at regular intervals for analysis. This sampling took about one minute. Each sample (film, disk or artefact) was then crushed or chopped as thoroughly as possible and analysed.

5.2.3.1 Diffuse reflectance fourier transform infrared spectroscopy (DRIFTS)

IR analyses were carried out using a SpectraTech DRIFTS collector (see Figure 2.4) which was placed in the Nicolet 510P spectrometer. A DTGS detector was used. Approximately 0.3 g of chopped sample was placed in the sample cup of the DRIFTS collector. The spectra were recorded using the following parameters:
Number of scans = 128
Resolution = 4 cm^{-1}
Electronic gain = 1

The spectra were recorded between 4000 and 600 cm^{-1}. For each spectrum, a background spectrum was first recorded (sample cup empty), which was subtracted from the sample spectrum. All data manipulation was carried out using OMNIC software. Spectra were converted to Kubelka-Munk units for quantitative analysis and were baseline corrected. For each sample (film, disk or artefact), two IR spectra were recorded.

The absorbance of the peaks of interest, i.e. the nitrate group (1650 cm^{-1}) and the plasticiser carbonyl group (1733 cm^{-1}) were ratioed against the absorbance of the peak at 1160 cm^{-1}, associated with the ring structure of the cellulose nitrate.

5.2.3.2 Ion chromatography

Sample solutions were analysed as described in 4.2.2. Duplicate injections were made for each sample.

5.2.3.3 Microanalysis

Samples were prepared and analysed as described in 4.2.5. Single measurements of % nitrogen were made for each sample.

5.3. Investigation of the influence of sulphate in degradation

Earlier work had suggested that high sulphate levels in the cellulose nitrate were a cause of increased degradation. To prove this theory, it was necessary to artificially degraded cellulose nitrate samples with high levels of sulphate and determine whether degradation occurs at a greater rate, compared to samples with no sulphate present.

5.3.1 Ageing of films

Procedure

Initial studies involved using thin films of approximately 200 μm thick, so that any degradation would be seen in the shortest possible time, due to the high surface exposed. High temperature (70 °C) and high humidity (75% R.H.) ageing conditions were also chosen to accelerate degradation, so that the studies could be conducted in a conveniently short time. Cellulose nitrate films containing <0.1, 2 and 5 mg g^{-1} sulphate (7 of each) were placed in three separate glass tanks and aged. Films were removed for analysis at intervals up to 264 hours. A small amount of film was retained for microanalysis and two aqueous extracts were prepared for ion chromatographic analysis (50 mg in 20 mL water). The remainder of the film was used for DRIFTS measurements. The experiment was then repeated with another three sets of films and the average is reported.

Results and discussion

Visible changes were noted in the films as they were aged. Films containing sulphate (2 and 5 mg g^{-1}) began to curl and became brittle after only 5 hours in the high temperature and high humidity conditions. After 48 hours, these films were turning brown and at 190 hours they were very dark brown and brittle. The films which contained negligible levels of sulphate did not show any colour changes after 240 hours but were curling and becoming brittle.

Analysis of the films by DRIFTS, ion chromatography and microanalysis (Table 5.1) also showed that degradation was greater in the films containing sulphate. There is a reduction in the IR ratios for the nitrate peak over time, for films containing 2 mg g^{-1} sulphate. There is also a slight decrease in the nitrate levels as determined from ion chromatographic analysis and the total nitrogen content. These reductions are more dramatic for the films containing 5 mg g^{-1} sulphate.

Table 5.1 **Films degraded at 70°C / 75% R. H- Analysis by IR (n=4), ion chromatography (n=4) and microanalysis (n=2).**

(a) Films contain <0.1 mg g^{-1} sulphate (by ashing)

hours	nitrate IR ratio 1650:1160 cm^{-1}	nitrate mg g^{-1}	oxalate mg g^{-1}	nitrogen %	
0	2.0 ± 0.2	0.3 ± 0.1	<0.05	10.3	10.2
5	1.9 ± 0.3	0.2 ± 0.1	<0.05	10.4	10.7
24	1.8 ± 0.3	0.2 ± 0.1	<0.05	10.7	10.5
48	1.8 ± 0.1	0.1 ± 0.1	<0.05	10.2	10.3
96	1.9 ± 0.2	0.3 ± 0.1	<0.05	10.5	10.3
190	2.0 ± 0.2	0.1 ± 0.1	<0.05	10.6	10.6
264	1.9 ± 0.2	0.2 ± 0.1	<0.05	10.5	10.6

(b) Films contain approximately 2 mg g^{-1} sulphate (by ashing)

hours	nitrate IR ratio 1650:1160 cm^{-1}	nitrate mg g^{-1}	oxalate mg g^{-1}	nitrogen %	
0	2.0 ± 0.1	0.7 ± 0.2	<0.05	10.6	10.5
5	2.0 ± 0.2	0.5 ± 0.1	<0.05	10.6	10.6
24	1.8 ± 0.1	0.5 ± 0.1	<0.05	10.3	10.5
48	1.9 ± 0.2	0.5 ± 0.1	<0.05	10.0	10.3
96	1.6 ± 0.2	0.3 ± 0.1	<0.05	9.8	10.1
190	1.6 ± 0.1	0.1 ± 0.1	<0.05	9.8	9.9
264	1.5 ± 0.1	0.2 ± 0.1	0.5 ± 0.05	10.0	9.7

(c) Films contain approximately 5 mg g^{-1} sulphate (by ashing)

hours	nitrate IR ratio 1650:1160 cm^{-1}	nitrate mg g^{-1}	oxalate mg g^{-1}	nitrogen %	
0	1.9 ± 0.1	1.0 ± 0.3	<0.05	10.6	10.4
5	1.8 ± 0.1	0.8 ± 0.2	<0.05	10.4	10.2
24	1.6 ± 0.2	0.6 ± 0.1	<0.05	10.2	10.0
48	1.6 ± 0.2	0.5 ± 0.1	<0.05	9.8	9.5
96	1.4 ± 0.2	0.6 ± 0.1	<0.05	9.0	9.0
190	1.3 ± 0.2	0.4 ± 0.1	0.7 ± 0.05	8.8	8.7
264	1.3 ± 0.2	0.4 ± 0.1	1.1 ± 0.1	8.5	8.1

Mean and standard deviation reported above for IR and IC analysis.

This suggests that some denitration is occurring, with the loss of nitrogen, from the films containing sulphate. No such losses were seen for the films with no sulphate.

The other interesting result from the experiment is the appearance of oxalate in the films containing 5 mg g^{-1} sulphate after 96 hours and after 190 hours for the films containing 2 mg g^{-1} sulphate. This confirms that, as with earlier analyses of the artefacts, after significant degradation has occurred, the cellulose chain is attacked, producing oxalate. Oxalate is detected first in the films containing 5 mg g^{-1} sulphate, proving that the rate of degradation is increased as sulphate levels are increased.

5.3.2 Ageing of disks

Although accelerated ageing of thin films gave a good indication of cellulose nitrate stability, it was necessary to repeat this experiment using thicker samples, more realistic of the artefacts. Cellulose nitrate disks containing <0.1, 2 and 5 mg g^{-1} sulphate were aged under identical conditions to the initial tests with films. The procedure for analysis was also identical to before.

Results and discussion

The disks containing no sulphate did not show any visible changes after 336 hours whereas the disks containing sulphate became brown and brittle after around 100 hours. The results of the chemical analyses (Table 5.2) were similar to those seen with the films. A decrease in the nitrate IR ratio and the % nitrogen is seen over time for the samples containing sulphate. However, the nitrate levels determined by ion chromatographic analysis show an increase for these samples. This indicates that as denitration occurs in the disks, there is a build up of nitrogenous gases. Over time, these gases are lost from the surface of the disk, as seen in the decrease in the nitrate value at 336 hours for the disks containing 5 mg g^{-1}. This build up is not seen with the films, as any gases formed are quickly lost from the surface. Oxalate is again present in the samples containing sulphate once considerable ageing has occurred. The disks containing 5 mg g^{-1} sulphate have notably higher oxalate levels after 240 hours compared with the films aged previously indicating that degradation has occurred to a greater extent. As degradation products, such as nitrogen dioxide, are able to build up in the disks, they in turn cause further degradation by physically

Table 5.2 **Disks degraded at 70°C / 75% R.H. - Analysis by IR (n=4), ion chromatography (n=4) and microanalysis (n=2). Disks contain varying levels of sulphate**

(a) Disks contain <0.1 mg g^{-1} sulphate (by ashing)

hours	nitrate IR ratio 1650:1160 cm^{-1}	nitrate mg g^{-1}	oxalate mg g^{-1}	nitrogen %	
0	1.8 ± 0.2	1.3 ± 0.3	<0.05	10.6	10.7
24	2.0 ± 0.2	1.3 ± 0.1	<0.05	10.1	10.7
72	1.9 ± 0.1	0.8 ± 0.2	<0.05	9.9	10.2
168	1.8 ± 0.1	1.2 ± 0.2	<0.05	10.1	10.5
240	2.1 ± 0.05	1.5 ± 0.4	<0.05	10.4	10.8
336	1.7 ± 0.1	1.0 ± 0.2	<0.05	10.0	10.2

(b) Disks contain approximately 2 mg g^{-1} sulphate (by ashing)

hours	nitrate IR ratio 1650:1160 cm^{-1}	nitrate mg g^{-1}	oxalate mg g^{-1}	nitrogen %	
0	2.0 ± 0.1	1.5 ± 0.2	<0.05	10.3	10.3
24	1.9 ± 0.2	1.3 ± 0.1	<0.05	10.2	10.6
72	1.9 ± 0.2	1.3 ± 0.1	<0.05	10.4	10.5
168	1.9 ± 0.3	1.2 ± 0.2	<0.05	10.3	10.2
240	1.7 ± 0.1	2.0 ± 0.1	<0.05	10.0	9.8
336	1.7 ± 0.2	2.7 ± 0.2	0.7 ± 0.1	9.5	9.4

(c) Disks contain approximately 5 mg g^{-1} sulphate (by ashing)

hours	nitrate IR ratio 1650:1160 cm^{-1}	nitrate mg g^{-1}	oxalate mg g^{-1}	nitrogen %	
0	2.0 ± 0.2	1.6 ± 0.2	<0.05	10.1	9.8
24	1.8 ± 0.1	1.4 ± 0.1	<0.05	9.5	9.7
72	1.8 ± 0.2	0.7 ± 0.1	<0.05	9.8	9.5
168	1.7 ± 0.1	1.5 ± 0.1	2.2 ± 0.1	8.9	9.3
240	1.6 ± 0.2	2.5 ± 0.1	7.4 ± 0.5	8.2	8.0
336	1.5 ± 0.2	3.4 ± 0.1	8.2 ± 0.4	7.3	7.4

Mean and standard deviation reported above for IR and IC analysis.

rupturing the plastic and allowing water and oxygen to penetrate easily. Hydrolytic degradation will then occur and the whole process is autocatalysed.

No significant physical or chemical changes were detected in the disks containing <0.1 mg g^{-1} sulphate throughout the duration of this study.

5.3.3 Ageing of artefacts

Procedure

A study was also carried out to investigate the influence of sulphate in cellulose nitrate artefacts. Analysis of swabs taken from a number of tortoiseshell hair clips (sample number 18), revealed that the objects contained varying levels of sulphate and nitrate. Four hair clips were selected which contained various combinations of high and low sulphate and nitrate levels. All the objects appeared undegraded and did not contain any traces of oxalate. These were then aged at 70 °C and 75% R.H. as before. Swabs were taken from different sections of the artefacts' surfaces at intervals, and analysed by ion chromatography. All analyses were made in triplicate. Small samples were also removed for microanalysis. Two % nitrogen measurements were made for each sample. IR measurements were not taken for two reasons. First, insufficient sample could be removed for DRIFTS measurements. Second, the earlier work had shown that the IR ratios did not change dramatically with degradation; nitrate levels determined by IC and % nitrogen being better indicators of denitration.

Results and discussion

All the artefacts appeared discoloured after 120 hours. The samples containing sulphate also appeared swollen and later became brittle and crumbled. The results of the analysis of the swabs are shown in Table 5.3. As with the disks, there is an initial increase in the nitrate levels and then a decrease, as gases are slowly lost from the samples. Oxalate is seen in all the artefacts after appreciable degradation has occurred. This is seen more rapidly and to a greater extent in the artefacts containing the higher sulphate levels. A greater reduction in the total nitrogen content is seen for the hair clips containing high sulphate levels, compared to those with lower levels (Figure 5.1). The graph confirms that sulphate levels are more important than nitrate levels in the degradation process, as samples (c) and (d) (containing sulphate)

Table 5.3 **Analysis of swabbed extracts of cellulose nitrate hair clips degraded at 70°C / 75% R.H. by ion chromatography (n=4) and microanalysis (n=2).**

(a)Hair clip contains ≈0.2 mg g^{-1} nitrate and ≈0.5 mg g^{-1} sulphate

hours	nitrate (mg L^{-1})	sulphate (mg L^{-1})	oxalate (mg L^{-1})
0	0.3 ± 0.04	0.5 ± 0.06	<0.02
24	1.2 ± 0.2	0.5 ± 0.08	<0.02
72	1.2 ± 0.1	0.6 ± 0.1	<0.02
120	4.6 ± 0.3	0.6 ± 0.07	<0.02
200	6.5 ± 0.4	0.6 ± 0.08	0.9 ± 0.3

(b)Hair clip contains ≈9 mg g^{-1} nitrate and ≈1.5 mg g^{-1} sulphate

hours	nitrate (mg L^{-1})	sulphate (mg L^{-1})	oxalate (mg L^{-1})
0	8.5 ± 0.3	1.5 ± 0.3	<0.02
24	8.3 ± 0.5	1.3 ± 0.1	<0.02
72	11.9 ± 0.4	1.4 ± 0.5	<0.02
120	16.8 ± 0.4	1.8 ± 0.4	0.5 ± 0.2
200	11.2 ± 1.5	1.6 ± 0.5	3.2 ± 0.1

(c)Hair clip contains ≈1 mg g^{-1} nitrate and ≈7 mg g^{-1} sulphate

hours	nitrate (mg L^{-1})	sulphate (mg L^{-1})	oxalate (mg L^{-1})
0	0.9 ± 0.2	6.9 ± 0.8	<0.02
24	3.6 ± 0.1	7.2 ± 1.1	<0.02
72	11.1 ± 1.1	7.5 ± 0.9	0.6 ± 0.1
120	12.5 ± 1.5	7.1 ± 0.6	3.3 ± 0.3
200	6.6 ± 0.1	7.4 ± 1.2	4.7 ± 0.1

(d)Hair clip contains ≈5 mg g^{-1} nitrate and ≈6 mg g^{-1} sulphate

hours	nitrate (mg L^{-1})	sulphate (mg L^{-1})	oxalate (mg L^{-1})
0	4.7 ± 0.1	5.7 ± 0.5	<0.02
24	5.2 ± 0.3	5.9 ± 0.7	0.2 ± 0.07
72	12.9 ± 0.6	4.9 ± 0.3	4.3 ± 0.3
120	11.2 ± 0.2	5.8 ± 1.2	4.5 ± 0.8
200	5.7 ± 0.2	5.3 ± 0.3	7.0 ± 0.2

Mean and standard deviation reported above for IR and IC analysis.

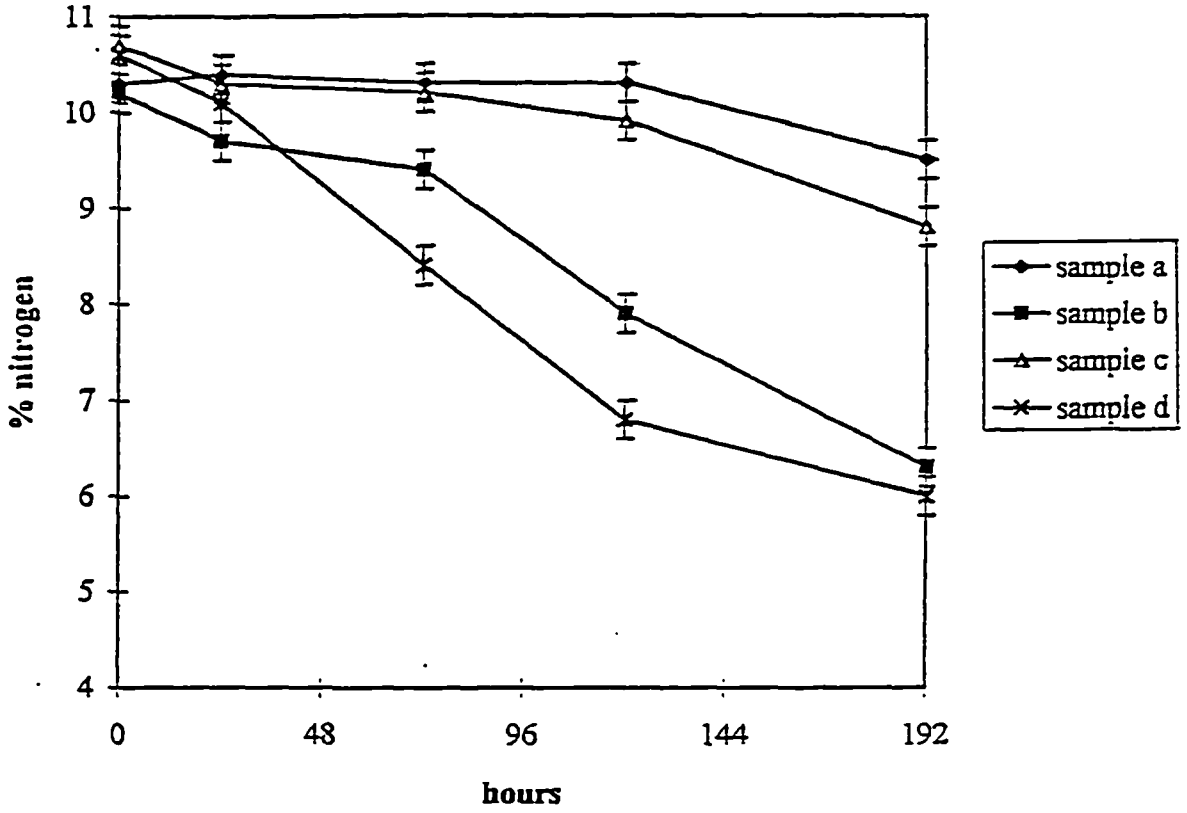

Figure 5.1 **Change in % nitrogen with time for four cellulose nitrate hair clips Hair clips degraded at 70 °C and 75% R.H..**
(a)Hair clip contains ≈0.2 mg g^{-1} nitrate and ≈0.5 mg g^{-1} sulphate
(b)Hair clip contains ≈9 mg g^{-1} nitrate and ≈1.5 mg g^{-1} sulphate
(c)Hair clip contains ≈1 mg g^{-1} nitrate and ≈7 mg g^{-1} sulphate
(d)Hair clip contains ≈5 mg g^{-1} nitrate and ≈6 mg g^{-1} sulphate

degraded to a far greater extent than samples (a) and (b). High nitrate levels do increase the extent of deterioration to some extent, as sample (b) shows a greater loss of % nitrogen than sample (a), after 200 hours.

5.4 Investigation of the influence of zinc oxide filler

Procedure

Cellulose nitrate disks containing <0.1 and 5 mg g^{-1} sulphate were degraded at 70 °C and 75% R.H.. In addition, disks containing 2% zinc oxide and 5 mg g^{-1} sulphate were degraded to test the theory that the presence of fillers may prevent degradation. The procedure for analysis is the same as in 5.1.2.

A similar experiment was conducted using three artefacts; (a) the tortoiseshell lid (contains <0.5 mg g^{-1} sulphate), (b) the handbag handle (contains 4 mg g^{-1} sulphate) and (c) the pink jewellery box (contains 0.5 mg g^{-1} sulphate and 5% zinc oxide filler). Four samples (2 x 2 x 0.3 cm) were removed from each artefact and degraded under identical conditions as before. Samples were removed at intervals. For each sample two aqueous extracts were prepared for ion chromatographic analysis and two samples were removed for microanalysis.

Results and discussion

The results from the analysis of the aged disks are shown in Figures 5.2 and Table 5.4. The decrease in the nitrogen content is not as great for the samples containing filler and sulphate, compared to those containing high sulphate levels only. This indicates that the presence of filler is, in some way, slowing the denitration process, probably by neutralising any acids formed and hence preventing them causing further degradation. No oxalate is detected in the samples containing filler and 5 mg g^{-1} sulphate until 336 hours, compared with 72 hours for samples containing only 5 mg g^{-1} sulphate, again confirming that the degradation has been retarded.

The results from the analysis of the artefacts are shown in Figures 5.3 and Table 5.5. The samples from the pink jewellery box do not degrade to the same extent as the other two artefacts which do not contain filler. There is no visible change in the artefact even after 240 hours, whereas the tortoiseshell lid appears swollen and the handbag handle is discoloured and brittle. There is no decrease in the overall nitrogen content for the pink jewellery box and no oxalate is detected throughout the ageing experiment. The other two artefacts both show degradation - loss of nitrogen and formation of oxalate, most dramatically with the handbag handle which has the higher sulphate level.

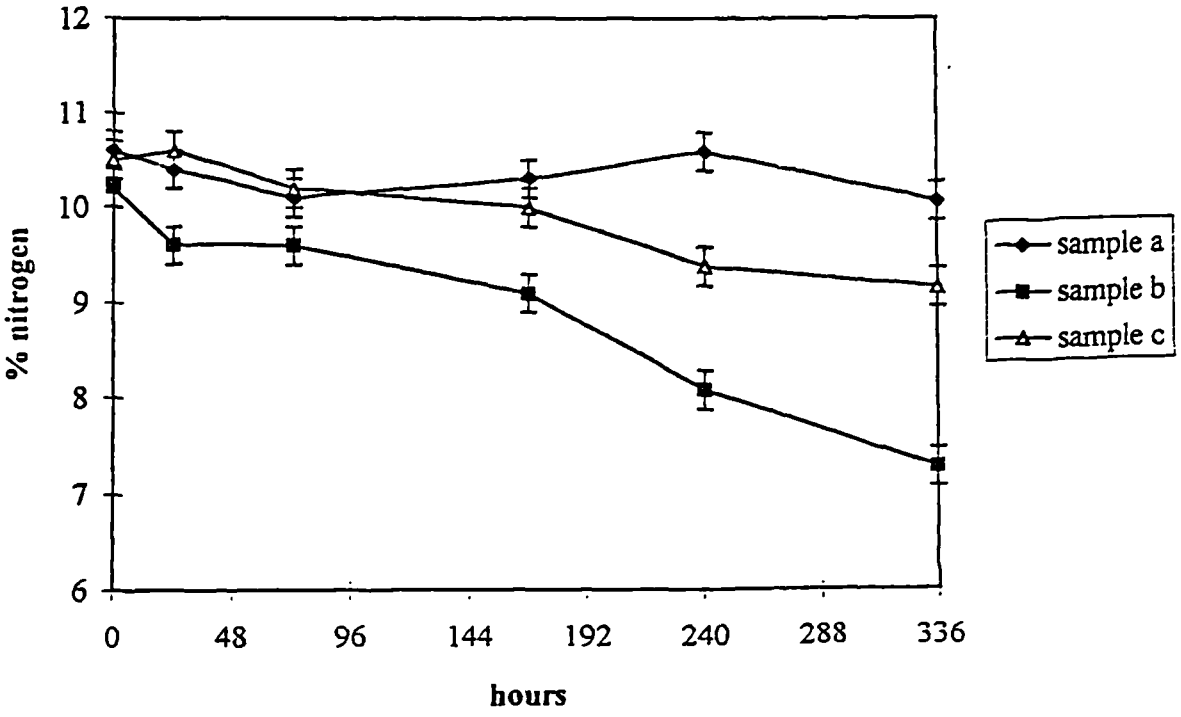

Figure 5.2 **Change in % nitrogen with time for cellulose nitrate disks containing (a) <0.1 mg g^{-1} sulphate, (b) 5 mg g^{-1} sulphate and (c) 5 mg g^{-1} sulphate + 2% zinc oxide filler. Disks degraded at 70 °C and 75% R.H..**

Table 5.4 **Concentrations of oxalate detected in extracts of cellulose nitrate disks aged at 70 °C / 75% R.H.. Concentrations are in mg g^{-1}.**

hours	disk contains <0.1 mg g^{-1} SO_4	disk contains 5 mg g^{-1} SO_4	disk contains 5 mg g^{-1} SO_4 + 2% zinc oxide
0	<0.05	<0.05	<0.05
24	<0.05	<0.05	<0.05
72	<0.05	0.3 ± 0.07	<0.05
168	<0.05	1.4 ± 0.1	<0.05
240	<0.05	6.3 ± 0.3	<0.05
336	<0.05	7.5 ± 0.2	1.2 ± 0.2

For each disk, two samples were taken and two measurements taken (n=4)
Mean and standard deviation reported above

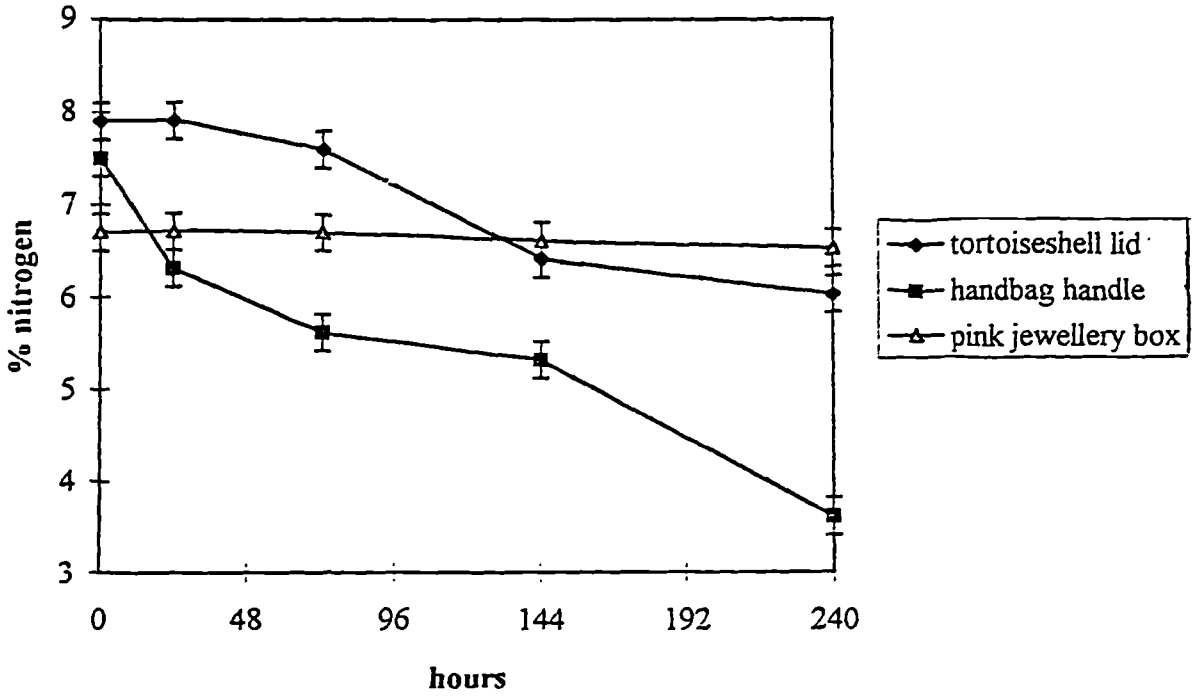

Figure 5.3 **Change in % nitrogen with time for three cellulose nitrate artefacts. Artefacts degraded at 70 °C and 75% R.H.**
(a) Tortoiseshell lid (12) - contains <0.5 mg g^{-1} sulphate
(b) Handbag handle (2) - contains 4 mg g^{-1} sulphate
(c) Pink jewellery box (10) - contains 0.5 mg g^{-1} sulphate and 5% zinc oxide filler.

Table 5.5 **Concentrations of oxalate detected in extracts of cellulose nitrate artefacts aged at 70 °C / 75% R.H.. Concentrations are in mg g^{-1}.**

hours	tortoiseshell lid (<0.5 mg g^{-1} SO_4)	handbag handle (4 mg g^{-1} SO_4)	pink jewel. box (<0.5 mg g^{-1} SO_4 + 5% zinc oxide)
0	<0.05	1.9 ± 0.5	<0.05
24	<0.05	3.0 ± 0.1	<0.05
72	0.7 ± 0.1	3.6 ± 0.2	<0.05
144	0.9 ± 0.1	3.6 ± 0.3	<0.05
240	1.2 ± 0.2	6.0 ± 0.4	<0.05

For each disk, two samples were taken and two measurements taken (n=4)
Mean and standard deviation reported above

Table 5.6 **Disks degraded at 70 °C and (a)12% R.H., (b) 55% R.H. and (c) 75% R.H. Analysis by ion chromatography. Disks contain approximately 1 mg g^{-1} sulphate (by ashing).**

(a) 12% Relative Humidity

hours	nitrate (mg g^{-1})	sulphate (mg g^{-1})	oxalate (mg g^{-1})
0	0.1 ± 0.02	1.2 ± 0.1	<0.05
24	0.1 ± 0.02	1.1 ± 0.1	<0.05
48	0.3 ± 0.04	1.1 ± 0.05	<0.05
96	0.6 ± 0.06	1.1 ± 0.04	<0.05
144	0.5 ± 0.1	1.1 ± 0.1	<0.05
240	0.4 ± 0.05	1.2 ± 0.1	<0.05

(b) 55% Relative Humidity

hours	nitrate (mg g^{-1})	sulphate (mg g^{-1})	oxalate (mg g^{-1})
0	0.2 ± 0.02	1.0 ± 0.03	<0.05
24	0.4 ± 0.1	1.0 ± 0.04	<0.05
48	2.9 ± 0.5	1.1 ± 0.1	<0.05
96	3.7 ± 0.4	1.1 ± 0.1	<0.05
144	2.6 ± 0.1	1.1 ± 0.1	0.4 ± 0.1
240	2.7 ± 0.4	1.2 ± 0.2	2.5 ± 0.1

(c) 75% Relative Humidity

hours	nitrate (mg g^{-1})	sulphate (mg g^{-1})	oxalate (mg g^{-1})
0	0.1 ± 0.05	1.3 ± 0.2	<0.05
24	6.4 ± 0.8	1.0 ± 0.1	0.1 ± 0.06
48	4.4 ± 0.6	1.0 ± 0.2	2.3 ± 0.1
96	3.7 ± 0.1	1.1 ± 0.03	5.2 ± 0.2
144	1.2 ± 0.1	1.0 ± 0.2	8.0 ± 0.2
240	1.1 ± 0.2	1.4 ± 0.3	9.4 ± 0.4

For each disk, two samples were taken and two measurements taken (n=4)
Mean and standard deviation reported above

Table 5.7 **Disks degraded at 50 °C and (a)12% R.H., (b) 55% R.H. and (c) 75% R.H. Analysis by ion chromatography. Disks contain approximately 1 mg g^{-1} sulphate (by ashing).**

(a) 12% Relative Humidity

hours	nitrate (mg g^{-1})	sulphate (mg g^{-1})	oxalate (mg g^{-1})
0	0.1 ± 0.04	0.8 ± 0.06	<0.05
24	0.1 ± 0.05	1.0 ± 0.1	<0.05
48	0.2 ± 0.05	0.9 ± 0.1	<0.05
96	0.2 ± 0.05	0.9 ± 0.07	<0.05
144	0.1 ± 0.02	0.9 ± 0.08	<0.05
240	0.2 ± 0.03	1.0 ± 0.1	<0.05

(b) 55% Relative Humidity

hours	nitrate (mg g^{-1})	sulphate (mg g^{-1})	oxalate (mg g^{-1})
0	0.3 ± 0.05	0.9 ± 0.1	<0.05
24	0.5 ± 0.06	1.0 ± 0.08	<0.05
48	0.6 ± 0.1	0.8 ± 0.07	<0.05
96	1.0 ± 0.1	0.8 ± 0.1	<0.05
144	1.2 ± 0.5	0.9 ± 0.2	<0.05
240	1.8 ± 1.1	0.8 ± 0.1	0.7 ± 0.02

(c) 75% Relative Humidity

hours	nitrate (mg g^{-1})	sulphate (mg g^{-1})	oxalate (mg g^{-1})
0	0.1 ± 0.05	0.9 ± 0.05	<0.05
24	2.8 ± 0.3	0.9 ± 0.1	<0.05
48	3.1 ± 0.3	0.9 ± 0.06	<0.05
96	1.8 ± 0.1	0.8 ± 0.07	0.4 ± 0.1
144	1.1 ± 0.08	0.9 ± 0.1	2.1 ± 0.3
240	0.7 ± 0.3	1.0 ± 0.2	4.7 ± 0.6

For each disk, two samples were taken and two measurements taken (n=4)
Mean and standard deviation reported above

5.5 Investigation of the influence of iron

Cellulose nitrate disks with approximately 0, 0.5 and 5 mg g^{-1} iron were aged at 70 °C and 75% R.H. to determine whether iron influenced the rate of degradation. All disks contained approximately 0.5 mg g^{-1} sulphate to accelerate degradation, so that the experiment could be run in a relatively short time. After 500 hours (3 weeks) all the disks had degraded to the same extent, both visibly and chemically. It was concluded that the iron was not accelerating the degradation, when present in the cellulose nitrate at levels up to 5 mg g^{-1}. However, it is possibley that when cellulose nitrate is in direct contact with iron (metal inserts, hinges, containers, e.t.c.) the degradation is accelerated.

5.6 Investigation of the effect of humidity on degradation

Procedure

Disks containing 1 mg g^{-1} sulphate were degraded at 12%, 55% and 75% R.H. and 70 °C over 240 hours to study the influence humidity plays in the degradation. Disks were removed at regular intervals and analysed as described in 5.3.2. This study was then repeated at 50 °C and at room temperature (approximately 18 °C).

Results and discussion

At 70 °C, samples in the more humid environments degraded at a far higher rate than those at 11% R.H. as indicated by a decrease in the % nitrogen (10.5% to 6.5% - see Figure 5.4) and formation of oxalate (Table 5.6). These samples also became brown and brittle over time. It is clear therefore that humidity is a major factor in the rate of degradation. Anions such as sulphate and oxalate will become hydolysed to acids in the plastic and cause increased deterioration.

At 50 °C, similar results were seen (Figure 5.5 and Table 5.7). The degradation is at a slightly slower rate due to the lower temperature. However, it is clear that even at 50 °C, severe degradation is occurring in high humidity environments.
In the final study at room temperature (≈20 °C), disks were left for 3 months, after which there was no visible change in any of the samples. The disks exposed to 75% R.H. had undergone very slight denitration however. Total nitrogen percentages had fallen from 10.5 % to 10% and nitrate levels determined by IC had increased from

0.5 to 1.5 mg g^{-1}, indicating that some degradation may have occurred even at this lower temperature.

5.7 Investigation of water uptake during ageing

Procedure

Cellulose nitrate disks containing 1 mg g^{-1} sulphate were degraded at 60 °C and three different values of relative humidity: 12%, 55% and 75%. The disks were weighed regularly over time to determine whether water was being absorbed by the cellulose nitrate during ageing. The experiment was carried out in duplicate.

Results and discussion

The results are shown in Figure 5.6. Disks degraded at 75% R.H. show an initial increase in weight (+5% after 24 hours), as water is quickly absorbed by the samples, then a steady loss in weight from the samples (-7% after 240 hours). This trend is also seen with samples degraded at 55% R.H., although the initial weight gain and final weight loss are not as notable. Samples degraded at 12% R.H. do not show any uptake of water during the experiment and only a slight loss of weight after 240 hours (1%).

This study suggests that the change in weight of a sample as it is degraded in a humid environment is due to two process (see Figure 5.7). There is an initial absorption of water by the cellulose nitrate which then reaches equilibrium. As the cellulose nitrate degrades there is a resultant loss of plasticiser and nitrogenous gases which increases over time.

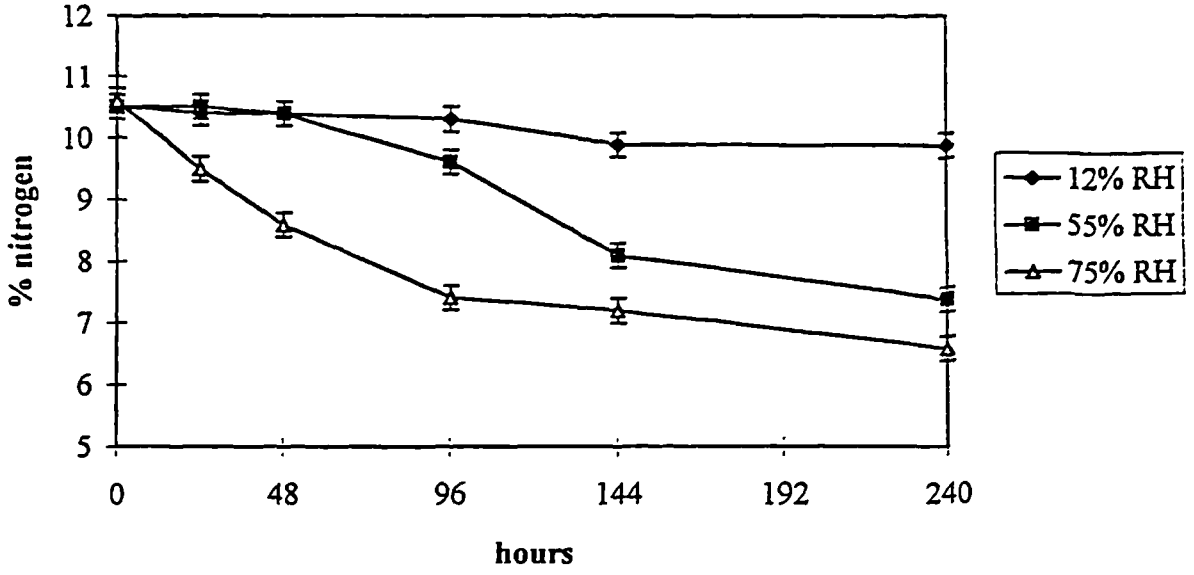

Figure 5.4 **Change in % nitrogen with time for cellulose nitrate disks degraded at 70 °C and (a)12% R.H., (b) 55% R.H. and (c) 75% R.H.. Disks contain approximately 1 mg g^{-1} sulphate (by ashing).**

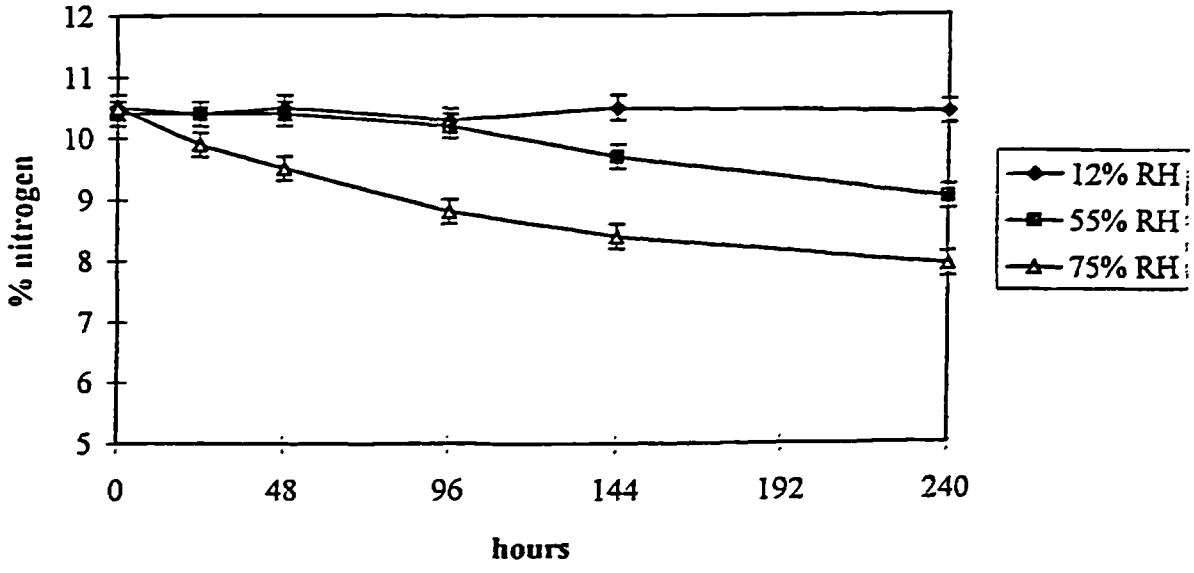

Figure 5.5 **Change in % nitrogen with time for cellulose nitrate disks degraded at 50 °C and (a)12% R.H., (b) 55% R.H. and (c) 75% R.H.. Disks contain approximately 1 mg g^{-1} sulphate (by ashing).**

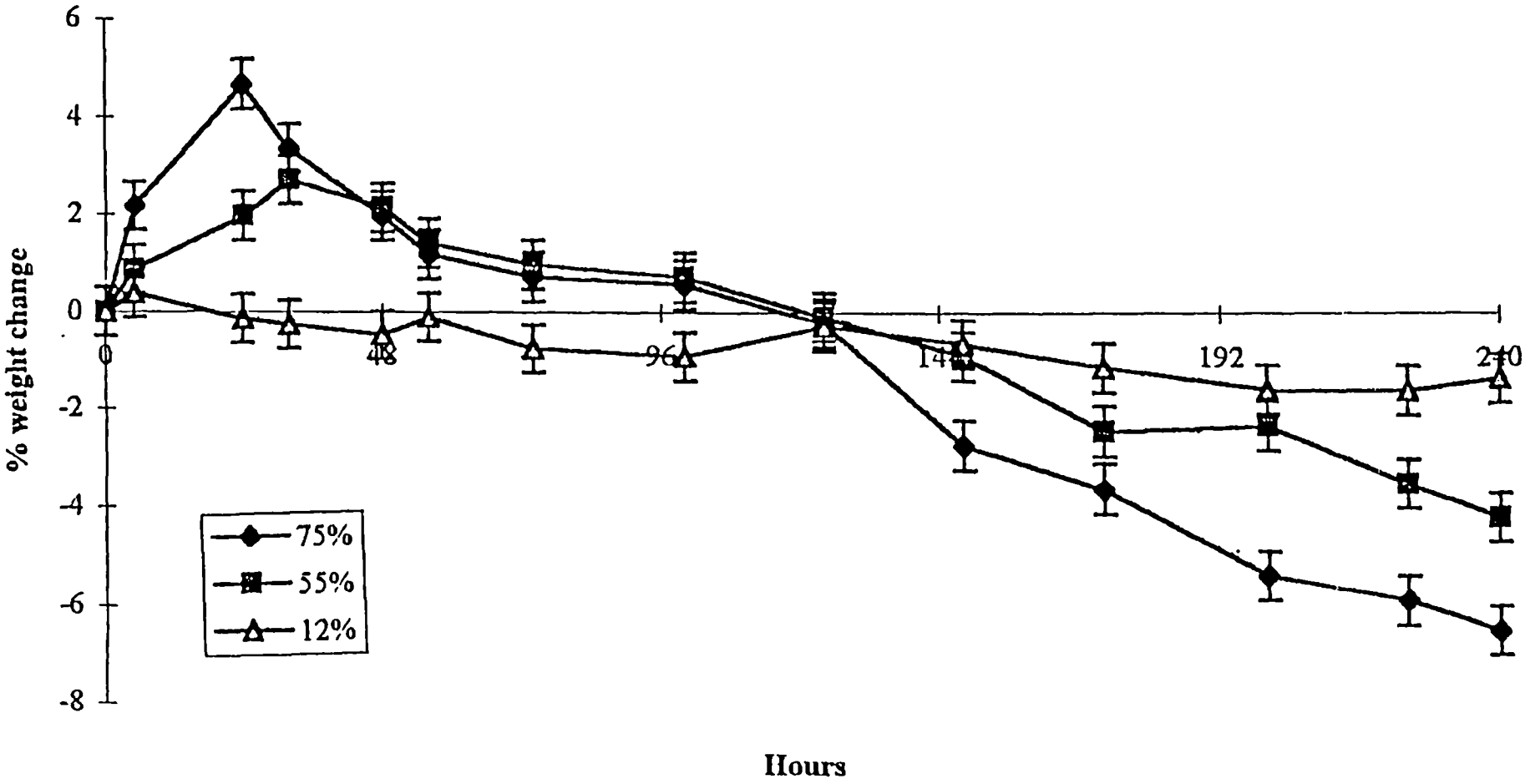

Figure 5.6 Change in the % weight of cellulose nitrate disks degraded at 60 °C and (a) 12% R.H., (b) 55% R.H. and (c) 75% R.H.. Disks contain approximately 1 mg g^{-1} sulphate (by ashing). (n = 3)

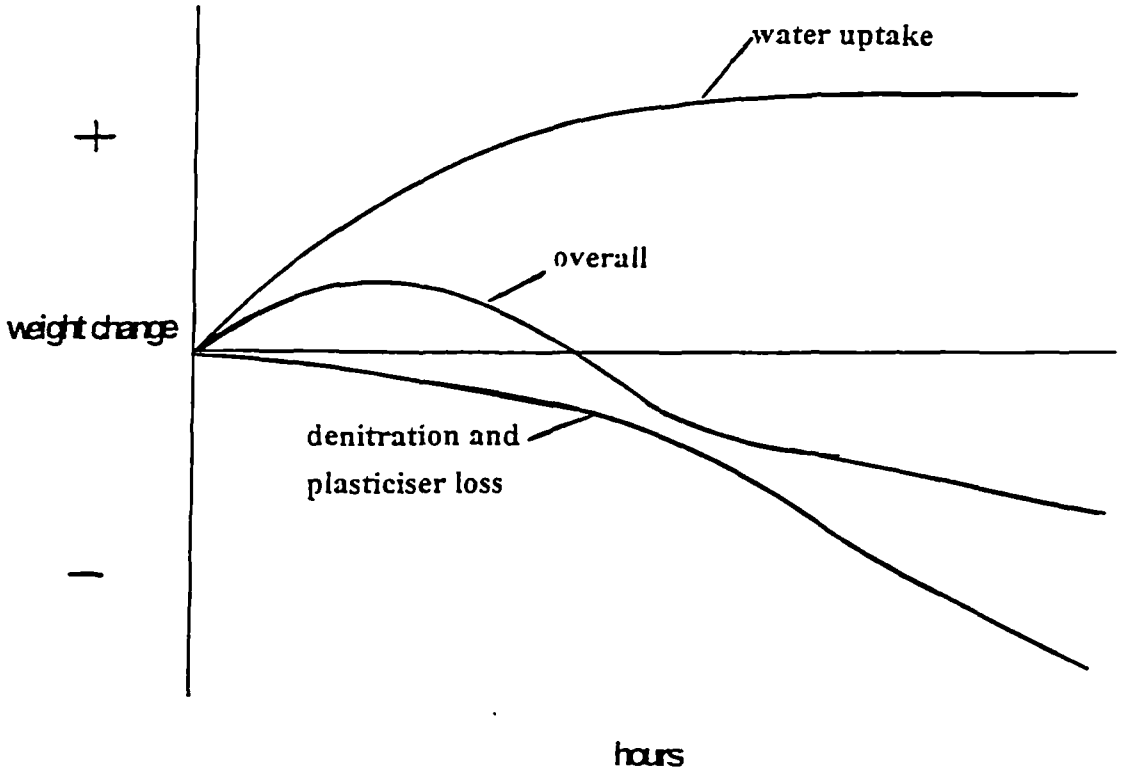

Figure 5.7 Change in weight of artefact as it degrades

5.8 Conclusions

A relatively straightforward procedure has been developed for determining the stability of cellulose nitrate using accelerated ageing tests. Ion chromatography and elemental microanalysis have proved to be extremely useful analytical techniques that can monitor the extent of degradation. The degradation processes of denitration and ring destruction (formation of oxalate) can be studied in both prepared cellulose nitrate samples and in artefacts.

This study has demonstrated that levels of sulphate in cellulose nitrate plastics increase the rate of degradation. Zinc oxide filler has been shown to slow the onset of degradation if sulphate is present in an artefact. Humidity levels, in which an artefact is stored or displayed, are very important, as high R.H. values have been shown to dramatically increase the rate of degradation.

References

1. Hamrang, A., *"Degradation and Stabilisation of Cellulose Based Plastics and Artifacts"*, Ph.D. Thesis, Manchester Metropolitan University, 1994.

2. Derrick, M., Daniel, V. and Parker, A., in *"Preventative Conservation: Practice, Theory and Research"*, Roy, A. and Smith, P., (eds.), IIC, London, 1994, 207-211.

3. Louvet, A., *"Study of the Degradation of Cellulose Nitrate Photographic Base"*, Ph.D. Thesis, Centres de Reserches sur la Conservation des Documents Graphiques, Paris, 1994.

4. Shashoua, Y., Bradley, S. M. and Daniels, V. D., *Studies in Conservation*, 1992, **37**, 113-119.

5. Feller, R. L., *"Accelersted Aging: Photochemical and Thermal Aspects"*, The J. Paul Getty Trust, California, 1994.

6. Edge, M., Allen, N. S., Hayes, M., Riley, P. N. K., Horie, C. V. and Luc-Gardette, J., *European Polymer Journal*, 1990, **26**, 623-630.

7. Green, J. W. in *"Methods in Carbohydrate Chemistry, vol. 3"*, Whistler, R. L., (ed.), Academic Press, London, 1963, 213-235.

CHAPTER SIX

MOLECULAR WEIGHT ANALYSIS OF CELLULOSE NITRATE USING GEL PERMEATION CHROMATOGRAPHY

Chapter Six - Contents

6.1 Introduction

Gel permeation chromatography (GPC) is a type of gel filtration chromatography suitable for the separation of polymer molecules according to size. As mentioned in 2.5, the technique involves passing a solution of the polymer through a column packed with a gel, which separates the polymer into fractions based on their size, which is influenced by molecular weight.

Cellulose nitrate, as with other polymers, does not consist of a particular molecule with a unique molecular weight, but rather a mixture of molecules with a molecular weight range which follows a distribution [1]. A study of the molecular weight distributions of undegraded and degraded samples, would provide useful information concerning the decay processes of cellulose nitrate and would indicate if chain scission is occurring. This in turn would provide a useful technique for assessing the extent of degradation in artefacts.

GPC is an attractive technique for degradation studies of artefacts, as it requires only small volumes of solution. In principle, it is also quite simple to understand, compared with other chromatographic techniques, as separation is based only on the size and shape of samples. The results are therefore highly predictable and reproducible [2]. However, it is first necessary to establish the validity of the procedures used. GPC studies of cellulose nitrate have been performed previously by several workers [3] and [4], but unfortunately no previous work concerning cellulose nitrate artefacts had been carried out prior to this work.

6.2 Experimental

6.2.1 Apparatus

A Pye Unicam PU 4003 pump was used. A tetrahydrofuran (HPLC grade) eluent was passed at a flow rate of 1 mL min^{-1} through two GPC columns (type 10^4 Å + 500 Å), each 32 cm long and connected in series in the order 10^4 Å, 500 Å. The columns were packed with PL gel Styrene 5 μm particles. A Philips PU 4206 refractive index (RI) detector was used at range 0.05 x 10^{-3} RI.

6.2.2 Sample preparation

The work involved the analysis of both samples from the artefacts and samples from films which had been aged. The films were prepared using a cellulose nitrate standard (procedure is described in 3.2.2) and aged at 70 °C and 75% R. H. Films contained approximately 1 mg g^{-1} sulphate.

Samples solutions were prepared by dissolving 20 mg of the crushed sample in 20 mL tetrahydrofuran (THF). Samples were left for 24 hours to ensure complete dissolution. Toluene was used as an internal standard for all solutions (0.5% (v:v)). The relative retention times of all peaks were calculated by dividing the t_r (retention time) values by the values for toluene.

6.2.3 Calibration

In order to relate retention times to molecular weight, the GPC column first had to be calibrated with standards of known molecular weight. Polystyrene standards were used for this purpose as they have narrow distributions. Three standards were used with molecular weights of 111000, 20500 and 4000. Solutions of each polystyrene standard in THF (2 g L^{-1}) were prepared. The solutions also contained 0.5% (v:v) toluene as an internal standard. A typical chromatogram for the standards is shown in Figure 6.1. The standard calibration curve of the polystyrene mixture was then prepared, based on a plot of ln (molecular weight) versus the relative retention time (Figure 6.2).

Cellulose nitrate has a expected molecular weight of 95000 to 30000 [5], so the three standards easily bracket this range. As seen in Figure 6.2, the calibration can be approximated by a linear relationship. However, to calculate the molecular weight averages and the distribution for polymers other than polystyrene by this calibration curve, it is necessary to transform molecular weight units in the curve to those for the polymer specified. The most common technique used to transform the molecular weight units is that of universal calibration. This states that the relevant parameter for calibration purposes is the hydrodynamic volume, measured as the product or intrinsic viscosity and molecular weight. This is based on the Mark - Houwink relation [6].

$$[\eta] = KM^{\alpha}$$

where $[\eta]$ is the intrinsic viscosity, M is the molecular weight and K and α are constants. This procedure requires accurate values of the Mark - Houwink parameters for both the sample and the standard used for the calibration. These must be for the same solvent and at the same temperature as the GPC analysis. For 25 °C using THF, $K = 1.2 \times 10^{-4}$ and $\alpha = 0.71$ for polystyrene and $K = 2.5 \times 10^{-4}$ and $\alpha = 1$ for cellulose nitrate [6].

A computer program was used for all data handling. The program was written by the Polymer Chemistry department of the University of Strathclyde especially for GPC analyses. For each peak (standard and sample), the elution volume (mm) to the start of the peak was first measured. The elution volume and peak height (mm) were then measured at 1 mm intervals along this peak and the data inputted in the form V(i), M(i) (elution volume, molecular weight). The program then calculated the average molecular weight for each sample.

6.3 Results and discussion

GPC analysis was carried out on a variety of artefacts, showing varying states of degradation. In general, it was found that the molecular weight distribution of the degraded artefacts was broader and had shifted towards lower molecular weights, compared to undegraded artefacts. Table 6.1 lists the average molecular weights calculated for a range of artefacts. Degraded artefacts generally have lower molecular weights, which may indicate that some chain scission has occurred in the artefacts during degradation. However, artefacts which exhibit no signs of deterioration show considerable variation in their molecular weights. It is likely that the molecular weight of the cellulose nitrate used to manufacture the artefacts was not constant and it is therefore difficult to compare directly different artefacts.

For this reason, the study was continued using prepared cellulose nitrate films so that the molecular weight of the starting material was constant. Films were aged and analysed over time to monitor any changes in molecular weight. Figure 6.3 shows the chromatograms of films aged for 0, 48, 96 and 144 hours. Films aged for longer were insoluble in THF. As the ageing time increased, the cellulose nitrate peak on the chromatograms became broader and again shifted to lower molecular weights.

This was confirmed by the calculated values for the molecular weights (Table 6.2), which show a decrease from 84000 to 67000. In chromatogram D, it is possible that a secondary peak is arising after the main peak. This suggests that non random degradation is occurring i.e. the degradation is following a defined pattern.

6.4 Conclusions

Although only initial studies have been carried out using gel permeation chromatography, the technique has proved to be applicable for analysing cellulose nitrate artefacts. The procedure is relatively simple and requires very little sample. This study has indicated that as cellulose nitrate artefacts degrade, chain scission occurs, resulting in a decrease in the average molecular weight. This correlates with the formation of oxalate which is detected once considerable degradation has occurred.

References

1. Crompton, T. R., *"Analysis of Polymers, an Introduction"*, Permagon Press, Oxford, 1989.

2. Ravindranath, B., *"Principles and Practice of Chromatography"*, Ellis Horwood Ltd., West Sussex, 1989.

3. Holt, C., Mackie, W. and Sellen, D. B., *Polymer*, **19**, 1978, 1421-1426.

4. Saunders, C. W. and Taylor, L. T., *Applied Spectroscopy*, **45**, 1991, 900-905.

5. *"Modern Plastics Encyclopaedia, vol. 2"*, Plastics Catalogue Corporation, London, 1947, 64-66.

6. *"Polymer Yearbook 2"*, Pethrick, R. A. (ed.), Harwood Academic Publishers, London, 1985.

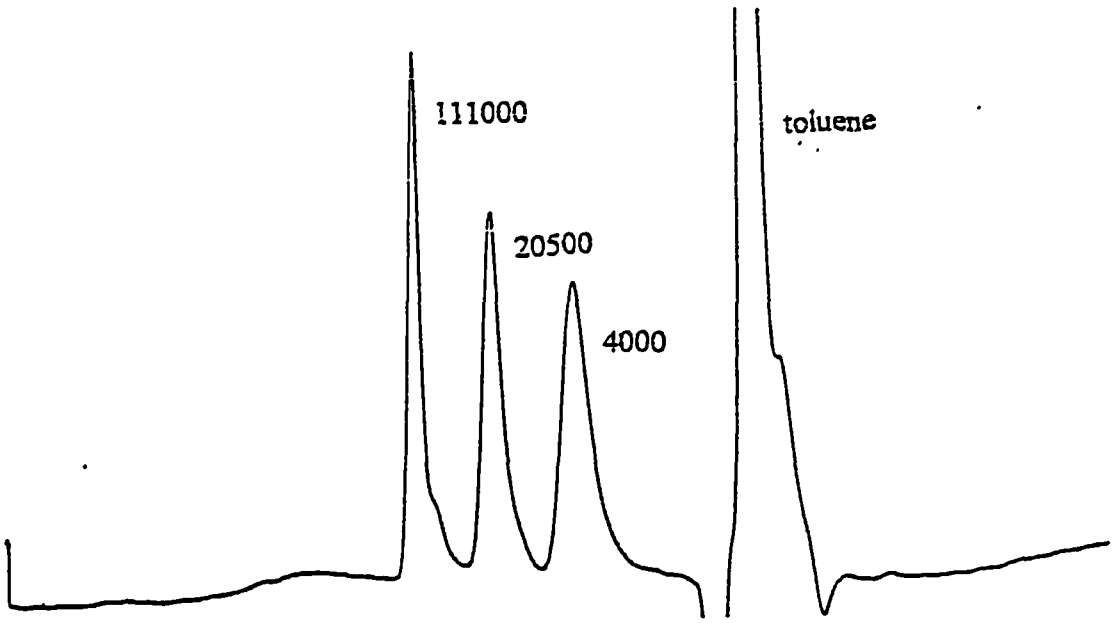

Figure 6.1 Chromatogram of polystyrene standard. Standard contains 2 mg L^{-1} of each polystyrene standard in THF (Molecular weights: 111000, 20500 and 4000) and 0.5% (v:v) toluene as an internal standard.

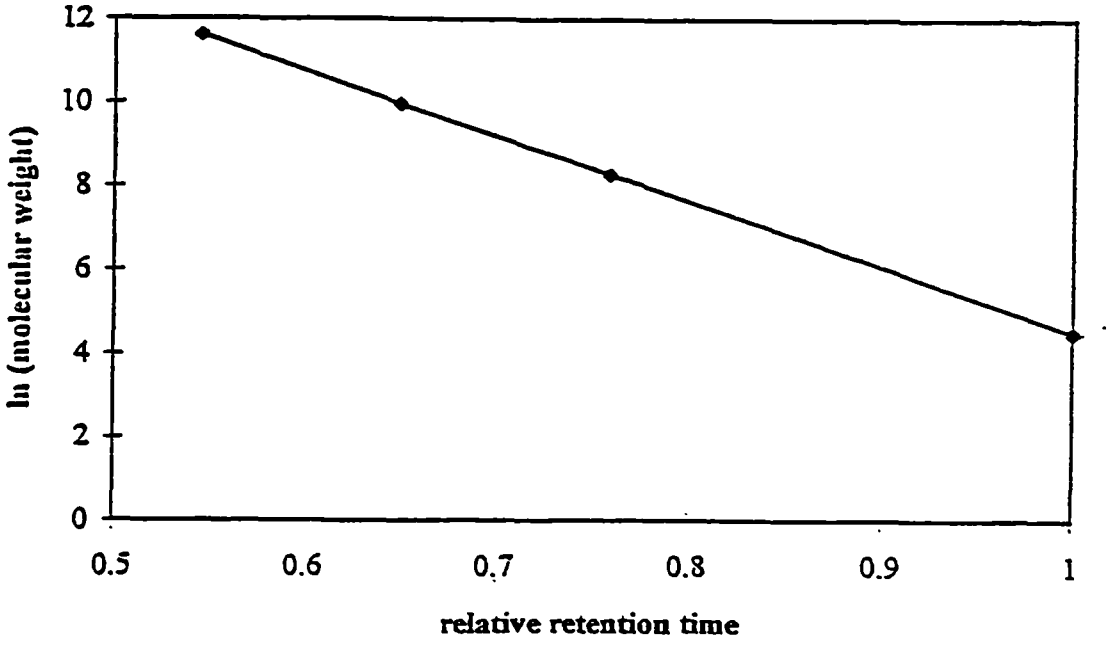

Figure 6.2 Plot of ln (molecular weight) versus relative retention time for polystyrene standard.

Table 6.1 Molecular weight averages calculated for artefacts

(A) Undegraded artefacts

Sample	Molecular weight average
napkin ring (17)	85000 ± 2000
tort. jewellery box (15)	63000 ± 1500
yellowed container (14)	67000 ± 1500
tortoiseshell lid (12)	79000 ± 3000

(B) Degraded artefacts

Sample	Molecular weight average
tortoiseshell box (1)	47000 ± 3000
handbag handle (2)	55000 ± 1000
green box (4)	67000 ± 4500
set square (5)	56000 ± 2000

Three measurements taken for each sample (n = 3)
Mean and standard deviation reported above

Table 6.2 Molecular weight averages calculated for films aged at 70 °C and 75% R.H.

Hours aged	Molecular weight average
0	84000 ± 1000
48	81000 ± 2000
96	74000 ± 1500
144	67000 ± 2000

Three measurements taken for each sample (n = 3)
Mean and standard deviation reported above

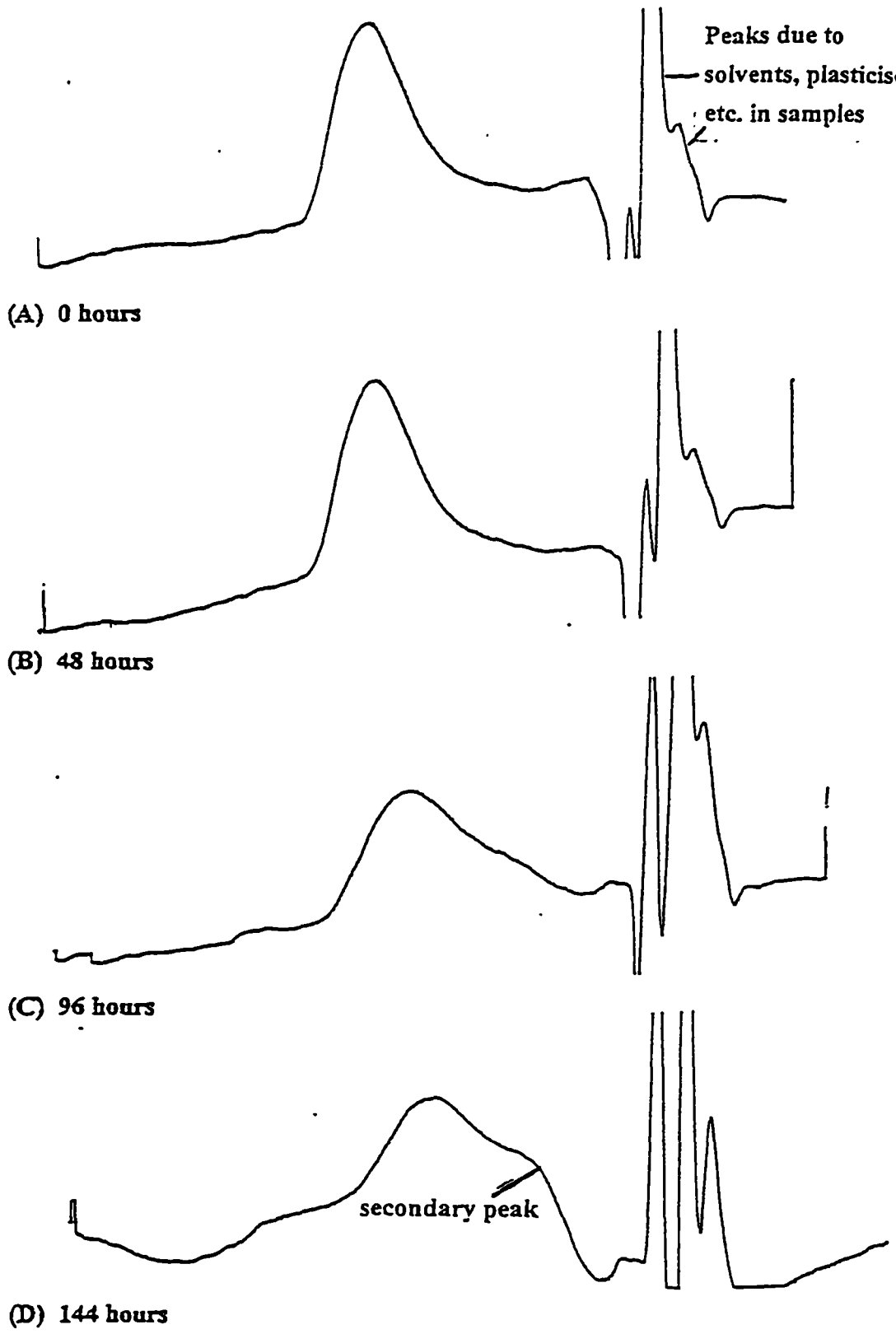

Figure 6.3 Chromatograms of films aged at 70 °C and 75% R.H.

CHAPTER SEVEN

CONCLUSIONS AND FUTURE WORK

Conclusions

The deterioration of cellulose nitrate artefacts is a complex problem facing conservators and conservation scientists, as there are many parameters which must be considered for understanding the overall degradation process. In this study, analysis of several cellulose nitrate artefacts and model samples revealed that the rate of deterioration may relate to trace sulphate levels. These are most likely to result from inadequate washing at the manufacturing stage. This was confirmed when laboratory model cellulose nitrate samples doped with sulphate were aged at 70 °C and 75% R.H. These samples underwent considerably more degradation compared to samples which did not contain sulphate, aged in identical conditions.

The presence of an inorganic filler, such as zinc oxide, in a cellulose nitrate artefact appears to slow, or even prevent, the degradation. Artefacts containing filler were found to be in generally better condition, even those which contained trace sulphate levels which affected the stability of the unfilled artefacts. This theory was confirmed when cellulose nitrate samples containing 5 mg g^{-1} sulphate and 2% zinc oxide were aged at 70 °C and 75% R.H. The degradation was minimal compared to aged samples containing 5 mg g^{-1} sulphate only.

Degradation studies carried out in this work indicated that humidity plays a very important part in the degradation process of cellulose nitrate. As the level of humidity increased, degradation processes occurred at a faster rate. Even at 50 °C, cellulose nitrate samples deteriorated significantly in humid environments (> 55% R.H.).

Accelerated ageing tests at above room temperatures and relative humidities allowed reaction rates to be increased so that reactions could be studied within a reasonably short time. While this created artificial conditions compared to those which an artefact in a museum store or display would normally be exposed to, the test pieces of cellulose nitrate mimicked the real time changes observed in historical cellulose nitrate plastics. The conclusions drawn from the accelerated ageing experiments are therefore considered valid models on which to base conservation strategies for three dimensional cellulose nitrate objects.

Analysis of artefacts and aged cellulose nitrate samples has revealed that chain scission occurs during the degradation process. Ion chromatographic analysis has

shown that oxalate is formed once considerable degradation has occurred. Its presence indicates that there is some destruction of the cellulose nitrate molecule during ageing. Studies involving gel permeation chromatography have also indicated that there is chain scission. There is a change in the molecular weight distribution as cellulose nitrate samples are aged, with a decrease in the average molecular weight.

During this study , several methods were developed to monitor some of the chemical and physical changes that occur as cellulose nitrate artefacts degrade. Basically, two approaches were taken for measuring degradation. The first was to determine how far the degradation process had already progressed. The second was to define a parameter that would allow a prediction to be made about the stability of cellulose nitrate artefacts.

Fourier transform infrared spectroscopy was used to monitor the loss of nitrate groups and the loss of plasticiser from artefacts as they degrade. A microscope attachment to the FTIR spectrometer enabled very small samples to be analysed with minimal preparation. Although the technique was not precise it would give an indication that degradation had taken, or was taking place. FTIR microspectroscopy is well suited for identifying unknown plastics in museum and art collections and for assessing degradation that has already occurred, in objects from which only minimal samples can be taken.

Levels of nitrate, sulphate and oxalate in the artefacts could be determined using ion chromatography. An aqueous extract of a 50 mg sample, or better still from a collectors point of view, a swab taken from an artefact's surface, was sufficient for determining the presence of these anions. High levels of nitrate and oxalate indicated that considerable degradation had already occurred. However, the level of leachable sulphate was found to be a reliable indicator for predicting stability in historical cellulose nitrate plastics. High (>5 mg g^{-1}) levels were associated with an already degrading artefact; low (<5 mg g^{-1}) levels equated with a stable system and intermediate levels (>0 mg g^{-1} and <5 mg g^{-1}) implied that the artefact could become unstable at some point in the future and should be monitored at regular intervals for signs of degradation.

The loss of nitrate from an artefact could also be measured by elemental analysis to calculate the % nitrogen content. However, it was found that even artefacts which appear undegraded had low nitrogen levels (≈7%). This technique may be better

suited to monitoring losses of nitrogen over a period of time and hence determining the rate of degradation.

Initial work to develop a method for analysing cellulose nitrate samples using gel permeation chromatography was also undertaken. The results from molecular weight determinations correlated with visual appearance and anion level determinations. Further work is recommended to identify the products formed during degradation.

Overall, it is clear that the degradation of cellulose nitrate artefacts depends on two factors; the presence of sulphate and humidity. Sulphate is important as it acts as a catalyst for chain degradation, seen by GPC analysis and the presence of oxalate and also acetate and formate. Sulphate also acts as a catalyst for denitration which is observed by FTIR measurements, ion chromatography and elemental analysis. In some instances sulphate does not correlate with degradation, where zinc oxide filler is present.

The degradation process is probably diffusion controlled. It is the diffusion of water to the reaction site, where the sulphate esters are hydrolysed, which is the critical factor for the degradation reaction. The diffusion is controlled by two factors. The humidity at which the cellulose nitrate is exposed to, i.e. the concentration of water at the surface and the permeability of the media. The loss of plasticiser affects this permeability. As it diffuses out, it leaves voids which increase moisture accessibility and the cellulose nitrate also becomes more rigid and is susceptible to stress cracking and crazing.

Therefore, to increase the lifetime of cellulose nitrate artefacts, the relative humidity should be low and the loss of plasticiser should be suppressed. Future research should examine ways of controlling plasticiser loss.

Recommendations for preserving artefacts

To fully understand the causes and the processes of deterioration and to accurately evaluate degradation, sophisticated laboratory techniques are required. As conservators rarely have the necessary equipment, funding or training required, it is important to recognise the need for accurate, simple methods for measuring chemical

properties to evaluate objects with potential stability problems. This work has shown that simple procedures can be used to assess an artefact's stability.

Once an object has been identified as cellulose nitrate, preferably by spectroscopic methods, a full visual inspection and report is essential. By assessing degradation visually, using a simple scheme similar to the one outlined in chapter 3, artefacts can be initially ranked. Artefacts determined to be exhibiting any effects of degradation should then be isolated as described in 3.3.1. Swabs could then be taken from the surface of the artefact for ion chromatographic analysis to determine nitrate, sulphate and oxalate levels. If any sulphate or oxalate is identified, or the level of nitrate is high, then the artefact should be separated from other objects to prevent acidic vapours attacking.

If surface deposits are identified on an artefact, they should be removed using a slightly damp swab. Water should be used sparingly and the surface dried immediately, to prevent penetration to the interior of the plastic. Further research is recommended to investigate cleaning methods and to evaluate any negative effects they may have on an object's stability.

Future research should also involve the development of possible stabilisation treatments for objects. This may possibly be achieved by using a combination of anti oxidants, light stabilisers and plasticiser. Hamrang [1] has carried out some work in this area, with promising results, but more research is needed. Coating artefacts with such a mixture may prevent moisture and oxygen from penetrating the artefact and may also neutralise acids or harmful degradation products. The relative efficiency of each component in a stabilisation system should be investigated to determine optimum concentrations. It is also important to determine whether the stabiliser system is penetrating the polymer matrix or simply coating the surface.

It has been shown by the use of accelerated ageing tests, that low temperature and low humidity environments are favourable for reducing degradation and objects should therefore be stored in controlled conditions. This would obviously reduce thermal and hydrolytic degradation in the artefact as well as decreasing the rate at which plasticiser is volatilised. Temperature and humidity should also be controlled so that constant levels are maintained. Fluctuations in the artefact's environment may result in changing stresses within the plastic, leading to cracking and distortion.

Artefacts should not be stored or exhibited in sealed containers so that deleterious gaseous degradation products are unable to build up. Future work is also suggested to investigate the use of passive sampling tubes to monitor levels of nitrogenous gases or plasticiser in storage cabinets.

The effectiveness of oxygen scavenging absorbents, such as Ageless©, could also be tested for cellulose nitrate preservation.

Finally, research is also needed to investigate the degradation of two other plastics. Cellulose acetate and PVC are two other plastics common in historical plastics collections which are also suffering from degradation. A better understanding of deterioration mechanisms and techniques of prevention and prediction is needed. When these become clearer, appropriate treatment can then be assessed for minimising further damage to collections.

1. Hamrang, A., *"Degradation and Stabilisation of Cellulose Based Plastics and Artifacts"*, Ph.D. Thesis, Manchester Metropolitan University, 1994.